

UNIVERSITA' VITA-SALUTE SAN RAFFAELE

FACOLTA' DI MEDICINA E CHIRURGIA

Corso di Laurea specialistica in Biotecnologie
Mediche, Molecolari e Cellulari

MOLECULAR MECHANISMS IN THE
PATTERNING OF MOUSE CORTICO-
CEREBRAL EMBRYONAL PRIMORDIUM

Relatore: Professor Giorgio Casari

Correlatore: Professor Antonello Mallamaci

Tesi di Laurea di:

Paola Cognigni

matr. 001114

Anno Accademico 2006-2007

Abstract

During the development of the forebrain, the margin between the cortex and the basal forebrain, termed pallial-subpallial boundary, functions as a signaling center for cortical patterning, a guidance element for migrating cells and axonal projections, and a sharp gene expression margin dividing pallial from subpallial gene expression domains. The aim of our work was to molecularly dissect positioning, establishment and function of this boundary region in the developing embryonic forebrain, using the mouse as our model organism.

We isolated the boundary structure through manual microdissection of the embryonic brain and artificially re-created boundary events in culture through mixed cultures of pallial and subpallial origin. Starting from these materials, via dedicated strategies for gene expression profiling and specific functional assays, we highlighted a variety of features and events pertaining to the boundary and its neighboring regions. Analysis of acute preparations provided us with evidence toward the existence of a highly metabolically active, fast-cycling population in the surroundings of the pallial-subpallial boundary, which we propose to be implied in development of paleocortex, classically assumed to arise and migrate from the ventralmost cortical primordium. In vitro boundary recreation showed several transcriptional programs being selectively activated by contact between cells bearing different positional identities. In particular, we found neuronal identity profiles, sets of transcription factors, and molecules regulating signaling responsiveness to be affected, in line with a proposed recapitulation of boundary formation events, in which an intricate interaction net among transcription factors and signaling molecules establishes the boundary and eventually defines local neuronal phenotypes. We propose several explanations that could account for the observed results; a particularly intriguing one calls for the involvement of Pax6 as a master gene in maintaining cortical identity in opposition to basal identity as a response to contact with subpallial-originated cells.

We finally suggest several planned lines of research to delve further into the implications of the current results, in order to pinpoint the molecular events involved in the development of the pallial-subpallial boundary.

Riassunto

Nello sviluppo del cervello, il margine tra la corteccia e il telencefalo basale, detto margine corticostriatale, possiede una funzione di centro segnalatorio nel patterning corticale, un elemento di guida per cellule migranti e proiezioni assonali e un netto confine di espressione genica che separa i domini di espressione palliali e subpalliali. Il nostro scopo è stato quello di analizzare a livello molecolare gli eventi di posizionamento, formazione e funzione di questa zona di confine durante lo sviluppo embrionale del cervello, utilizzando il topo come modello.

Abbiamo isolato la struttura di confine mediante microdissezione manuale del cervello embrionale e ricreato artificialmente eventi di confine in coltura, mediante miscele di cellule di origine palliale e subpalliale. Da questo materiale, utilizzando strategie di profilatura dell'espressione genica e specifiche prove funzionali, abbiamo osservato svariate caratteristiche ed eventi relativi al confine e alle zone circostanti. L'analisi di preparazioni acute ci ha offerto indicazioni sull'esistenza di una popolazione cellulare altamente attiva metabolicamente e in rapida proliferazione nei dintorni del margine corticostriatale, che proponiamo possa essere implicata nello sviluppo della paleocorteccia, che si considera classicamente derivata dal primordio corticale più ventrale. La ricreazione in vitro di eventi di confine ha mostrato l'attivazione selettiva di vari programmi trascrizionali solo in caso di contatto tra cellule di diversa identità posizionale. In particolare, abbiamo osservato la variazione di profili di identità neuronale, gruppi di fattori trascrizionali e molecole coinvolte nella risposta a segnali, coerentemente alla nostra proposta di una ricapitolazione di eventi di formazione di confine, in cui un'intricata rete di interazione tra fattori trascrizionali e molecole segnalatorie origina il confine per poi definire fenotipi neurali locali. Proponiamo diverse spiegazioni per i nostri risultati; particolarmente affascinante è il possibile ruolo di Pax6 come regolatore di alto livello nel mantenimento di un'identità corticale in contrasto con un'identità basale in risposta al contatto con cellule provenienti dal subpallio.

Infine, suggeriamo alcune linee di ricerca previste per l'approfondimento dei risultati correnti e delle loro implicazioni, allo scopo di identificare gli eventi molecolari coinvolti nello sviluppo del margine corticostriatale.

Index

Abstract	5
Riassunto	7
Index	9
Introduction	13
EMBRYOGENESIS OF THE MOUSE CENTRAL NERVOUS SYSTEM: AN OVERVIEW	13
<i>Neural tube formation</i>	13
<i>Cortical neuronogenesis</i>	14
DEVELOPMENTAL MECHANISMS	16
<i>Cellular events</i>	16
Cell cycle regulation.....	16
Programmed cell death.....	17
Adhesion and migration	17
Differentiation.....	18
<i>Regulatory elements</i>	19
Transcription factors.....	19
Morphogens	20
<i>Coordinates</i>	21
Time.....	21
Position.....	21
GENERAL PATTERNING MECHANISMS	24
<i>Adjacent transcription domains</i>	24
<i>Boundary definition</i>	25
<i>Acquired boundary features</i>	25
<i>Compartment constraint</i>	26
<i>Secondary patterning</i>	27
<i>Guidance and barrier function</i>	27
PATTERNING REGIONS IN THE DEVELOPMENT OF THE ROSTRAL CNS	29
<i>Dorsoventral axis</i>	29
Floor plate and roof plate	29
<i>Anteroposterior axis</i>	29
Anterior Neural Ridge	29
Isthmus	30
Zona Limitans Intrathalamica	31
AREA PATTERNING OF THE CEREBRAL CORTEX	31
<i>Cortical boundaries</i>	32
Cortical hem.....	32
Cortical anti-hem	33
Commissural Plate	33
<i>Morphogen sources and axis definition</i>	34
<i>Spatial patterning transcription factors</i>	34
CORTICOSTRIATAL BOUNDARY	36
<i>Gene expression margins</i>	36
<i>Signaling role</i>	36
<i>Boundary-restricted expression patterns</i>	37
<i>Guidance functions for axons and migrating cells</i>	37

Materials and methods.....	39
EMBRYONIC TISSUE RETRIEVAL.....	39
<i>Animal husbandry</i>	39
β -actin-EGFP ^{+/+} mice.....	39
<i>Microdissection and tissue preparation</i>	39
<i>Cell cultures</i>	40
RNA TECHNIQUES.....	41
<i>RNA extraction and purification</i>	41
<i>Microarray hybridization</i>	41
Affymetrix platform.....	42
<i>Real-Time PCR</i>	43
Primer pair selection	43
Standard preparation.....	44
Sample preparation	44
RT-PCR reaction.....	44
Data analysis	45
Primer sets.....	45
IMMUNOHISTOCHEMISTRY AND IN SITU HYBRIDIZATION.....	46
<i>Histological sample preparation</i>	46
<i>Cell cycle marker immunohistochemistry</i>	47
BrdU/IdU administration.....	47
Pretreatment of sections.....	47
Antibodies	48
Cell cycle data analysis.....	48
<i>In situ hybridization</i>	49
Probe selection and cloning.....	50
Probe synthesis.....	51
Pretreatment of sections.....	52
Hybridization and washing of sections	52
Digoxigenin revelation	53
<i>Microphotography and editing</i>	53
Results.....	55
ACUTE PREPARATIONS	55
<i>Dissection quality control</i>	55
RT-PCR.....	56
<i>Preliminary microarray hybridization</i>	56
Data filtering	57
Ontology classification	58
<i>RT-PCR</i>	59
Confirmation of microarray data.....	59
Temporal kinetics.....	60
<i>In situ hybridization</i>	63
FUNCTIONAL ASSAYS.....	66
Cell cycle analysis.....	67
COCULTURES.....	68
<i>Dissection quality and biological identity in culture</i>	68
RT-PCR on acutely dissected and cultured material.....	68
RT-PCR on cocultured material	69
<i>Microarray hybridization</i>	71
Whole-transcriptome dynamics.....	71
Local boundary patterning events	73
Homotypical expression shift.....	75
<i>Striatal-like features of the cocultures</i>	77
An emerging GABA-ergic signature.....	77

<i>Cortical-like features of the coculture</i>	77
Involvement of retinoic acid signaling	77
A master gene for transcription factor regulation.....	78
Discussion	81
ACUTE PREPARATIONS	81
<i>Features of the isolated population</i>	81
<i>Putative identity of the population</i>	81
<i>Tissue distribution patterns of analyzed genes</i>	82
Ddah1 and NO signaling	82
COCULTURES	84
<i>Recreation of contact events</i>	84
Molecular counterparts of contact events	84
<i>Contact-specific events</i>	85
<i>Identity shift events</i>	85
Kinetic regulation	86
Instructive regulation.....	86
<i>RA signaling</i>	87
<i>Pax6 signature upregulation</i>	88
Conclusions	89
List of abbreviations	91
Appendices	95
APPENDIX A.....	95
APPENDIX B.....	97
APPENDIX C.....	102
APPENDIX D.....	106
Bibliography	111
Acknowledgements	121

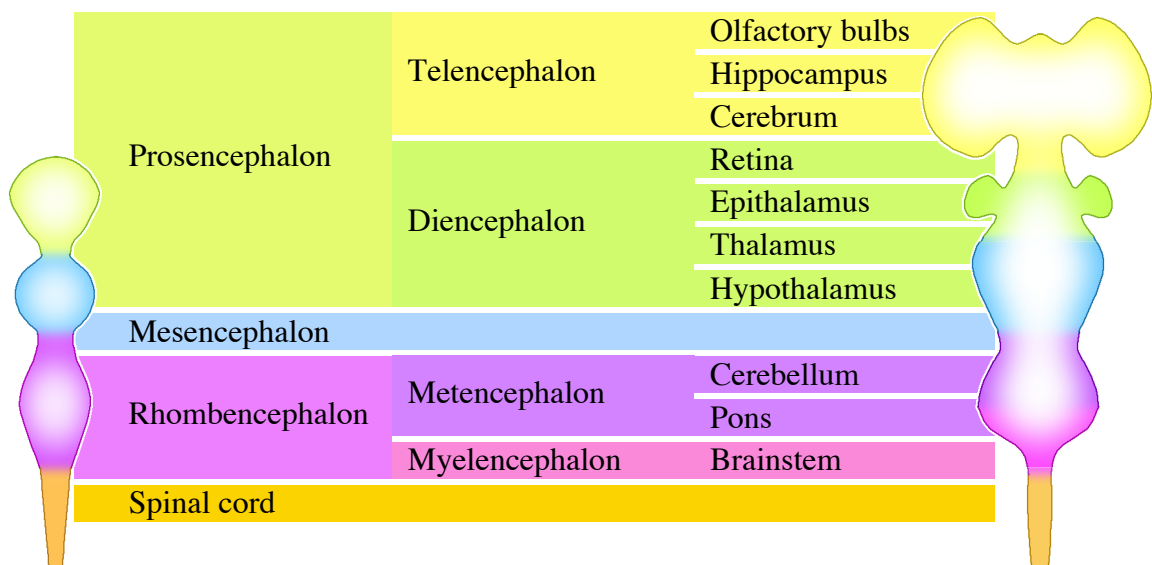
Introduction

Embryogenesis of the mouse central nervous system: an overview

Neural tube formation

Neural tissue is derived from the neural plate, a region of dorsal ectoderm with a columnar cellular phenotype which, after gastrulation, thickens and rises at its borders, invaginates and closes dorsally to form a hollow cylinder, the neural tube (Gilbert 7th edition, 2003). Cells at the interface between the dorsal neural tube and the overlying epithelium, called neural crest cells, acquire a migratory behavior and are bound to give rise to peripheral neurons, melanocytes and other cell types (Dupin et al., 2007).

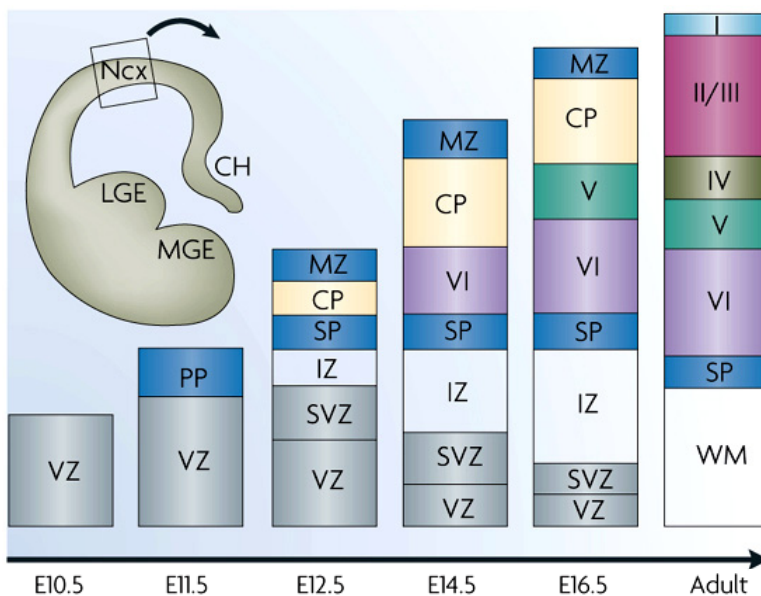
The neural tube will on the other hand give rise to the central nervous system, namely the brain, brainstem and spinal cord. Widening and folding its cylindrical shape, the neural tube develops flexures, defining initially three vesicles which outline the major subdivision of the brain: the forebrain, midbrain and hindbrain, while the posterior spinal cord does not swell into a vesicle. The three primary vesicles are later further refined into five secondary vesicles, each progressing to give rise to different elements of the central nervous system (Gilbert 7th edition, 2003).



- **Fig. 1** A schematic view of the different anatomical components and their embryological derivation, adapted from Gilbert 7th edition, 2003.

Cortical neuronogenesis

Neural progenitors are generated adjacent to the lateral ventricles, in the ventricular and later subventricular zone layers; they are bipolar in morphology, radially oriented and in contact with both the ventricular and pial surfaces. Newborn neurons can translocate to their final destination following a radial direction, thus remaining close to their generation place, and settle at distinctive radial levels, depending on their birthdates (Nadarajah and Parnavelas, 2002). This is how the laminar arrangement of the cortex is obtained, comprising six layers in the neocortex and three in the archicortex and paleocortex, which differ in terms of cell type and arrangement, projection targets and molecular markers (Aboitiz, 1999). This radial migration route is typically undertaken by the future pyramidal neurons, a large population of excitatory (glutamatergic) cortical neurons (Rash and Grove, 2006).



- **Fig. 2** The preplate (PP), the first neuronal structure to develop at E11.5, is split into the pial marginal zone (MZ) and the ventricular subplate (SP) by the incoming cortical plate (CP) neurons, which migrate radially from the proliferative ventricular zone (VZ) and subventricular zone (SVZ) up to the MZ. This gives rise to the layered structure of the cortex, in which deeper layers are older and more superficial ones younger. By adulthood, the proliferative layers are depleted and the overlying intermediate zone (IZ) has turned into white matter (WM). From Molyneaux et al., 2007.

However, newborn neurons can also follow a tangential migration route reaching a final destination that can be very distant from their birth place; clonally-related cells are therefore found dispersed throughout the cortex. It is the case, most prominently, of interneurons, inhibitory (γ -aminobutyric acid or GABA-ergic) neurons that are found intermingled and in contact with pyramidal neurons, but appear to be largely born outside the cortex,

in the medial and caudal ganglionic eminences of the subpallium (de Carlos et al., 1996) (Metin et al., 2006). Other migratory routes are known, such as the rostral migratory stream bringing lateral ganglionic eminence-born neurons to the olfactory bulbs, and the lateral cortical stream, giving rise to paleocortical neurons from the pallial-subpallial boundary (Marin and Rubenstein, 2001).

The combination of these mechanisms results in a varied population comprising, in each area, of clonally-related, locally-born cells together with cells that were born in a different area and have migrated to their final location, generally carrying functional and morphological differences that allow for a higher complexity. It is supposed that each neurogenetic compartment imparts unique characteristics to locally-born cells, providing a larger array of elements to cortical circuitry (Kiecker and Lumsden, 2005) (Molyneaux et al., 2007).

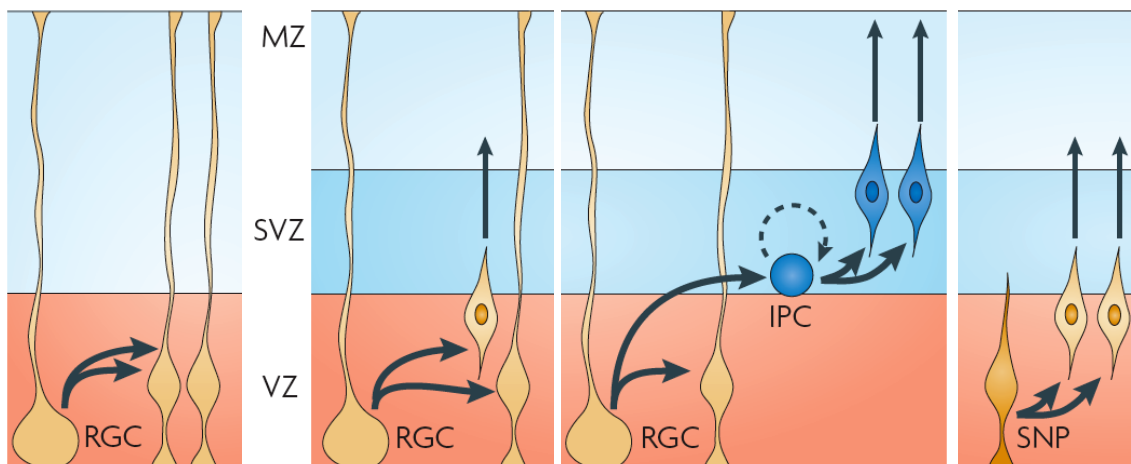
Developmental mechanisms

During embryogenesis, tissues must progressively acquire diversity in order to give rise to the variety of cellular identity, tissutal behavior and system function found in the mature organism. The undifferentiated primordium must therefore be able to partition itself and undertake varied morphogenetic routines in order to generate anatomical and functional differences. This partitioning mechanism can in turn be iterated, in order to sub-divide territories and generate further diversity in specification.

Cellular events

Cell cycle regulation

Growth, at the level of tissues, organs and the organism as a whole, is the most apparent event of embryogenesis. It necessarily implies a sustained proliferation at the cellular level, but modes and time of proliferation are also regulated and coordinated by developmental cues. The time of maintenance of a proliferative state and the duration of cell cycle determine the number of mitoses a progenitor goes through, and therefore its clonal expansion; it appears that the regulation is largely exerted at the level of G1



- Fig. 3 Several proposed proliferation modes in cortical neuronogenesis. Radial glia cells (RGC) can divide symmetrically (a) or asymmetrically, yielding another RGC along a postmitotic neuron (b) or an intermediate progenitor (IPC), still able to proliferate for a limited number of cycles but very restricted (perhaps unipotent) in its differentiation choices (c). Terminal differentiative divisions seem to arise from short neural precursors (SNP), no longer in contact with the pial surface. MZ, marginal zone; SVZ, subventricular zone; VZ, ventricular zone. Adapted from Dehay and Kennedy, 2007

phase, whose duration correlates with the progression of differentiation: self-renewing cells show a shorter cell cycle than differentiating ones (Dehay and Kennedy, 2007).

The proliferation of neuroblasts can occur in symmetrical and asymmetrical fashion, with symmetrical stem cell divisions being more frequent in early neuronogenesis to be later replaced by asymmetrical self-renewing and finally symmetrical differentiative divisions; additionally, transitional steps can be found such as intermediate progenitors (Kriegstein et al., 2006). Moreover, areal expansion can be obtained not only with an inducing signal, but also with a localized proliferative signal acting on already-specified cells. The exit from cell cycle is furthermore regulated as it is often tied to specification and/or differentiation.

Programmed cell death

The elimination of unnecessary cells is a natural process in development and was indeed discovered in *C. elegans* embryogenesis (Ellis and Horvitz, 1991); it has afterwards been recognized as an extremely common developmental event, used to create hollow structures, separate digits and, in the central nervous system, weed out excess cells (Baehrecke, 2002) (Meier et al., 2000). It has been repeatedly found that in late development, correct axonal targeting is necessary to provide neurons with life-maintaining signals; therefore, a higher number of neurons than necessary must be produced at the beginning, so that misrouted ones can be eliminated (Raff et al., 1993). However, an earlier apoptotic mechanism must take place during neuronogenesis, as shown by the phenotype of Caspase 9 knock-out embryos, in which the apoptotic pathway is largely blocked: by E13.5, gross alterations of prosencephalic development are apparent, with thickened ventricular walls and virtually absent ventricular cavities (Kuida et al., 1998).

Adhesion and migration

Different adhesion properties underlie tissue dynamics and are instrumental to the morphological events of embryogenesis; as an example, the folding and closure of the neural tube relies on the expression of the adhesion molecule n-cadherin instead of e-cadherin which is instead typical of the epithelial part of the ectoderm. This, together with a change in cell shape that causes the tissue to fold inward, is necessary for the

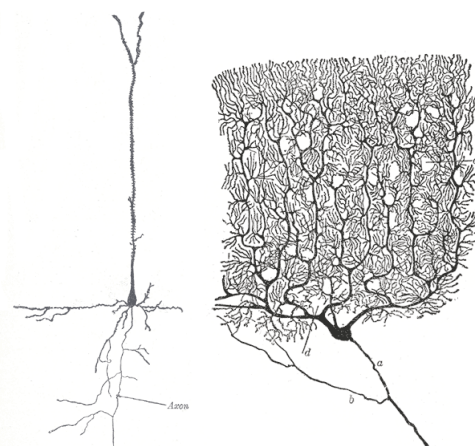
detachment of the neural plate borders from the adjacent epithelium; in fact, this event is disrupted if the epithelium is instructed to express n-cadherin along e-cadherin (Fujimori et al., 1990).

Cell adhesion and migration is necessary also for the correct positioning of cells within a developing tissue or organ. The cerebral cortex, which is characterized by a laminar structure, takes advantage of a radial mode of migration to dislocate neurons born from the same layer (along the ventricular surface) to different depths within the overlying cortical plate (Nadarajah and Parnavelas, 2002). Adhesion molecules must then be regulated according to positional information in order for the migrating cells to detach from the radial glia scaffold and localize in the correct layer; the molecule reelin, expressed by layer-1 Cajal-Retzius neurons, is fundamental in relaying layer information to migrating neurons (Forster et al., 2006), as in the absence of this protein mouse cortex shows layer disorganization and inverted stratification (Gleeson and Walsh, 2000).

Neurons also show other modes of migration, as for example the chain-like, non-radial migration that is employed by neurons whose final location is distant from their birthplace, such as subpallial-born interneurons. Molecular cues in this case are less clear; it appears that the same molecules that are in charge of area patterning can provide positional information to migrating cells (Osterfield et al., 2003).

Differentiation

Differentiation of a neuron requires the emission and guidance of the axon and development of one or more dendrites, the acquisition of the ability to synthesize and secrete of one or more neurotransmitters and finally to generate an electrical activity. Differences in all these characteristics are found among different classes of neurons and are fundamental to attain a correct neuronal network establishment and function: as an example, the major neuronal compo-



- **Fig. 4** Pyramidal neuron and Cajal-Retzius cell, after Ramón y Cajal. a. Axon. b. Collateral. c and d. Dendrons. Adapted from Gray, 1918

nents of the cerebral cortex, pyramidal neurons and interneurons, differ in terms of morphology (pyramidal neurons have a typical structure, with a triangular soma, a single vertical apical dendrite and several basal dendrites, that interneurons lack), projection target (long-range intracortical, subcortical and subcerebral structures as opposed to local connections), secreted neurotransmitter (glutamate for the former, GABA and various neuropeptides for the latter) and therefore synaptic effect (pyramidal neurons are excitatory and interneurons inhibitory), migration mode (radial versus tangential) and many molecular determinants (Molyneaux et al., 2007).

At the time of cell cycle exit, neuronal features are already defined in the form of specific transcriptional patterns, regulated by spatial and temporal cues received at the progenitor stages (Salie et al., 2005); however, interactions between the maturing post-mitotic neuron and the surroundings, most notably at the level of the axon's growth cone, can give rise to signals that act retroactively on the neuronal body and further define cellular identity and survival (Hippenmeyer et al., 2004).

Regulatory elements

Transcription factors

The activation of the coordinated array of cellular events that must take place in each partition is regulated by a number of transcription factors, whose mutual interplay and interaction with external cues is necessary to carry out the developmental fate of the cell expressing it and in turn to localize, define and mould the region in which they take effect.

Among the principal transcription factors involved in the development of the central nervous system there are homeodomain proteins, including empty spiracle homeobox (Emx), distal-less homeobox (Dlx), LIM homeobox (Lhx) and GS homeobox (Gsh) proteins, and basic helix-loop-helix factors (bHLHs), including Neurogenin, Olig and E-type proteins (Bertrand et al., 2002). Genes encoding for these factors and the molecular circuitries they are involved in are conserved across a wide evolutionary spectrum, as a large number of genes involved in developmental pathways have their homologues in *Drosophila* and have been first identified in that model through mutagenesis screenings, only to find that their homologues (often several of them) in vertebrates also carry out patterning functions. Such is the case, for example, of *Drosophila*'s

empty spiracles (*ems*) and orthodenticle (*otd*) genes, whose mammalian counterparts are the members of the *Emx* and *Otx* families, which outline areal identities in the brain (Finkelstein and Boncinelli, 1994).

Transcription factors can act by regulating several aspects of neuronal fate. They may promote a proliferating progenitor state, as is the case with the *Hes* and *Id* families of bHLH factors (Ross et al., 2003). They may promote exit from cell cycle and pan-neuronal as well as subtype-specific differentiation programs: this is the case with proneural genes such as *Ngn1*, *Ngn2* and *Mash1* (Bertrand et al., 2002). In turn, each regional identity is tightly correlated to a specific pattern of transcription factor expression; as an example, within the telencephalon *Emx1*, *Emx2* and *Pax6* are typically expressed in the pallium, while *Dlx5* and *Gsh2* are subpallial genes (Schuurmans and Guillemot, 2002). Within each region, different expression patterns are also observed, underlying reciprocal interaction loops; *Emx2* and *Pax6*, both expressed in the cortical primordium, have opposite gradients, high caudomedial to low rostralateral and reverse, respectively (Mallamaci and Muzio, 2000).

Morphogens

Regional information that is to be acquired by neighboring cells is relayed through soluble factors that can generate a gradient active over long-range distances (i.e. several cell diameters). Such a molecule can elicit different sets of intracellular events through a series of threshold-regulated responses; consecutive domains are thus defined and their distribution is a function of the distance from the signaling source (Osterfield et al., 2003). A molecule with these characteristics is defined as a morphogen and tissue that is able to secrete a morphogen and induce several cellular fates in neighboring regions is named an organizer (Rhinn et al., 2006). Some morphogens active in CNS patterning are Bone Morphogenetic Proteins (BMPs) (Liu and Niswander, 2005), Fibroblast Growth Factors (Fgfs) (Mason, 2007), Wingless analogs (Wnts) (Ciani and Salinas, 2005) and Sonic Hedgehog (*Shh*) (Fuccillo et al., 2006).

Morphogens provide positional information to the cortical map, often via dose-dependent regulation of transcription factor genes nested around their sources, as well as by interacting with one another in order to define and restrict each other's domain of influence (Ohkubo et al., 2002). Moreover, they may directly regulate cell cycle pro-

gression (Cayuso and Marti, 2005), stem cell maintenance (Aubert et al., 2002), axon growth (Sanchez-Camacho et al., 2005) and guidance (Bovolenta, 2005).

Coordinates

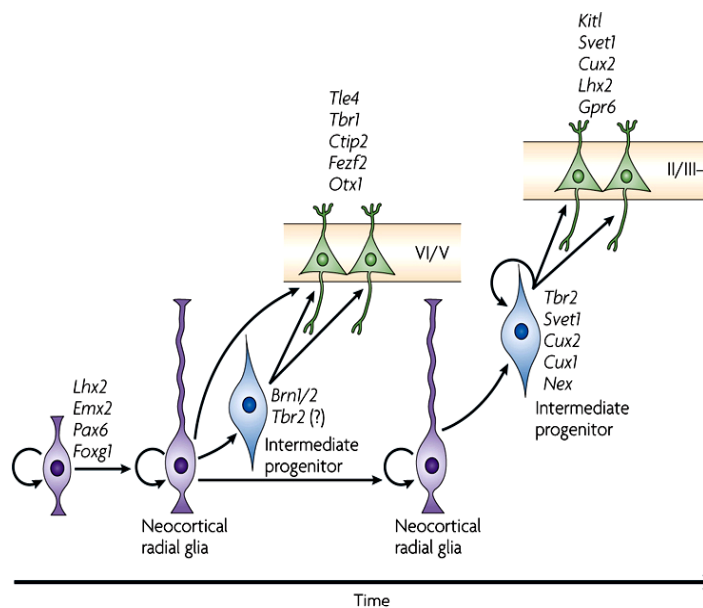
Time

Developmental events, being part of a progressive, finely-tuned process, need a strict timing control in order to harmonize with one another and bring about sequential passages; one such sequential mechanism is involved in layer specification in the cortex, where neuroblasts leaving the proliferative layers at subsequent times migrate radially to settle into progressively more external layers, each with a different cellular identity, depending on the neuron's birthdate (Kriegstein et al., 2006). As to the codification of time, two mechanisms seem to be in action: the response to concentration of a transacting signal, which accumulates or decreases in a time-dependent manner; and an intrinsic "cell-cycle counter" based on epigenetic markers (Caviness et al., 2003).

Position

Developmental routines must be activated within a tissue in the correct spatial map, both in relation to the rest of the embryo and relatively to its own borders. Thus, positional identity may be acquired from external clues emanating from adjacent tissues, as well as from sources that are part of the tissue itself (Molyneaux et al., 2007).

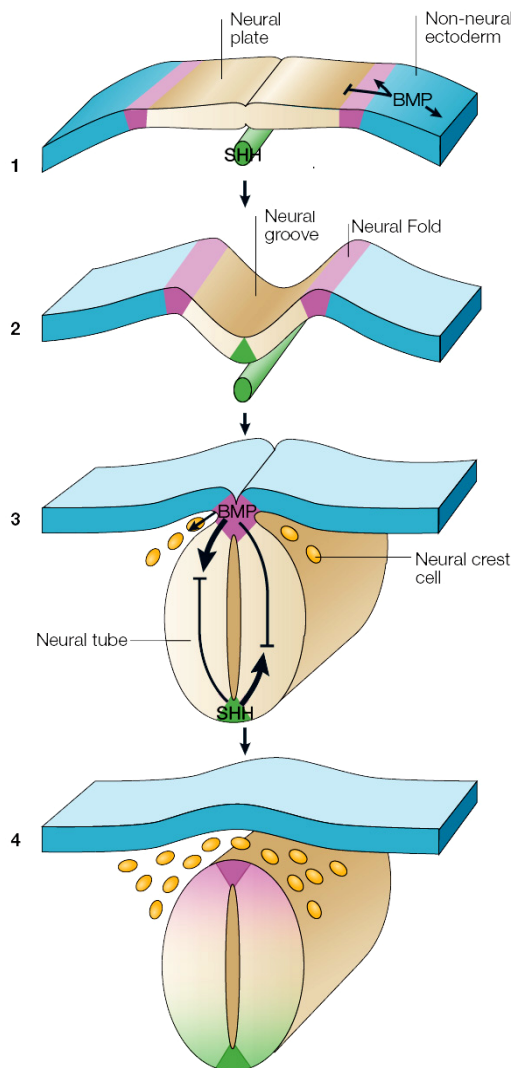
Defining the major coordinates involves more than one signaling center; infor-



- **Fig. 5** A model of the interaction between genes encoding positional information (gradient-expressed transcription factors, i.e. Emx2 and Pax6) and temporal information (early, deep-layer bound transcription factors such as Brn1 and 2, and late, superficial-layer bound ones such as Svet1 and Cux2) in defining the distinct molecular signatures of differentiating neurons. From Molyneaux et al., 2007.

mation from each axis is then available to individual cells allowing for the activation of different threshold responses.

Dorsoventral axis



- **Fig. 6** A schematic view of the neural tube formation and the signaling sources involved. Notochordal SHH and ectodermal BMP sources induce the formation of the roof and floor plate respectively, with opposite and mutually-repressing SHH and BMP signaling establishing a molecular patterning across the dorsoventral axis of the neural tube.

Within the neural tube, the dorsoventral patterning relies initially on external signals: at the earliest stages of neural tube formation, the neural epithelium is constrained between BMP-secreting tissue, defining the edge between neural and non-neural epithelium; at the same time, an external, mesodermic source, the notochord, secretes the morphogen Sonic Hedgehog (Shh), which is in turn also expressed in the adjacent midline neural tissue. The invagination of the neural fold brings the BMP-expressing epithelial borders together, while the closure of the neural tube exposes the ventralmost (previously midline) tissue to signals from the notochord and the dorsalmost (previously marginal) to BMP-secreting epithelium. BMP function is further regulated by inhibitors, such as noggin and chordin, secreted by ventrally-placed mesoderm (Patten and Placzek, 2002) (Lupo and Harris, 2006). The adjacent neural tissue begins in turn to express the same molecules, and a double, divergent dorsoventral gradient is established which is known to regulate the arrangement of neuronal identity along the dorsoventral axis, thanks to a multiple-threshold response which was observed in vitro, where the administration of different

doses of Shh induced the differentiation of neuroblasts into different classes of ventral neurons (Liem and Jessell, 2000).

Anteroposterior axis

The anteroposterior axis is on the other hand patterned by intrinsic cues emanating from the rostral and caudal end of the neural plate and relies on several secreted molecules: anterior identity, which appears to be default, is counteracted by a posteriorizing signal based on Fgfs, Wnts, Nodal and retinoic acid (Gamse and Sive, 2000). After neural tube closure, signaling centers arise to maintain and refine the anteroposterior axis: the anterior margin of the neural plate (anterior neural ridge, ANR), the zona limitans intrathalamica (ZLI, between prosomeres 2 and 3) and the midbrain-hindbrain boundary (MHB). Both the ANR and the MHB secrete molecules of the Fgf family, most prominently Fgf8 which thus appears to have a stereotyped role in AP (anteroposterior) patterning (Rhinn et al., 2005). Wnts and their antagonists, such as Dickkopf1, Cerberus and Frizzled-related proteins, are also involved in anteroposterior axis definition, with Wnt function yielding a posterior fate while antagonists are expressed anteriorly (Ciani and Salinas, 2005). Finally, in the middle, at the ZLI, there is a prominent source of Shh (Fuccillo et al., 2006).

General patterning mechanisms

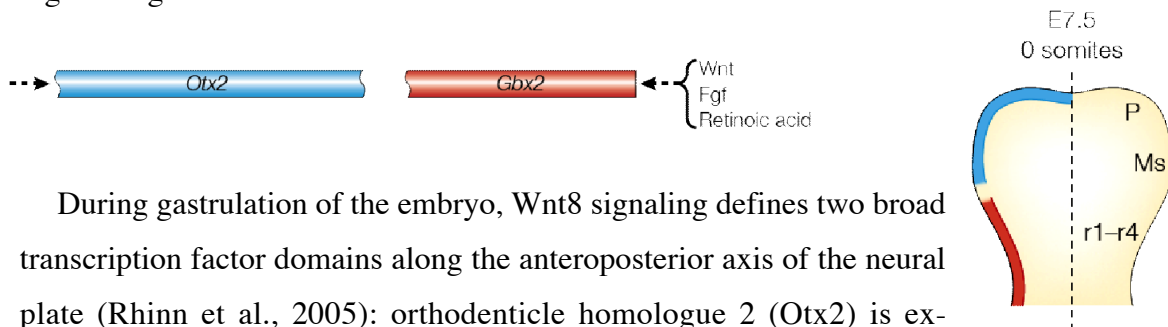
Molecular events that control CNS patterning and cortico-cerebral arealization in particular show a variety of actors, interactions and peculiarities; however, certain programs appear to be frequently employed and can be used to outline a model pattern formation mechanism.

The isthmus organizer, one of the first patterning centers to be identified and one of the best characterized, has been used to provide molecular examples of the general mechanisms posited.

For references, see Kiecker and Lumsden, 2005; Raible and Brand, 2004; Wurst and Bally-Cuif, 2001; Rhinn et al., 2006. All figures adapted from Wurst and Bally-Cuif, 2001.

Adjacent transcription domains

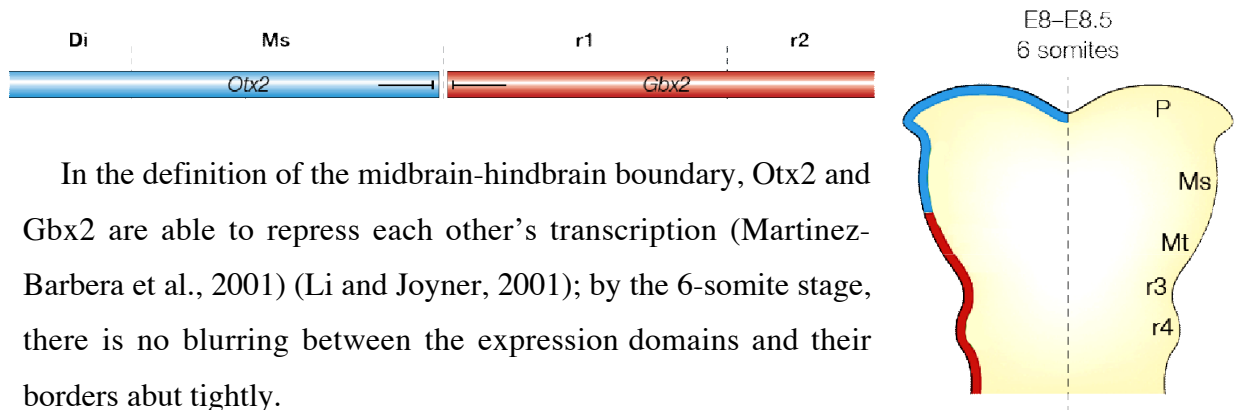
Primary patterning, established by early signals on the tissue at the time of its formation, defines adjacent morphogenetic fields at the molecular level. Differential gene expression on broad, partially overlapping domains is the substrate for subsequent patterning events that occur around the borders of the field and allow for further partitioning and regionalization.



During gastrulation of the embryo, Wnt8 signaling defines two broad transcription factor domains along the anteroposterior axis of the neural plate (Rhinn et al., 2005): orthodenticle homologue 2 (*Otx2*) is expressed rostrally, while gastrulation brain homeobox 2 (*Gbx2*) more caudally (Broccoli et al., 1999). At the 0-somite stage (E7,5), the border between the expression domains is blurred and partially overlapping, but a first level of regional specification is already in place, as the *Otx*-expressing region is bound to give rise to the forebrain and midbrain, while the *Gbx2*-expressing region will develop into hindbrain. The boundary between them corresponds anatomically to the isthmus, a narrowing of the neural tube at the border between mesencephalon and metencephalon.

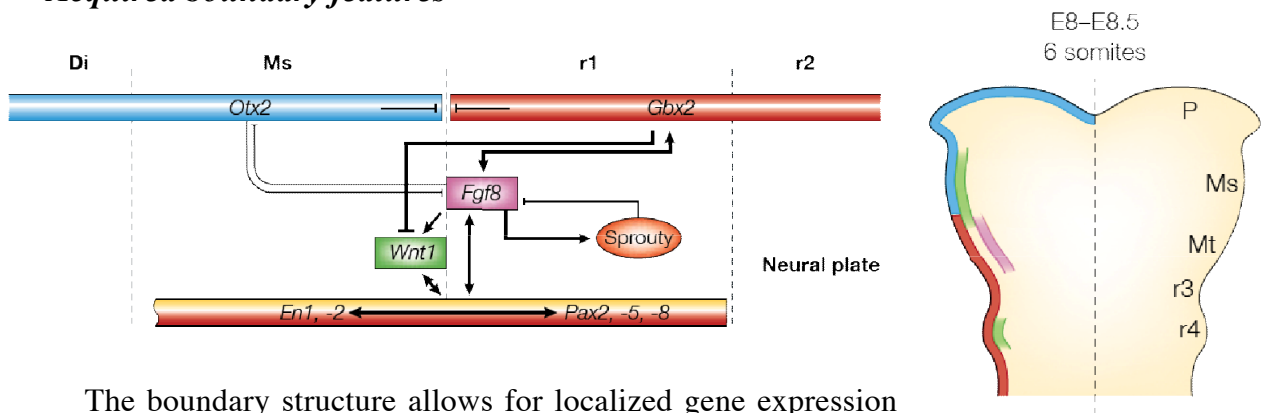
Boundary definition

Transcription factors expressed in the same region are generally connected by mutual regulation loops, which refine the localization of each. In particular, a partial, graded overlap can be sharpened by means of a mutual repression, thus establishing two populations of cells expressing one or the other exclusively, separated by a sharp boundary.



In the definition of the midbrain-hindbrain boundary, *Otx2* and *Gbx2* are able to repress each other's transcription (Martinez-Barbera et al., 2001) (Li and Joyner, 2001); by the 6-somite stage, there is no blurring between the expression domains and their borders abut tightly.

Acquired boundary features



The boundary structure allows for localized gene expression which is refined through complex regulatory loops; in particular, a secreted molecule can be expressed locally if it is secreted by one territory and induced by a product of the other territory. This restricts the supporting loop to the frontier and can be further spatially refined with inhibitory molecules acting outside of the boundary region. The secreted molecule's activity can be additionally regulated by spatially limiting the expression of its receptors and/or desensitizing the adjacent fields via appropriate negative feedback circuitries.

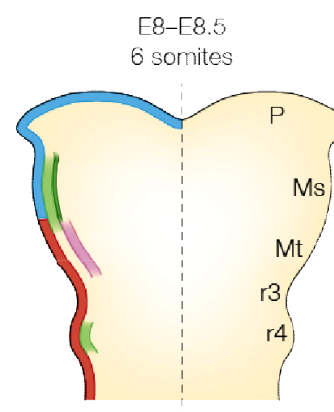
Wnt1 and *Fgf8* are secreted by the *Otx2* and *Gbx2*-expressing domains, respectively,

but they also directly and indirectly (through the induction and interaction of other transcription factors of the Engrailed and Pax families) stimulate each other's production; this local expression outlines the boundary and adds a new element in spatial patterning. Three fibroblast growth factor (Fgf) receptors, Fgfr1, Fgfr2 and Fgfr3, are present across midbrain and hindbrain, at the level of the boundary: the latter two are sharply downregulated, leaving Fgfr1 alone to account for Fgf function in this region, which can therefore differ in its intracellular response (Saarimaki-Vire et al., 2007). Inhibitors of Fgf signaling such as Sprouty, which can block the Fgf-8 self-inducing loop if it falls under a certain threshold, are also present across the boundary area to limit the spreading of Fgf8's expression domain (Minowada et al., 1999).

Compartment constraint

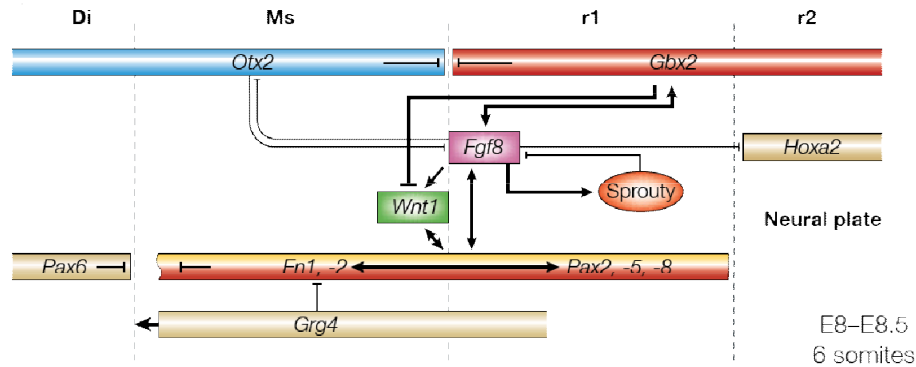
The molecular definition of a boundary can affect its tissutal features by activating intracellular signaling cascades as well as subsequent gene transcription; the boundary region can therefore be recognized through the expression patterns of such genes and acquire local characteristics, such as a reduced proliferation rate and differentiation (Bally-Cuif and Hammerschmidt, 2003) or cell surface molecules. In particular, local expression of cadherin and ephrin expression has been found to take place, resulting in a homotypical adhesion preference: this induces a cell sorting that "smoothens" the surface of the boundary. In fact, if artificially mixed, cells from different regions (i.e. pallium and subpallium) are able to segregate homotypically (Götz et al., 1996). This can result in lineage restriction of a region, defined then compartment, as no cells from neighboring areas can intermingle with them and participate in tissue construction (Inoue and Tanaka, 2001).

Within the midbrain-hindbrain boundary, a local expression of e-cadherin (Shimamura et al., 1994) and PB-cadherin (Kitajima et al., 1998) appears to superimpose with the level of Wnt1, as is observed in other Wnt1-expressing regions of the CNS; this could also account for the particular structure of the isthmus, which is anatomically recognizable as a narrowing of the neural tube.

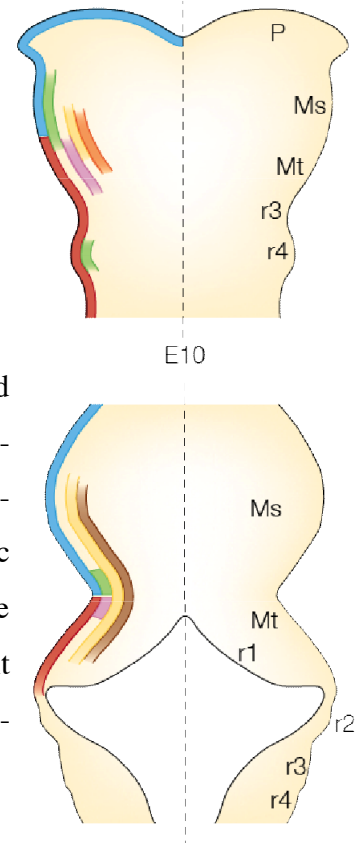


Secondary patterning

The diffusion of soluble factors secreted locally by the boundary region can in effect define a new organizer; such a secondary patterning center can induce gradient-dependent responses on both sides of the boundary, but the pre-existing differences in the intracellular signaling cascades can cause the different compartments to give rise to completely different responses.



The secondary patterning function acquired by the midbrain-hindbrain boundary appears to be largely mediated by Fgf8; rostrally, it is necessary to polarize the dorsal mesencephalon, which will give rise to the tectum; caudally, it induces the adjacent tissue to acquire cerebellar fate. Ectopic Fgf8 expression can lead to the ectopic induction of gene patterns such as tectum polarization and cerebellar markers (Lee et al., 1997). In addition, Fgf8 cooperates with Shh, which defines the dorsoventral orientation, in regulating neuronal phenotypes: i.e., dopaminergic neurons of the substantia nigra develop just rostrally of the MHO, in a ventral position, and their location is dependent on Shh for the dorsoventral position and Fgf8 for the anteroposterior position (Ye et al., 1998).



Guidance and barrier function

Along with the patterning role they often take up, other functions are typical of boundary regions and are connected both with the secretion of morphogens and the sharp change in gene expression pattern they exhibit: secreted molecules can be used as

chemoattractants or repulsants (Charron and Tessier-Lavigne, 2005), while regionalized gene expression allows for expression of anchored repulsive and attractive factors, effectively creating barriers to axonal growth. Boundaries can then guide the migration of incoming axons, which have been proposed to use the surface between gene expression domains as a localizing cue and scaffold (Sanchez-Camacho et al., 2005), and also contribute positional information to tangentially migrating cells in the form of soluble signaling molecules as well as permissive and non-permissive substrates for adhesion and migration (Testaz et al., 2001) (Jarov et al., 2003).

The axonal projection of the trochlear nerve use the midbrain-hindbrain boundary as their cue to cross the brain from dorsal to ventral and might receive positional information from the same molecules that take part in the boundary development itself, such as Wnts (Lyuksyutova et al., 2003) or Fgf8 (Irving et al., 2002), or the gene patterning of the region could localize the expression of repellent guidance molecules such as semaphorin Sema3F and neuropilin2 used by the axons in trajectory guidance (Watanabe et al., 2004).

Patterning regions in the development of the rostral CNS

Several boundary regions with patterning functions have been characterized in the central nervous system of mouse and their function appears to be largely preserved throughout vertebrate evolution (Molnar et al 2006). A schematic view of the localization, features and function of organizer regions characterized in the mouse central nervous system is presented here.

For references, see Ragsdale and Grove, 2001; Rhinn et al., 2006; Rash and Grove, 2006.

Dorsoventral axis

Floor plate and roof plate

In the early events of neural tube formation, external sources of Shh ventrally and BMPs and Wnts dorsally signal the dorsoventral axis to the neuroepithelium. These morphogens are in turn expressed by the adjacent neural tissue, so that Shh is secreted by the ventralmost part of the neural tube and BMPs and Wnts by the dorsalmost part (Lupo and Harris, 2006). These signaling centers, in which neuronogenesis is largely absent or very delayed (Bally-Cuif and Hammerschmidt, 2003) are termed floor and roof plate respectively and provide the early area map with dorsoventral positional information.

As embryogenesis proceeds, Shh expression spreads into the developing medial ganglionic eminence (MGE), which arises from the ventromedial domain of the neural tube, identified by the expression of NK2 homeobox 1 (Nkx2.1) (Fuccillo et al., 2006), while BMPs and Wnts diffuse into the presumptive archicortex, which arises from the dorsalmost neural tube, identified by the expression of Emx1 and Emx2 (Shimogori et al., 2004).

Anteroposterior axis

Anterior Neural Ridge

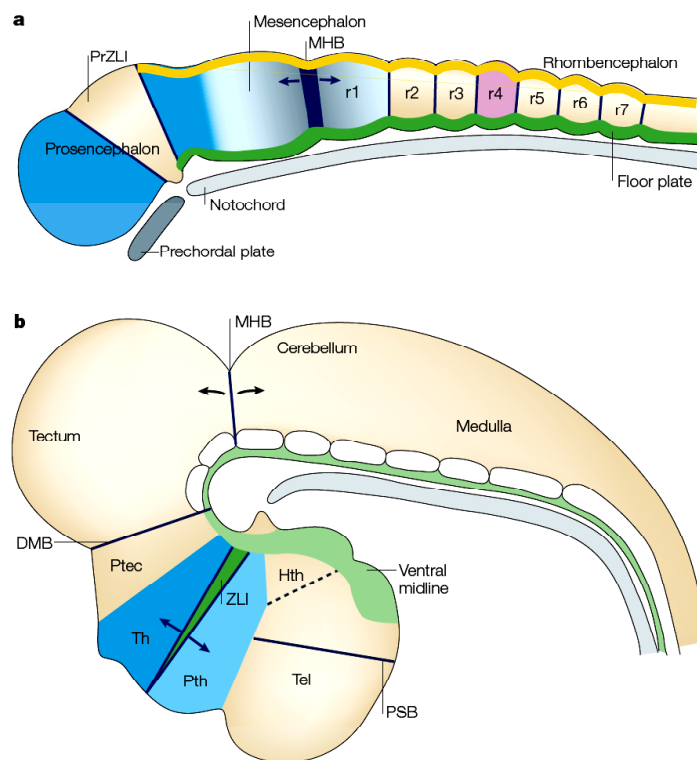
Forms at the anterior limit of the cortical primordium; its signaling function during corticogenesis is mediated by Fgf8 and Fgf15.

The ANR has the fundamental role of relying anteroposterior position information to

the developing telencephalon; in fact, an artificial source of Fgf8 placed in the posterior telencephalon causes a shift towards anterior fates, which is oriented as a mirror image of the native anterior telencephalon (Shimogori et al., 2004). Along its role within the cortex, the ANR also interacts with neural crest cells migrating rostrally to provide the developing telencephalon with cranial structure and vascularization and is therefore necessary for the correct formation of the entire head and facial structure (Creuzet and Martinez, 2006).

Isthmus

Forms at the boundary between the metencephalon and mesencephalon, expressing Wnt1 rostrally and Fgf8 caudally as signaling molecules. (Wurst and Bally-Cuif, 2001) Typical gene expression patterns are characterized by a rostral restriction of Otx2 while Gbx2 is expressed caudally, (Raible and Brand, 2004) with a defining and positioning role for the organizer itself; in turn, the signaling function is necessary to define the antero-posterior axis of the adjacent regions. Fgf8 appears to mediate most of the boundary's function,



- **Fig. 7** A schematic representation of patterning centers in vertebrate development, using avian brain as an example. SHH signaling is represented in green (along the floor plate/ventral midline and in the ZLI), Fgf signaling in dark blue/purple (MHB, rhombomere 4, also in the anterior neural ridge, not shown) and Bmp signaling in orange (roof plate). Boundaries with a recognizable morphology and cell compartment restriction are located at the pallial-subpallial boundary (PSB), adjacent to the zona limitans intrathalamica (ZLI), at the diencephalon – midbrain boundary (DMB) and between adjacent rhombomeres. Hth, hypothalamus; Ptec, pretectum; Pth, prethalamus; Tel, telencephalon; Th, thalamus. Adapted from Kiecker and Lumsden, 2005.

as these can be vicariated by Fgf8-soaked beads; Wnt1 might cooperate by acting primarily on proliferation rate regulation, thus participating in controlling population sizes after than their specification (Panhuysen et al., 2004).

Zona Limitans Intrathalamica

Forms at the boundary between the thalamus (formerly dorsal thalamus) and prethalamus (formerly ventral thalamus) (Scholpp et al., 2007). It splits the anterior neural plate into two distinct domains, responding to Fgf signaling coming from ANR and isthmus in different fashions: the rostral domain expresses Forkhead box G1 (Foxg1) and differentiates as telencephalon, the caudal one expresses Engrailed 2 (En2) and differentiates as mesencephalon (Garcia-Lopez et al., 2004). Moreover, signals coming from the ZLI induce Gbx2 and Dlx2 expression in thalamus and prethalamus, respectively. Although several signaling molecules are expressed by this structure, such as Wnts, Fgfs and Shh, its function appears to be mediated mostly by Shh, which is necessary and sufficient for thalamus and prethalamus induction (Kiecker and Lumsden, 2004). However, Wnts are also necessary to maintain thalamus differentiation, while the prethalamus is not affected by their removal: this may underlay a role in inducing a competence difference between the two areas which would be necessary for a different response to the same signaling molecule. It should be remembered that Shh has generally a ventralizing function, being expressed along the floor plate of the neural ridge and maintaining such a ventral domain of expression along the neural tube; only in the ZLI, it is possible to find a dorsal expression of Shh (Lim and Golden, 2007).

Area patterning of the cerebral cortex

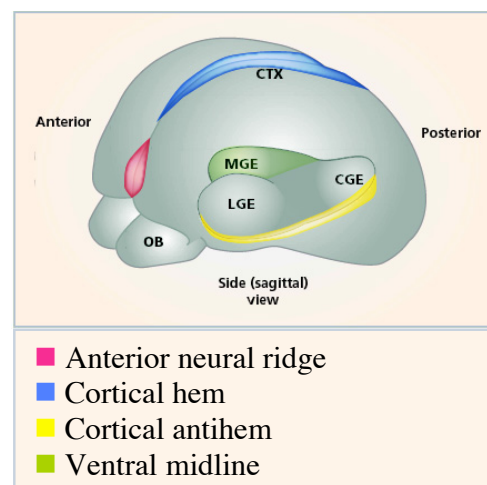
The adult cortex is characterized by sharply-bordered areas with anatomical and functional differences (although not, apparently, by specific individual gene expression: it is rather patterned by different superimposed domains of a number of genes); the origins and mechanism of development of this areal pattern have been debated (O'Leary et al, 1989). It is now clear that the first spatial identities are encoded in the cortical tissue already at the time of its generation, in the form of specific gene expression patterns. Signaling sources located in different points on the perimeter of the developing cortex

then take on the role of delineating positional information; subsequent transcriptional cascades and interactions are responsible for the refinement of the areal map, the sharpening of borders between areas and the correct connections with afferent axons, which in turn contribute to the fine-tuning of their targets (Grove and Fuguchi-Shimogori, 2003) (Rash and Grove, 2006) (Guillemot et al., 2006).

Cortical boundaries

Cortical hem

Forms at the boundary between the hippocampus, the medialmost part of the cortex, and the non-neural choroid plexus, located along the midline of the embryo. As the dorsal midline of the telencephalic vesicle invaginates, giving rise to the two telencephalic hemispheres, the adjacent neuroepithelium gets increasingly thinner, while a secreting epithelium is found between the telencephalic hemispheres, which matures into the choroid plexus. The thinning neuroepithelium, which has disappeared by the time of birth, has in turn signaling functions and is known as the cortical hem. Consistently with its dorsal origin, the cortical hem's function

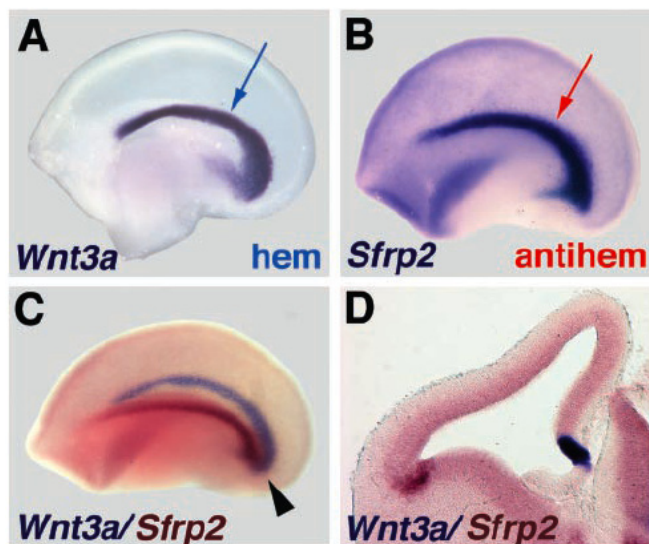


- **Fig. 8** Localization of the known patterning centers affecting cortical arealization.

Ctx, cortex; LGE, lateral ganglionic eminence; MGE, medial ganglionic eminence; CGE, caudal ganglionic eminence; OB, olfactory bulb. Adapted from Corbin et al, 2001.

is mediated by Wnt signaling: within the telencephalon, genes *Wnt3a*, *5a* and *2b* are found exclusively in this structure (Grove et al., 1998). Wnt signaling from the hem is necessary for hippocampal formation, presumably by expanding an already specified population of cells through proliferative signals (Grove and Fukuchi-Shimogori, 2003). Molecules of the BMP family are also secreted and contribute toward the segregation of medial neuroepithelium and choroid plexus epithelium (Shimogori et al., 2004). The formation of the cortical hem is dependent on LIM-homeodomain factors, in particular *Lhx2* and *Lhx5*, which show complementary distribution (throughout the cortex except

the hem for Lhx2, only the hem for Lhx5) and function (loss of Lhx5 blocks the formation of hem and choroid plexus, with a disruption of hippocampal morphology; loss of Lhx2 expands dramatically the hem and choroid plexus at the expense of the cortex) (Zhao et al., 1999) (Monuki et al., 2001).



- **Fig. 9** Molecular localization of cortical patterning centers as revealed by whole-mount in situ hybridization. From Assimacopoulos et al., 2003.

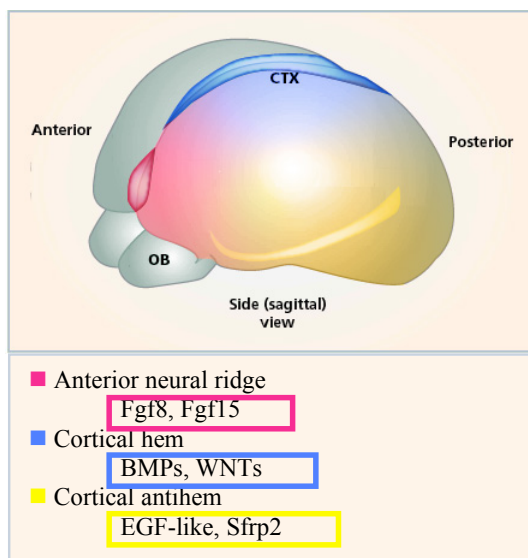
cases of EGF-secreting patterning centers (Assimacopoulos et al., 2003). Moreover, it is likely to antagonize Wnt signaling coming from the hem, via the secretory product Sfrp2, and to contribute to Fgf signaling, via expression of Fgf7. Its location suggests that it may interact with both the hem and commissural plate to establish positional coordinates for cortical arealization.

Commissural Plate

Forms as a derivate of the ANR, at the closure of anterior neural folds. Its function is also mediated by Fgfs, such as Fgf8, Fgf17 and Fgf18 and controls anterior regional fates in a similar manner to its predecessor ANR. It borders on the medioposterior margin with the cortical hem, which expresses a completely different set of morphogens connected with Fgfs by reciprocal inhibition loops (O’Leary et al., 2007).

Cortical anti-hem

Forms at the boundary between the pallium (cortex) and subpallium (basal ganglia), positioned as a “mirror image” of the cortical hem in respect to the cortex. Its signaling function seems to rely on a relatively infrequent secreted factor family for nervous system development, the epidermal growth factor (EGF) family; there are however other



- **Fig. 10** Morphogen gradients across the cortex. The superimposition of different families of signaling molecules allows for a different combination to be received by each portion of the cortical surface, encoding positional information in regard to the tissue's margins. Ctx, cortex; OB, olfactory bulb. Adapted from Corbin et al., 2001.

of the transcription factors involved have now been identified and their expression patterns characterized, which seem also to rely on opposing gradients to establish their respective domains (Mallamaci and Stoykova, 2006).

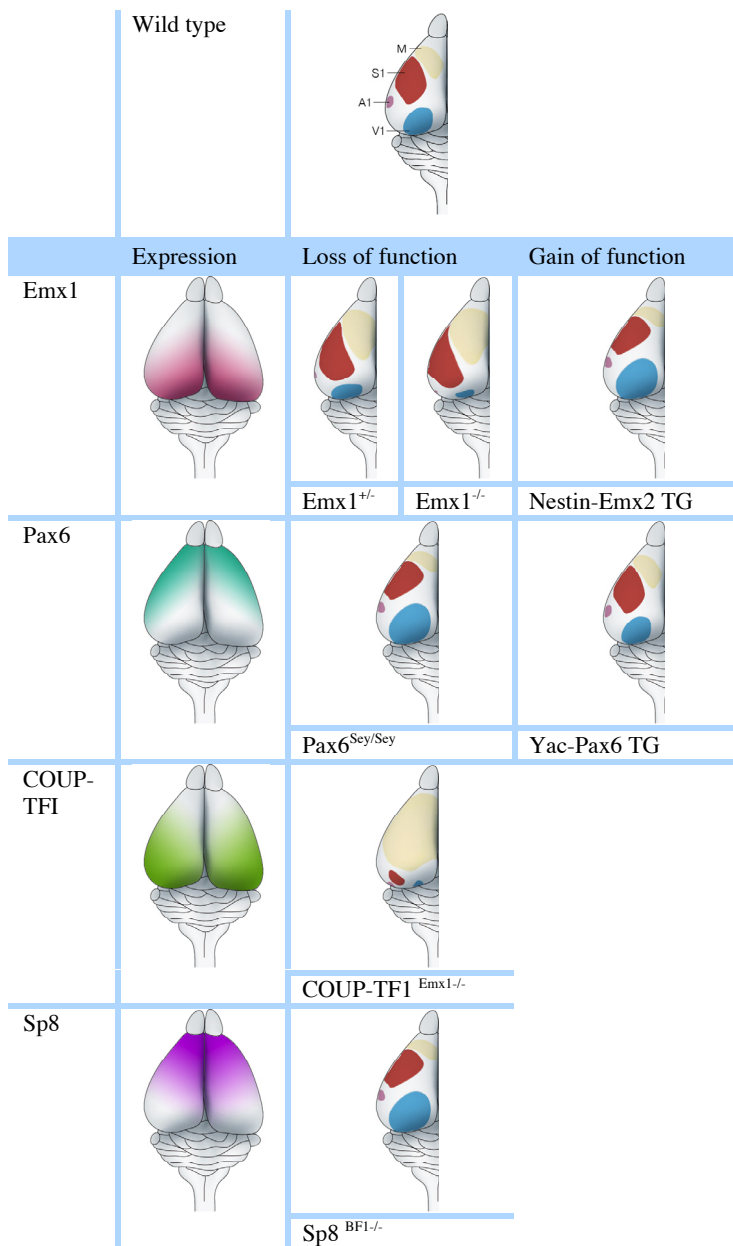
Emx2 and Pax6 (Muzio et al., 2002) (Bishop et al., 2000) have been characterized first and they exhibit a complementary distribution, high caudomedial to low rostro-lateral and opposite, respectively; COUP-TFI (Armentano et al., 2007) and Sp8 (Griesel et al., 2006), more recently studied, are expressed in a high caudolateral to low rostromedial and opposite, respectively. They interact with each other, as well as receiving information from morphogen gradients, to define their expression domain, through direct as well as more complex routes. For example, Sp8 expression is closely entwined with Fgf8 expression from the commissural plate, through reciprocal induction patterns; however, their effect on cortical arealization are contrasting, underlying distinct patterning mechanisms (Sahara et al., 2007).

Morphogen sources and axis definition

Patterning centers that exert their effect on the developing cortex are located at its margin: at the rostromedial pole, the commissural plate secretes Fgfs; caudomedially, the cortical hem secretes BMPs and Wnts; and laterally, the cortical antihem secretes EGFs. In addition, the MGE is a source of ventral Shh.

Spatial patterning transcription factors

Graded gene expression within the proliferating compartment induced by morphogen concentration has been found to regulate the relative size and position of cortical areas in the mature brain; some



- **Fig. 11** A summary of the expression patterns and observed phenotypes in loss and gain of function transgenic mice for putative arealization transcription factors. Pax6^{Sey} (Small eye) allele is an expressed, non-functional form of Pax6 protein with a less severe phenotype than the knock-out. COUP-TFI and Sp8 loss of function mutants were developed through Cre-lox technology, as knock-outs were not informative; Emx1 and BF1 promoters were used respectively to limit the loss of function to the cortical area. Adapted from O’Leary et al., 2007, Lopez-Bendito and Molnar, 2003.

When loss-of-function and gain-of-function experiments were performed, the relative position and size of cortical areas appeared to be affected, rather than cortical size, showing that their effect takes place after cortical specification; however, the removal of both Emx2 and Pax6 caused the loss of the cortex, which was specified instead to sub-pallial fates, underlining a role in corticogenesis of this gene pair (Muzio et al., 2002); the alterations were consistent with the gene’s expression pattern, thus demonstrating a real patterning function. Interestingly, when afferent (i.e. thalamocortical) connections were established, they often connected to the correct functional area, even if spatially shifted (O’Leary et al., 2007). This did not occur in COUP-TFI null mice, as several non-cortical structures were also altered; this, coupled with the perinatal mortality of these mutants, has made it necessary to engineer the gene out of

cortical neuroblasts (Emx1-expressing) only to show its patterning effect, which is characterized by a marked increase in frontal areas at the expense of caudal domains (Armentano et al., 2007).

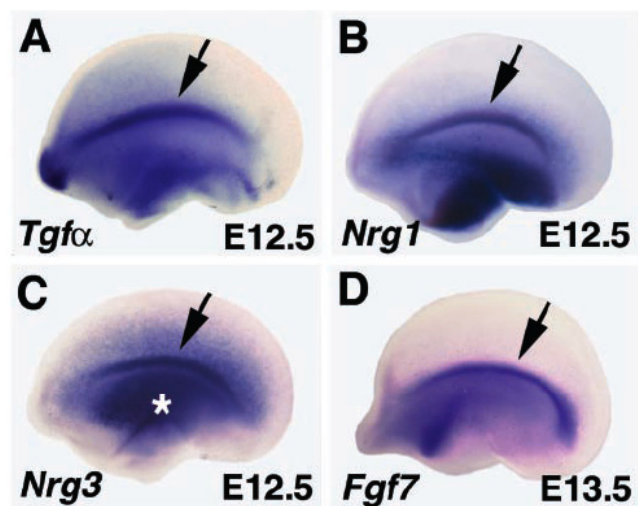
Corticostriatal boundary

Gene expression margins

A sharp border between gene expression patterns can be observed just ventrally to the sulcus between the cortex and the adjacent lateral ganglionic eminence. Several genes whose expression domains span the pallium such as Emx1, Tbr2, Ngn2 and Pax6, and the subpallium, such as Gsh1 and 2 and Mash1, show an abrupt downregulation along the boundary. Two such genes, Pax6 and Gsh2, are involved in mutual repression and appear to be instrumental in positioning the border itself (Toresson et al., 2000), as their expression overlaps at the putative boundary which is in turn sharpened; mutants lacking Pax6 or Gsh2 activity do not show the morphological and molecular determinants of the corticostriatal boundary; as such, gene expression domains are blurred and subpallial identity is shifted dorsally in the first case, while pallial identity expands into the subpallium in the second case (Yun et al., 2001).

Signaling role

Among the genes whose expression is restricted to the pallial-subpallial border, there are some that strongly suggest a patterning role as a secondary organizer: several secreted factors of different families are found here, in particular members of the EGF family such as Transforming growth factor alpha ($Tg\alpha$) and Neuregulins 1 and 3 (Nrg1 and Nrg3); Secreted

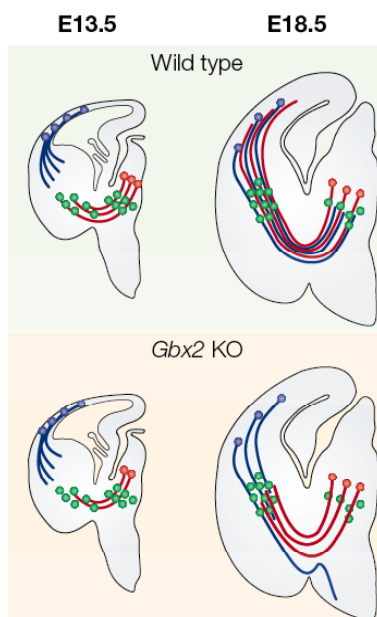


- Fig. 12 Expression patterns of antihem-specific genes; from Assimacopoulos et al., 2003.

frizzled-related protein 2 (Sfrp2), a secreted Wnt antagonist, is expressed locally as early as E10.5 (Kim et al., 2001) and Fgf7 expression is also transiently localized in the boundary region, which has been termed “antihem” for its symmetrical position in regards to another cortical patterning center, the cortical hem (Assimacopoulos et al., 2003).

Boundary-restricted expression patterns

Narrow expression domains of specific transcription factors develop adjacent to the antihem, on both sides of it. This is the case, for example, of the gene developing brain homeobox 1 (Dbx1), which is expressed along the ventricular surface at the ventralmost pallium, just lateral of the boundary; conversely, Ets transcription factor ER81 (Er81)



- **Fig. 13** Axon guidance disruption at the level of the pallial-subpallial border in *Gbx2*^{-/-} mice, in which the boundary structure fails to form properly: incoming thalamocortical projections (red) do not proceed into the cortex, and corticofugal axons (blue) are misrouted at the boundary. Adapted from Lopez-Bendito and Molnar, 2003.

and Teashirt 1 (Tsh1) (Caubit et al., 2005) are located just medial from the boundary, at the dorsalmost subpallium. It is tempting to speculate these domains may arise as a response to patterning molecules diffusing from the antihem. In this respect, some defects observed in the absence of Pax6, in this boundary and its surroundings, may be due to the loss of the signaling functions that it performs (Assimacopoulos et al., 2003).

Guidance functions for axons and migrating cells

Birthdating and Di-labeling studies show that the progeny of pallial-subpallial boundary neuroblasts can be found relatively far, populating various structures of the basal limbic system (pyriform cortex, amygdala and nucleus accumbens); this can only be attained through tangential migration, which has been demonstrated to draw from both the pallial (Pax6-positive) and subpallial (Gsh2-positive) populations and was

termed lateral cortical stream. If the boundary is disrupted, as in Gsh2 knock-out mice, the stream does not correctly appear and the limbic system is malformed (Carney et al., 2006).

The pallial-subpallial border appear also to have a guidance function for afferent axons, such as thalamocortical projections: in case of boundary disruption due to the removal of Gsh2, the incoming growth cones are misrouted and their connection never correctly form, due to structural defects at the level of the boundary and the lack of expression of guidance molecules such as semaphorins (Jones et al., 2002).

Materials and methods

Embryonic tissue retrieval

Animal husbandry

Wild type female mice of CD1 genetic background were mated overnight with β -actin-EGFP^{+/-} or wild type males of similar genetic background and inspected at 9.00 A.M. on the following day for the presence of vaginal plug; noon of this day was assumed to correspond to embryonic day 0.5 (E0.5). At the required times, pregnant females were anesthetized by CO₂ administration and killed by cervical dislocation; embryos were harvested and treated according to the necessary procedure. In case of matings with β -actin-EGFP^{+/-} breeders, harvested embryos were identified as EGFP positive or negative by fluorescent microscopy.

β -actin-EGFP^{+/-} mice

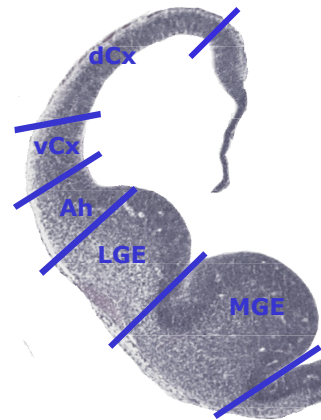
Transgenic mice constitutively expressing enhanced green fluorescent protein were used as a source for primary neuroblast cell cultures. The transgenic strain was obtained from Jackson laboratories (strain code C57BL/6-Tg(ACTB-EGFP)10sb/J) and subsequently backcrossed onto a CD1 background. Embryos used for cell cultures were isogenic by at least 7/8 to CD1 (founders were backcrossed to CD1 for at least three generations).

The transgenic cassette contains, along the sequence coding for the enhanced form of green fluorescent protein (EGFP), chicken beta-actin promoter and cytomegalovirus enhancer, beta-actin intron and bovine globin poly-adenylation signal. Resulting heterozygous mice express high levels of the fluorescent protein in all tissues save hair and erythrocytes, and thus can be easily genotyped by simple observation under natural light or UV transillumination. Homozygous animals were not generated as they are reported to be perinatally lethal by the supplier.

Microdissection and tissue preparation

Embryos were dissected in ice-cold PBS supplemented with 0,6% glucose; from

each telencephalic vesicle, meninges were removed and the cortex, corticostriatal boundary, lateral and medial ganglionic eminences were separately harvested, while the caudal ganglionic eminence, olfactory bulbs and hippocampus were discarded. In microdissections designed to yield acute RNA, the cortical field was further subdivided into ventral and dorsal cortex and harvested material was kept in ice-cold RNAlater (Ambion) during the time of the dissection. For each experiment, material from at least 4 separate embryos was retrieved.



- **Fig. 1** Coronal section of E12.5 mouse telencephalon, highlighting the microdissected fields in relation to morphological structures.

Cell cultures

Primary neuroblasts were harvested from E11.5 embryos as previously described; material from at least 5 embryos was collected for each of the following fields: cortex, corticostriatal boundary and lateral and medial ganglionic eminences. Harvested tissues were dissociated to single cells through repetitive pipetting and the number of cells was quantified in a Burker chamber.

Cells were plated at a density of 150,000 cells per 0,4 cm² well in 200 µl of medium on Nunc 96-well multiwell plates; in each well, cells were plated in either homotypical cultures (150,000 cells from the same field preparation) or heterotypical cultures (75,000 cells from a field preparation and 75,000 cells from a different one). When possible, heterotypical cultures were assembled from material retrieved from EGFP positive and negative embryos respectively, in order to verify by fluorescence microscopy the correct mixing of the different cell populations. The following homotypical cultures were prepared: cortex (Cx/Cx), corticostriatal boundary (Ah/Ah), lateral ganglionic eminence (LGE/LGE), medial ganglionic eminence (MGE/MGE); and the following heterotypical cultures: cortex/lateral ganglionic eminence (Cx/LGE), cortex/medial ganglionic eminence (Cx/MGE).

Cells were cultured for 24 hours at 37° C in 5% CO₂-supplemented atmosphere, in 200 µl/well of DMEM-F12 + Glutamax (Sigma) - 0.1% BSA (Sigma) – 0.6% glucose

(Sigma) – 1X N2 (Invitrogen) – 20ng/ml bFGF (Invitrogen) – 20ng/ml EGF (Invitrogen) – 1X penicillin/streptomycin solution (Sigma) – 1X fungizone (Gibco) - 2µg/ml heparin (Gibco).

RNA techniques

RNA extraction and purification

RNA was extracted from samples using TRIzol Reagent (Invitrogen) according to manufacturer's instructions and resuspended in sterile deionized water. Agarose gel electrophoresis and spectrophotometric measurements (NanoDrop ND-1000) were employed to estimate quantity, quality and purity of the resulting RNA. In case of RNA used as a template for microarray hybridization, a DNase digestion step was included (RQ1 RNase-free Dnase, Promega), followed by column purification (RNEasy Mini kit, Qiagen); sample quality was furthermore assayed with an Agilent 2100 Bioanalyzer, for a quantitative estimate of RNA degradation.

Microarray hybridization

Large-scale transcriptome analysis were performed taking advantage of microarray technology, which allows for the explorative characterization of differential gene expression patterns from which functional features could be inferred.

Expression microarray platforms contain a large collection of DNA probes corresponding to numerous known transcript sequences, each represented by a number of discriminating cDNAs or oligonucleotides attached to a solid surface in small discrete spots; several reference spots are also present as well as internal controls and probes for known housekeeping genes. A suitably prepared sample, or a pair of differently-labeled samples to be compared, will hybridize to the DNA spots according to sequence complementarity rules, as defined by the stringency of washing procedures; sample labeling results in detectable signal localized onto individual spots which is proportional to the amount of transcript within the sample that is complementary to the probe of each spot.

An image of the hybridized chip can be acquired with a high-resolution scanner and specific software is used to link each spot's image and signal intensity to the molecular identity of the probe. In case of single-sample hybridization, an absolute value is ob-

tained representing the particular sample's expression pattern; in dual-sample hybridization, differences or ratios between the two preparations' gene expression are obtained.

Affymetrix platform

Affymetrix chips contain short (25 nucleotide), chemically synthesized probes attached covalently to a quartz surfaces; they are employed for single-sample hybridizations. The sample labeling, hybridization and data acquisition were performed by Helena Krmac at the CBM s.c.r.l. Functional Genomics lab and statistical analysis was carried out by Paola Roncaglia in Stefano Gustincich's Laboratory of Neurogenomics at SISSA, Trieste.

The GeneChip® Mouse Genome 430A 2.0 Array (Affymetrix) was used for hybridization experiments; it contains 22,600 probe sets relative to 14,000 known mouse genes and transcription variants.

Labeling of the sample was performed with Illumina TotalPrep RNA Amplification Kit starting from 500 ng of purified RNA. Chip hybridization was carried out on Affymetrix platform and the hybridized chip was scanned with an Affymetrix GeneChip Scanner 3000.

Statistical analysis on the samples was performed with either dChip software (www.dchip.org) or R (cran.r-project.org) and Bioconductor (www.bioconductor.org) software for quality assessment and pre-processing (background subtraction, normalization and summarization) followed by Multiexperiment Viewer (MeV, <http://www.tm4.org/mev.html>), part of TM4 Microarray Software Suite (<http://www.tm4.org>) (Saeed et al., 2003) for statistical analysis, data set comparison and data filtering.

When three samples were compared at the same time, the One-way Analysis Of Variance (ANOVA) test (Zar, 1999) was used to select statistically relevant variations and Pavlidis Template Matching (PTM) (Pavlidis and Noble, 2001) was applied to select genes exhibiting the pattern of interest; when the comparison was performed between two samples, the Significance Analysis of Microarray (SAM) test (Tusher et al., 2001) (Chu et al., 2002) was used to select genes with significant expression differences and to quantify the change extent, setting a maximum False Discovery Rate (FDR) of 0 or 0,1, as stated in the text.

Real-Time PCR

Quantitation of a chosen sequence within a DNA sample can be accomplished through Real-Time Polymerase Chain Reaction (RT-PCR). The technique is based on the acknowledgement that the polymerase chain reaction shows an exponential kinetic, as product amount is doubled at every reaction cycle until one of the reagents becomes limiting. Within the exponential phase, the only independent variable is the initial concentration of the template that the specific set of primers is able to amplify, and thus can be inferred from the reaction's behaviour, if it is possible to monitor it before the plateau is reached; this is accomplished through fluorescence-based detection on appropriate optical read thermocyclers.

The SYBR Green technique makes use of a cyanine dye able to complex with double-stranded DNA and emit strong green fluorescence ($\lambda_{\text{max}} = 522 \text{ nm}$) after excitation from blue light ($\lambda_{\text{max}} = 488 \text{ nm}$). The fluorescence quantifies the amount of double-stranded DNA within the reaction which, if the primer pair has been chosen correctly, will represent target amplification. Fluorescence readings are then plotted against cycle number on a logarithmic scale; at the fluorescence reading at which the signals are distinguishable from background noise, a threshold is placed, and for each curve the cycle number at which the threshold is crossed (C_t) can be identified. Being the detectable amplification signal that is furthest from the plateau phase, the C_t is the best indicator of reaction behaviour and thus starting concentration.

C_t values can be transformed into absolute values given that a standard titration curve constructed from known quantity samples has been run along the unknown experiments. The standard curve offers the additional advantage of testing the primer set and reaction conditions, as a plot of the known concentrations of the standards against their C_t on a logarithmic scale should lie on a straight line with a slope of $-0,30103 (\log_{10} 1/2)$ meaning that each cycle has in fact doubled the amount of product and that C_t s reflect this correctly (i.e., two samples with a factor of 2 between their concentrations reach their C_t exactly one cycle apart).

Primer pair selection

Primers were designed to amplify regions of roughly 100 bp in length. The region chosen for the amplification was tested for the existence of paralogous genes or tran-

scription variants; the former were excluded and when possible, a set of primers encompassing most documented variants was chosen. All primer pairs were designed to span across an intron, in order to avoid amplification from genomic sequences. Oligonucleotide properties were assayed informatically with NetPrimer (<http://www.premierbiosoft.com/netprimer/index.html>). The potential formation of secondary structures and undesired self- and cross-dimers was taken into account, especially if annealing appeared potentially productive (giving rise to a polymerase attach site and leading to undesired amplification). Furthermore, at the end of each RT-PCR a melting curve step was included, to discriminate potential parasite amplifications of smaller sequences within the reaction.

Standard preparation

For each primer pair, a PCR amplification was carried out with the following cycle settings: 5' at 98,0 C, (1' at 98,0 C, 1' at 58,0 – 62,0 C, 1' 30'' at 72,0 C) x 5, (1' at 95,0 C, 1' at 58,0 – 62,0 C, 1' 30'' at 72,0 C) x 30, 10' at 72,0 C. The exact annealing temperature was optimized for each primer pair. The amplification product was run on agarose gel, checked for correct size and absence of undesired amplifications, extracted with Qiaex II DNA purification system (Qiagen) and resuspended in sterile deionized water. After spectrophotometric quantitation at 260 nm, six serial 1:50 dilutions were prepared starting from a concentration of 1 ng/μl; discarding the first dilution, the resulting 5 points were used as samples in the RT-PCR, spanning a range of six factors of ten from 10000 to 0,0016 fg/reaction.

Sample preparation

RNA was collected from E11.5, E12.5 and E13.5 embryos as described above. Reverse transcription was performed with SuperScriptIII (Invitrogen) according to manufacturer's instruction; as transcription primers, a mixture of anchored oligo-dT primers (sequence TTTTTTTTTTTTTTTTTTTVN, 20 μM) and random hexamers (5 μM) was used.

RT-PCR reaction

The following reagents were assembled for each individual reaction, as suggested by

the manufacturer: iQ SYBR Green Supermix (Bio-Rad) 5 µl, forward primer 250 nM, reverse primer 250 nM, DNA template 0,5 µl, sterile deionized water to 10 µl. Reaction mix was prepared in a single batch and dispensed in the required wells for every plate. Each sample and blank (sterile deionized water) was loaded in independent triplicates. The reaction was run on a Bio-Rad Mini Opticon MJ Mini thermocycler with the following cycle parameters: 3' at 95,0 C, (10'' at 95,0 C, 35'' at 65,0 C) x 40, optical reads at 65,0 C and 80,0 C; at the end of the run, a melting curve step was performed with the following parameters: from 60,0 C to 95,0 C, optical reads every 0,5 C. Data was collected through Bio-Rad's supplied Opticon Monitor 3 software.

Data analysis

Sample C_t calculation, standard curve interpolation and absolute quantifications were performed by Opticon Monitor 3 software, along with the relative standard deviation statistics. Housekeeping reference gene choice was aided by geNorm software (<http://medgen.ugent.be/~jvdesomp/genorm/>) (Vandesompele et al., 2002). Normalization, comparison and graphical elaborations were performed on Microsoft Excel 2003.

Primer sets

The following primer pairs were employed for RT-PCR:

Emx1/Fw AGCGAGCCTTTGAGAAGAATCACTACGTGG

Emx1/Rev GGAACCCCTTCTTCTTCTGCTCAGACTCC

Fgf7/Fw CCGTGGCAGTTGGAATTGTGGCAATCAAAG

Fgf7/Rev CCTCCGCTGTGTGTCCATTTAGCTGATGC

Dbx1 FW CGTTCCAACCCTTTATCAGATCCTCCTATTTCC

Dbx1/Rev GCTTGCTGATGTACTTCTGCTTCTGGAACG

bAct/Fw AGATTACTGCTCTGGCTCCTAGCACCATGAAG

bAct/Rev CTGCTTGCTGATCCACATCTGCTGGAAG

Sfrp2 FW CCAAGAATGAGGACGACAACGACATCATGG

Sfrp2 REV GAGCCACAGCACGGATTTCTTCAGGTCC

Nkx2.1 FW GGAAGTGGATGTCTCCTCGGAAAGACAGC

Nkx2.1 REV ATGCCCACTTTCTTGTAGCTTTCCCTCCAGG

Oprm1 FW CCTCTTTGGAAACTTCCTGGTCATGTATGTGATTG

Oprm1 REV CCAAAGGGCCACGTTCCCATCAGGTAG
Gapd FW CAACAGCAACTCCCCTCTTCCACCTTCG
Gapd REV GGTGGTCCAGGGTTTCTTACTCCTTGGAGG
Tbp FW ATTCTCAAACCTCTGACCACTGCACCGTTG
Tbp REV TTAGGTCAAGTTTACAGCCAAGATTCACGGTAG
Anapc5 FW GCTAATTGAAGAATCGTGTCTCAGC
Anapc5 REV GATCATGTGGCGCAGGAACAG
Atp5b FW AGGAGACCATTAAAGGATTCCAGCAG
Atp5b REV AGTGCTGCCTTTGGCTGGAGTC
Ddah1 FW CATGCAACAGATGAGTGACCATCG
Ddah1 REV ACAGGGATCAGTAGATGGTCCTTGAG
Eif5 FW TAGTGATGATTTGGAAAGAACTGTAGAAGAGC
Eif5 REV GATGTGTGGGATCTTGGAGATCAGC
Rpl35 FW GAAGGAGGAGCTGTTGAAACAACCTGGACG
Rpl35 REV TCTTTTTGAGTCTGGTTAATAACAGTGAGGACTCG
Ldhd FW CTCCTCCTTCTTGTAGAGCCGGAGTC
Ldhd REV AGCCTCATCATCTGCAACGGACG
Psmb7 FW GCAAGATGGCGGCTGTGTGCG
Psmb7 REV CAAGAACTATGCCATCCTTATACACCACC
Sept5 FW CGGCCACCATGAGCACAGGAC
Sept5 REV GCCACCATGAGCGTGAAGTCG

Immunohistochemistry and in situ hybridization

Histological sample preparation

Embryos were dissected in ice-cold PBS supplemented with 0,6% glucose and fixed in 4% paraformaldehyde/PBS overnight at +4°C. The following day, they were repeatedly washed in PBS, equilibrated in PBS/Sucrose 30% solution and then included in Killik cryostat embedding medium subsequently frozen on dry ice. Embryos were cut at 10µm using a Microm HM550 cryostat, and sections were mounted on Menzel-Glaser SuperFrost Plus slides. Slides were stored at –80 °C.

Cell cycle marker immunohistochemistry

The fraction of proliferating cells and their cell cycle duration were analyzed through the administration of halogen-labeled deoxynucleotide analogs, Bromodeoxyuridine (BrdU, Sigma) and Iododeoxyuridine (IdU, Sigma). These small molecules are easily taken up by cells but can only be incorporated into the DNA during its synthesis, namely, S phase, thus marking only cells that are actively proliferating. The labeled cells can later be visualized by immunohistochemistry, as antibodies against BrdU exclusively and both analogs are available. Moreover, cells that have exited cell cycle can be recognized in immunohistochemistry by the expression of neuro-specific class III beta-tubulin (Tuj1).

By administering both analogs, modulating the times of administration and comparing the fraction of marked cells, it furthermore is possible to quantify the duration of the cell cycle and the relative duration of its phases.

BrdU/IdU administration

Wild type CD1 females were mated to wild-type CD1 males; at 12.5 days post coitum (dpc), BrdU and IdU were administered at the concentration of 50 µg/g of body weight to pregnant dams by intraperitoneal injection, as this concentration has been reported to label all S-phase nuclei (saturation labeling) (Takahashi et al., 1992). At scheduled times, pregnant females were anesthetized by CO₂ administration and killed by cervical dislocation.

Labelling times were 2h 30' for IdU and 50' for BrdU. Harvested embryos were fixed and sectioned as described above; three littermate embryos were analyzed. Brains were cut frontally and 12 equivalent representations were generated from each; cell counts were performed on relevant sections from one representation per embryo, monolaterally.

Pretreatment of sections

Slides were warmed to room temperature and left to dry for at least 30 minutes. Sections were post-fixed 5 minutes in 4% paraformaldehyde, followed by three washes in PBS. For the antigen retrieval, slides were boiled in 10 mM citrate buffer pH 6, for 5 minutes. Once cooled, the slides were kept at room temperature for at least 40 minutes.

Sections were first incubated in HCl 0,5 N for 10 minutes and finally treated in 0.1 M borate buffer pH 8.5 for 10 minutes. Sections were washed in PBS 5 minutes, three times and incubated in Blocking solution (PBS 1X; FBS 10%; BSA 1 mg/ml; Triton X100 0.1%) for 1 hour in humid chamber at room temperature. Primary antibody was incubated at the concentrations listed below in blocking mix overnight at +4°C.

The following day, slides were washed in PBS 5 minutes, three times and incubated in the fluorophore-conjugated secondary antibody at the concentration of 1:1000, for 2 hours at room temperature. Sections were then washed in PBS 5 minutes, incubated in DAPI 1:200 in PBS for 20 minutes, washed in PBS 5 minutes again, and finally mounted with VectaShield mounting medium (Vector Laboratories) and sealed with nail enamel.

In case of double immunofluorescence reactions, before the slide mounting, the blocking and incubation steps were repeated for the second primary and secondary antibody pair, providing adequate controls for any possible cross-reactivity.

Antibodies

Anti BrdU-IdU, mouse monoclonal, clone B44 (Becton Dickinson), 1:50

Anti BrdU, rat monoclonal, BU1/75 (ICR1) (Abcam), 1:500

Anti neuro-specific classIII beta-tubulin, mouse monoclonal, clone TuJ1 (BabCo), 1:1000

Anti mouse IgG Alexa Fluor 488, goat monoclonal (Molecular Probes, Invitrogen)

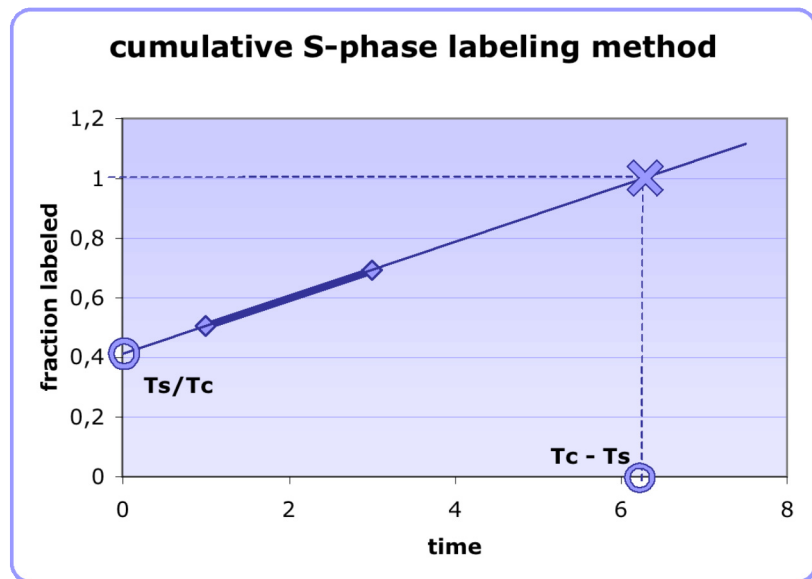
Anti rat IgG Alexa Fluor 594, donkey monoclonal (Molecular Probes, Invitrogen)

Cell cycle data analysis

Bromodeoxyuridine (BrdU), an analog of thymidine, is incorporated into DNA during the S-phase of the cell cycle. Total cell cycle length, T_C , and S-phase length, T_S , were determined by the cumulative S-phase labeling method (Takahashi et al., 1993).

As the thymidine analogs are only incorporated during DNA synthesis, only a fraction of the cycling cells are labeled with this method. Such a fraction represents the ratio between S-phase duration and whole cell cycle duration for a instantaneous analog administration (it should be noted, however, that such immediate administration is impeded by the delay due to the pregnant mother's blood flow and therefore sufficient la-

being is only obtained after at least 30' from injection; after that, it rises linearly. Finally, it reaches a plateau corresponding to the totality of the proliferative population after a time that is equal to the entire cell cycle minus the length of the S-phase: such a delay is necessary - in fact



- **Fig. 2** A diagram of T_s and T_c calculation from S-phase labeling. Observed fractions (diamonds) can be used to extrapolate the intersection with labeled fraction = 1 (cross) and = 0 (circle).

- to allow cells that had completed DNA synthesis just before the beginning of the experiment to re-enter S-phase and be labelled. Given these premises, the combination of different analogs injected at different times allows for the detection of time/labeled fraction pairs, from which it is possible to estimate by extrapolation the duration of the S-phase and of the total cell cycle.

Adjacent sections stained for BrdU and IdU/Tuj1 respectively were analyzed correspondingly. On each pair of sections, fields of matching area representing ventricular layers of cortex, corticostriatal corner and lateral ganglionic eminence were selected, marginally delimited by the neuron-specific Tuj1 signal and radially defined according to the direction of radial glia, as detectable from DAPI signal. For each field, the total numbers of nuclei labeled by the two distinct halogens were quantified, in order to calculate the labeling index (labeled cells as a proportion of total cells).

In situ hybridization

The spatial distribution of a transcript within a tissue can be studied by annealing a labeled complementary RNA fragment onto histological preparations and then detecting the label's position through a chromogenic reaction.

Target transcripts were cloned into bacterial expression vectors containing RNA polymerase transcription start sites able to transcribe independently both orientations of the insert. RNA polymerases with a specificity for the different transcription start sites (SP6, T7 and T3) were employed to synthesize labeled RNA sequences, by providing a mixture of NTPs containing digoxigenin-labeled UTP. By choosing the appropriate direction of transcription, either antisense or sense strand RNA were synthesized, to be used as probe and control respectively, after checking for the absence of known antisense transcription in the locus of the probe.

When applied to a properly-treated histological preparation, the probes bind to complementary RNA sequences and localize with them. The digoxigenin attached to the probe can subsequently be bound by a specific antibody conjugated with the enzyme alkaline phosphatase, which catalyzes a colorimetric reaction when supplied with appropriate substrates, thus providing a localized signal representing the localization of the desired RNA sequences within the histological sample.

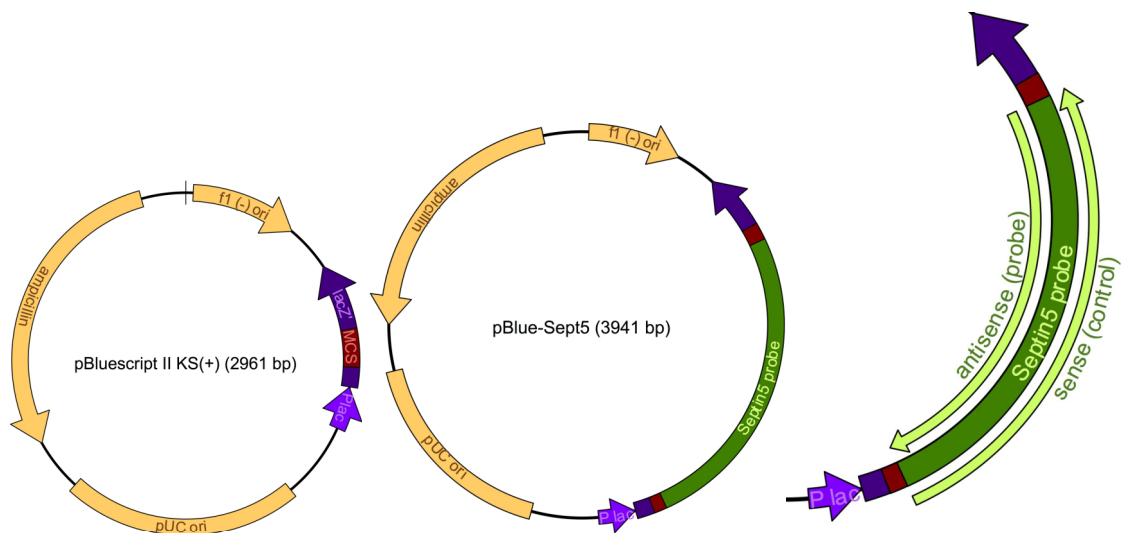
Probe selection and cloning

Target genes were screened against available databases (UCSC Genome Browser, <http://genome.ucsc.edu/>, (Kent et al., 2002), Feb 2006 and July 2007 Mus musculus assemblies; Ensembl Genome Browser, <http://www.ensembl.org/index.html> (Hubbard et al., 2007), NCBI m37 April 2007 Mus musculus assembly) for the absence of paralogous genes and antisense transcription at the selected locus. The following probes were used: Anapc5 (PCR amplified, Genbank NM_021505, nt 15-850); Ddah1 (PCR amplified, Genbank BE283964, nt 1-1098); Sept5 (PCR amplified, Genbank AF033350, nt 1017-2003).

PCR primers containing appropriate restriction sites were designed to amplify a region of 0,8-1,2 kb of the desired transcript and cloned into pBluescript KS(-) (Stratagene) Escherichia coli expression vector. All basic DNA standard methods (extraction, purification, ligation) as well as bacterial cultures and transformation, media and buffer preparations and agarose gel electrophoresis were performed according to Sambrook et al., 1989. DNAs were transformed in the *E.coli* DH5 α strain. Restriction enzymes were obtained from Roche and Promega, and used according to manufacturer's suggestions. Ligation reactions were performed with LigaFast Rapid DNA Liga-

tion System (Promega). DNA fragments were purified from agarose gel with the Qiaex II DNA purification system (Qiagen). Small-scale plasmid preparations (mini-preps) from transformants were made using the alkaline lysis method described by Maniatis et al., 1989. Large scale preparations (maxi-preps) were done by purification on Qiagen columns (Plasmid Maxi Kit, Qiagen).

Single stranded RNA probes were synthesized through in vitro transcription of sequences cloned into pGEM (Promega) or pBluescript vectors which contain specific RNA polymerase promoter sites. Plasmids for use in transcription reactions were linearized with appropriately placed restriction enzymes, purified by phenol/chloroform extraction and finally resuspended in deionized water.



- **Fig. 3** Maps of cloning and probe synthesis for a representative gene (Septin 5).

Probe synthesis

According to the manufacturers' instructions, the following reagents were assembled on ice in an eppendorf tube: 1-2 μg linearized DNA; 4 μl Transcription Optimized 5x Buffer (Promega); 2 μl 0,1M DTT (Invitrogen); 2 μl 10x Dig labelling mix (Roche); 1 μl 40U/ μl RNaseOUT (Invitrogen); 1 μl 20U/ μl RNA polymerase (either SP6, T3 or T7, Promega); deionized water to 20 μl . The reaction was incubated at room temperature overnight. The following day RNA transcripts were precipitated and resuspended in 20 μl of sterile deionized water, 2 μl of RNA probe were run on denaturing agarose gel

against known weight markers (total RNA preparations quantified by spectrophotometry) for quantification. Probes were diluted to a concentration of 50 ng/ μ l and stored at -80°C .

Pretreatment of sections

In order to improve signal and reduce the background, sections were subjected to several pre-treatment steps before the hybridization probe was applied. The following protocol is adapted for cryostat-cut sections.

Slides were left to dry for at least 30 minutes. After this step slides were immersed in 4% paraformaldehyde in PBS for 10 minutes and then washed in PBS, twice for 5 minutes. Slides were immersed in HCl 0,2 M for 5 minutes, then washed in PBS, three times for 2 minutes, and incubated in 0,5 μ g/ml of proteinase-K (Roche) in 50 mM Tris-HCl pH 8,5mM EDTA, at 30°C for 10 minutes. The proteinase K reaction was stopped by washing slides in Glycine 4 mg/ml in PBS for 5 minutes, twice. Slides were washed in PBS for 5 minutes, twice, then immersed in 4% paraformaldehyde in PBS for 10 minutes and subsequently washed in PBS, for 4 minutes, twice. The slides were rinsed in distilled water and finally placed in a container with 0,1 M Triethanolamine-HCl pH 8 set up with a rotating stir bar for 5 minutes. 0,4 ml of acetic anhydride were added twice for 5 minutes each, then slides were washed in deionized water twice for 2 minutes. Finally, the slides were left to dry for at least 30 minutes and used on the same day for hybridization.

Hybridization and washing of sections

The hybridization mix (Denhardt's Salts 1X, DTT 50mM, Polyadenylic acid 500 μ g/ml, Ribonucleic acid transfer 53,5 μ g/ml, Dextran sulphate 10 %, Formamide 50%) was added with either 15 or 45 μ l probe/slide, then heated to 80°C for 10 minutes and applied to the slides. Clean parafilm coverslips were applied to increase the uniform spreading of the hybridization mix over the sections. Slides were placed horizontally in a sealed plastic slide box, together with paper soaked in 50% formamide, 5X SSC and incubated overnight at 60°C . The following day, slides were removed and placed in a slide rack in a solution of 5X SSC, 0.15% β -mercaptoethanol at room temperature for 30 minutes, in order to remove the coverslips. Slides were incubated in stringent buffer

(50% formamide, 2X SSC, 0.15% β -mercaptoethanol) at 60°C for 30 minutes. They were then washed with NTE buffer (0.5M NaCl; 10 mM Tris-HCl pH 8; 5 mM EDTA) two times for 15 minutes each, and incubated with 2X SSC for 15 minutes, then 0.2X SSC for 15 minutes.

Digoxigenin revelation

Slides were pre-treated and washed as described; from this point, slides were incubated in B1 solution (0.1 M Tris-HCl pH 7.4; NaCl 0.15 M) for 5 minutes. Sections were blocked in B1 solution containing 10% of heat inactivated fetal bovin serum (FBS, Gibco) for 1 hour at room temperature. Slides were next incubated in B1 containing 0.5% FBS and the anti-Digoxigenin antibody conjugated with alkaline phosphatase enzyme (α Dig-AP, Roche) at the concentration of 1:2000, overnight at +4°C. The following day sections were washed three times in B1 solution before incubation in B2 buffer (0.1 M Tris-HCl pH 9.5; 0.1 M NaCl; 50 mM $MgCl_2$) containing the chromogenic substrates: 3.5 μ l of NBT (Nitro blue tetrazolium chloride, Roche) and 3.5 μ l BCIP (5-Bromo-4-chloro-3-indolyl phosphate, toluidine salt, Roche) for each ml. The ongoing development of these sections was followed using a bright field Olympus CHT microscope.

Microphotography and editing

Micrographs of immunofluorescence slides were taken with a Leica DM6000B microscope equipped with an AxioCam MRc5 digital microscope camera and acquired with Axiovision AC version 4.2 software. Micrographs of in situ immunohistochemistry were taken with a Nikon Eclipse 80i microscope equipped with a Digital Sight DS-2MBWc digital microscope camera (Nikon) and acquired with NIS-Elements AR 2.30 imaging software (Nikon).

Electronic files were processed on a Macintosh G4 computer with NIH Image and Adobe Photoshop CS2 software.

Results

Acute preparations

In order to obtain initial data about the molecular characterization of the corticostriatal boundary and its immediately flanking fields, we have chosen to isolate this region from embryonic telencephalic vesicles by manual microdissection and to look for gene expression patterns that show a marked local difference as compared to the neighboring fields. Such acute preparations were therefore intended mainly to collect total RNA.

In the choice of the most appropriate embryonic stage for the initial stages of our analysis, we have referred to published data showing that a peculiar transcriptional profile at the corticostriatal boundary and its surroundings is established between E11.5 and E13.5 (Muzio et al., 2002) (Bielle et al., 2005) (Assimacopoulos et al., 2003). We have chosen to collect the material specifically at E12.5 for several reasons: the molecular diversification processes that take place in the structure are underway; the size of the embryonic brain is such that sufficient material can be collected for multiple analyses and the manual microdissection technique can be replicated with sufficient reliability; and also, littermates at this stage show better synchronization in their development as compared to previous gestational ages.

Dissection quality control

Dissections were performed as described in Materials and methods. The following samples were collected separately:

- the corticostriatal boundary (i.e., the boundary region properly called plus its immediate surroundings, Ah);
- the ventral half of the neocortex (vCx);
- the dorsal half of the neocortex and the archicortex (dCx);
- the lateral ganglionic eminence (LGE);
- the medial ganglionic eminence (MGE).

We afterwards chose not to include the MGE in analyses as it does not appear to have a direct relevance to the search for corticostriatal boundary events.

The quality and correct design of the dissection procedure were assessed by selecting a panel of known regionally-bound transcripts able to discriminate between the desired areas, and detecting their presence and relative abundance in each sample through RT-PCR technique. The following genes were chosen:

- Emx1 (empty spiracles homolog 1 (Drosophila)): cortex (Yun et al., 2004)
- Oprm1 (opioid receptor, mu 1): LGE (Zhu et al., 1998)
- Nkx2.1 (NK2 homeobox 1): MGE (Nery et al., 2001)
- Dbx1 (developing brain homeobox 1): antihem (Bielle et al., 2005)
- Sfrp2 (secreted frizzled-related protein 2): antihem (Assimacopoulos et al, 2003)
- Fgf7 (fibroblast growth factor 7): antihem (Assimacopoulos et al, 2003)
- Actb (actin, beta, cytoplasmic): housekeeping
- Gapdh (glyceraldehyde-3-phosphate dehydrogenase): housekeeping
- Tbp (TATA box binding protein): housekeeping

From geNorm (Vandesompele et al., 2002) analysis of housekeeping genes, Tbp and Gapdh were indicated as best normalizers and Gapdh was selected for subsequent analyses.

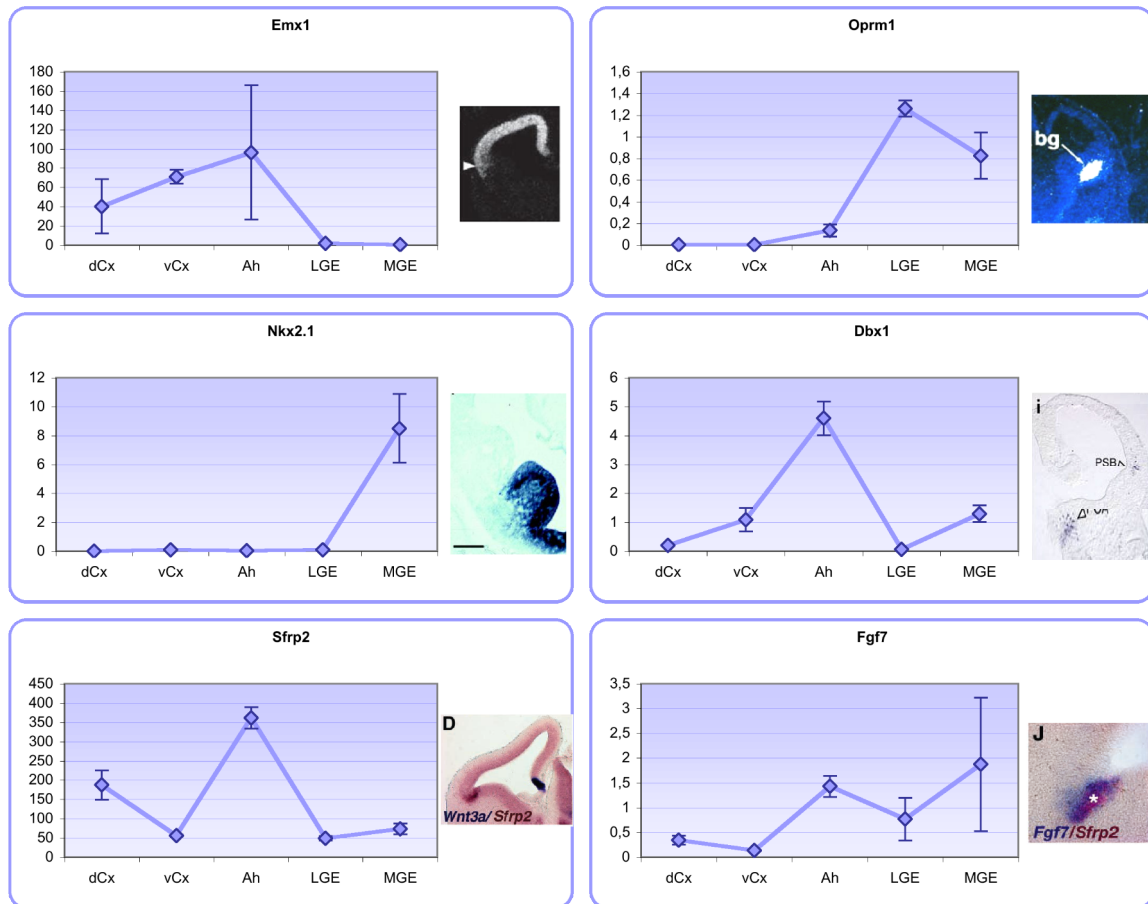
RT-PCR

The dissection procedure appears to distinguish correctly the different fields as defined by localized gene expression patterns, as shown by the results in Fig. 1. The comprehensive results of areal marker RT-PCR are listed in Appendix A.

Preliminary microarray hybridization

The dissected material was used to extract RNA for hybridization on a set of Affymetrix Mouse Genome chips, chosen as an explorative tool to identify possible molecular targets for further investigation. The samples that were hybridized were dCx, Ah and LGE, representing the region of interest and its closest neighboring regions.

The comprehensive results of the hybridization reactions are listed in Appendix B.



- **Fig. 1** Microdissected tissue RT-PCR profiling for area markers. The markers' localization as characterized in literature is shown on the side of the graphs. Expression values are normalized against Gapdh expression and are shown in arbitrary units. In situ images from Yun et al., 2004 (Emx1); Zhu et al., 1998 (Oprm1); Nery et al., 2001 (Nkx2.1); Bielle et al., 2005 (Dbx1); Assimacopoulos et al., 2003 (Sfrp2 and Fgf7).

Data filtering

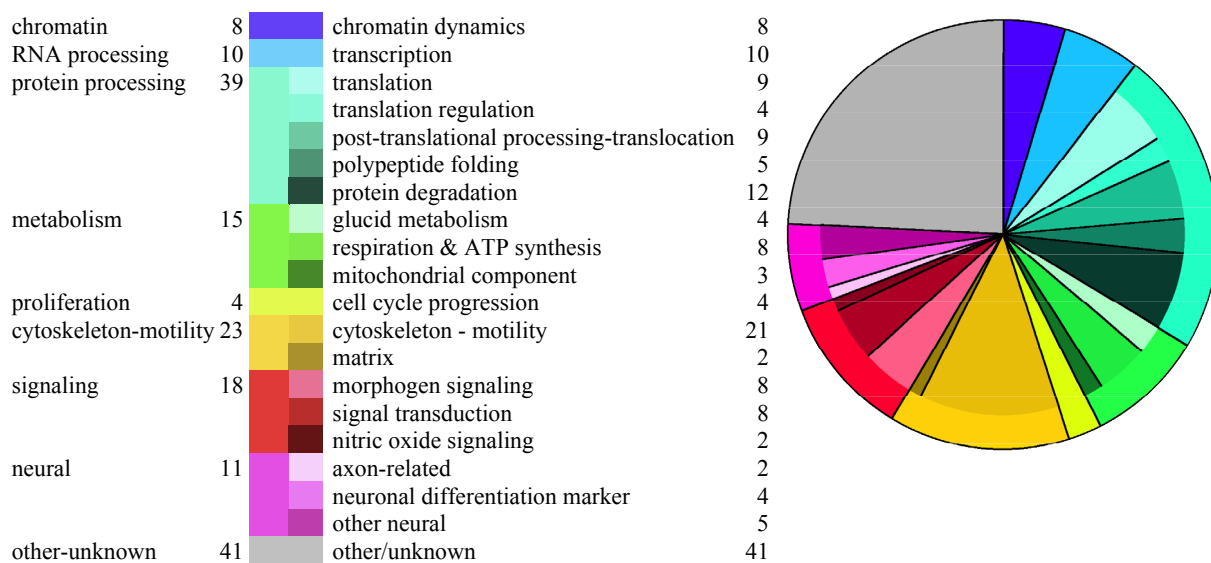
In order to identify molecular signatures of morphogenetic events that are activated by or happen within the boundary, we have decided to apply a two-direction filter against both neighboring fields: only genes showing a convergent, substantial change both between the Ah sample and the Cx sample, and between Ah and LGE, were considered. Particular attention was reserved for samples showing a higher signal in Ah than in both Cx and LGE.

Several levels of stringency were tested, both a 3-fold and a 4-fold change, and either considering the entire full length of transcripts or only the probes relative to the 3' end

of known messenger RNAs (this would make the analysis less affected by RNA degradation). A list of filtered genes, included in Appendix B, was obtained.

Ontology classification

Differentially expressed genes selected by the filter described above were classified according to their established or presumptive function in cell physiology. Several categories emerged, outlining a set of cellular processes that appeared to be coherently upregulated in our region of interest. In particular, metabolism (both aerobic and anaerobic), protein synthesis, processing and turnover, cytoskeleton dynamics, cell cycle progression and chromatin remodeling seemed to be particularly vigorous, suggesting a dynamic cell population undergoing a highly plastic and metabolically demanding phase. Other classes of related genes were found: telencephalic markers associated with the ventral telencephalon and neuronal markers, suggesting an ongoing neuronal differentiation process within the isolated population; a few genes related to morphogen signaling, perhaps connected with the corticostriatal boundary's patterning function; and some genes related to nitric oxide synthesis and regulation, which appears quite intriguing given the role of nitric oxide in regulating neuronogenesis kinetics (Cheng et al., 2003).



- Table 1

In order to further explore these data, we have selected a few genes from several major functional categories identified by ontology, choosing candidates with a strong, well-polarized signal and representative of their class. Before any additional characterizations, we have decided to confirm the data with a different technology, in this case RT-PCR.

RT-PCR

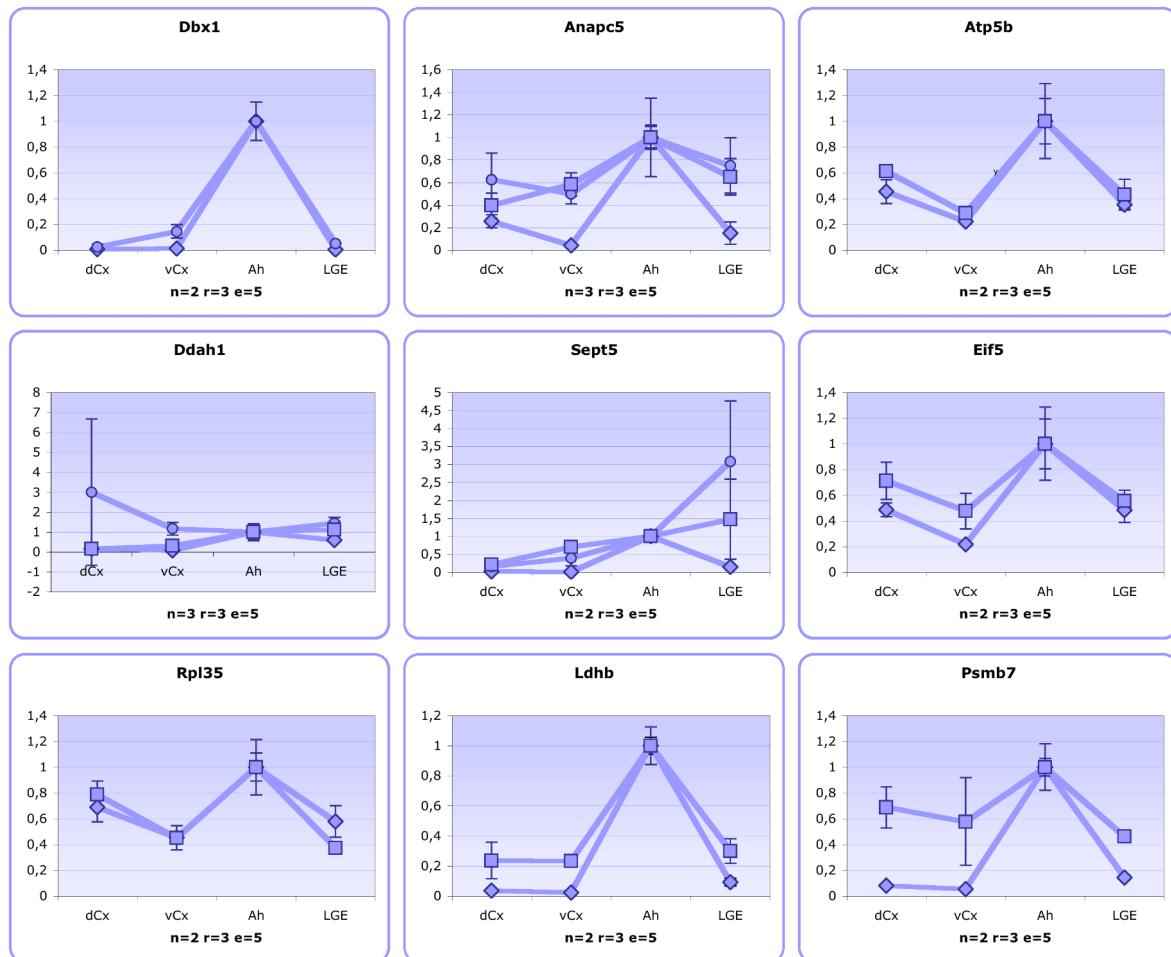
Confirmation of microarray data

The following genes were chosen as representative of functional classes for RT-PCR confirmation:

- Anapc5 (anaphase-promoting complex subunit 5) *Cell cycle progression*
- Atp5b (ATP synthase, H⁺ transporting mitochondrial F1 complex, beta subunit) *Metabolism – Respiration & ATP synthesis*
- Ddah1 (dimethylarginine dimethylaminohydrolase 1) *Signaling – Nitric oxide signaling*
- Eif5 (eukaryotic translation initiation factor 5) *Protein processing – Translation*
- Ldhb (lactate dehydrogenase B) *Metabolism – Glucid metabolism*
- Psmb7 (proteasome (prosome, macropain) subunit, beta type 7) *Protein processing – Protein degradation*
- Rpl35 (ribosomal protein L35) *Protein processing – Translation*
- Sept5 (septin 5) *Cell cycle progression*

Each gene was tested on two or three independent preparations equivalent to the ones used for hybridization and normalized for Gapdh; the results are shown in Fig. 2.

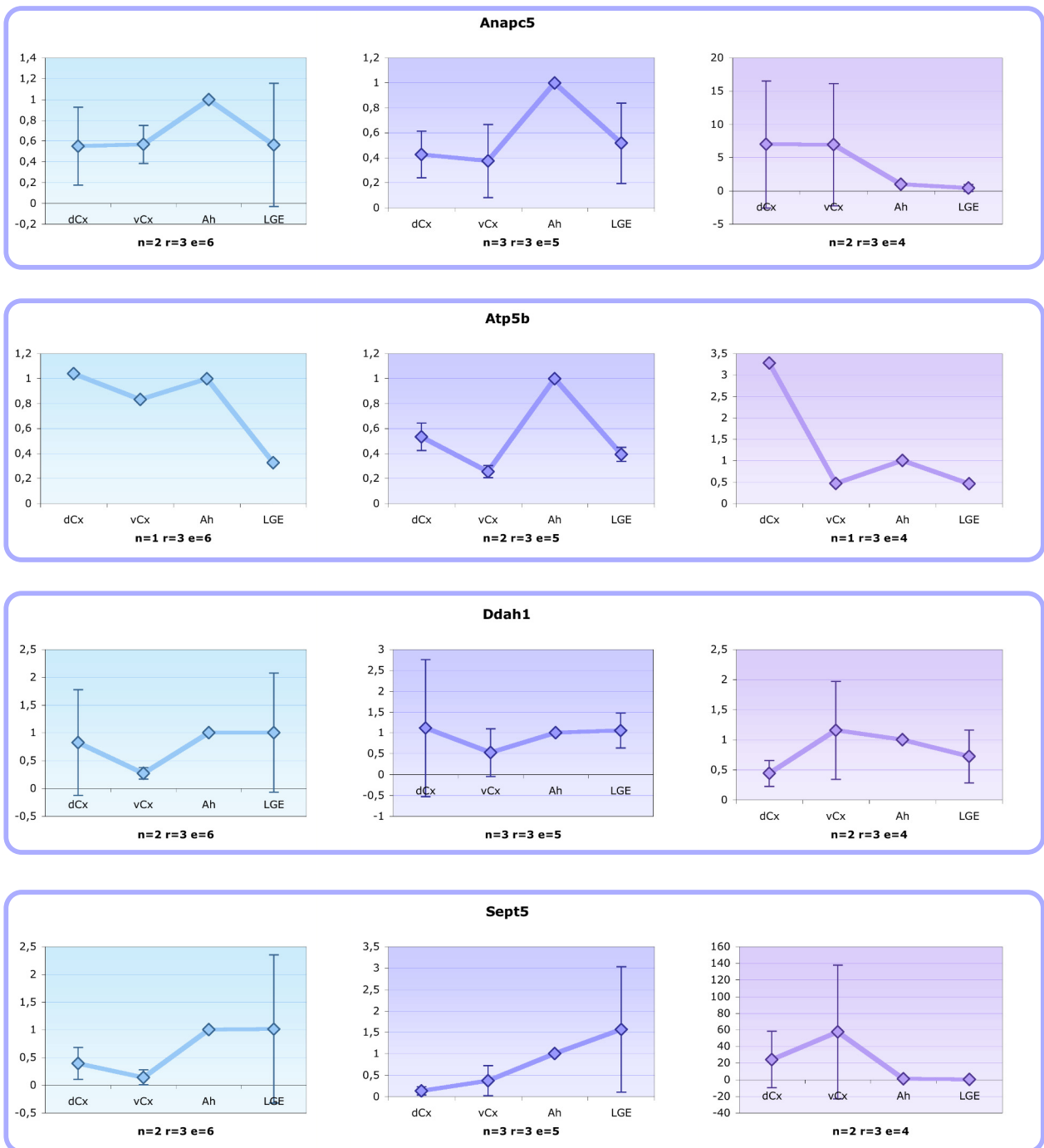
We observed that the majority of RT-PCR results were highly reproducible and consistent with microarray results; this was the case for Anapc5, Atp5b, Eif5, Ldhb, Psmb7 and Rpl35. Only a subset of the genes under investigation (Ddah1 and Sept5) exhibited more variable profiles, often not consistent with microarray results. In particular, an additional reaction was run for Ddah1, Sept5 and Anapc5 as their pattern suggests a higher expression in the basal telencephalon.



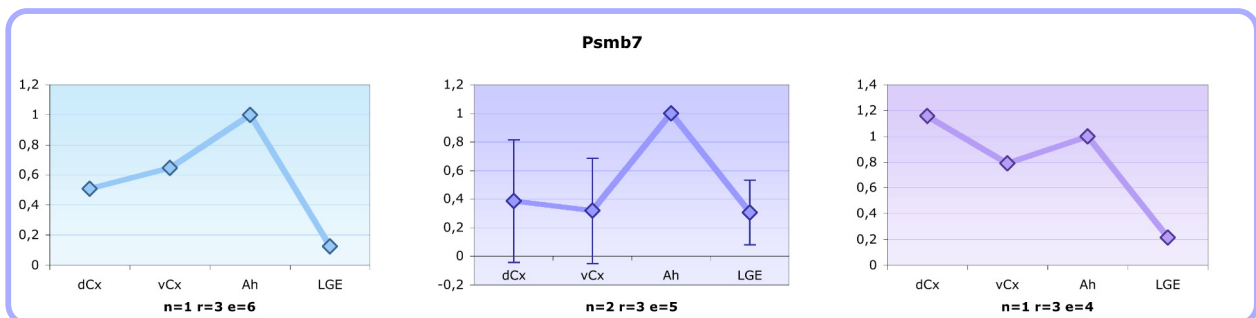
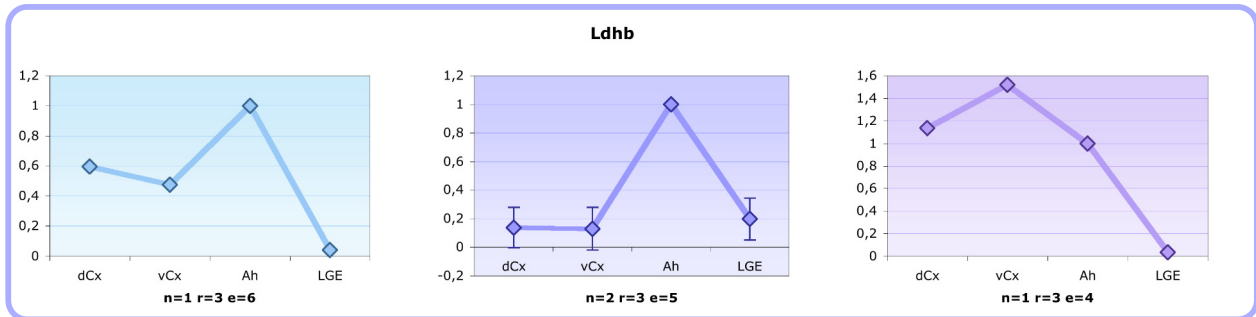
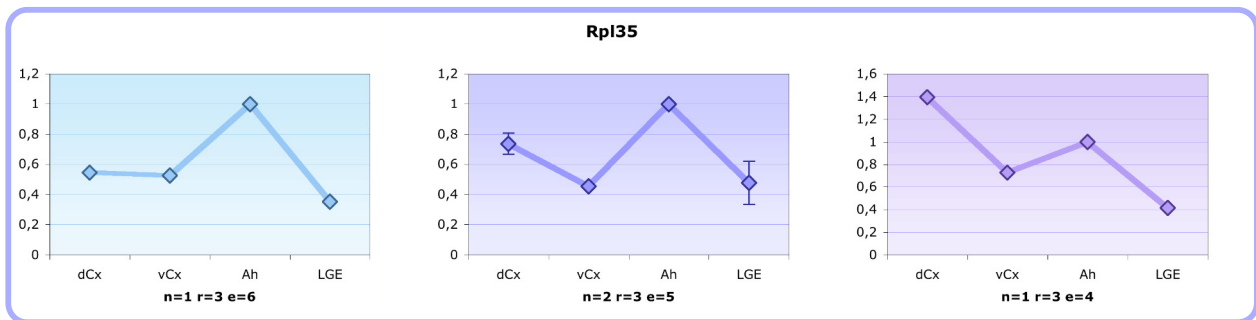
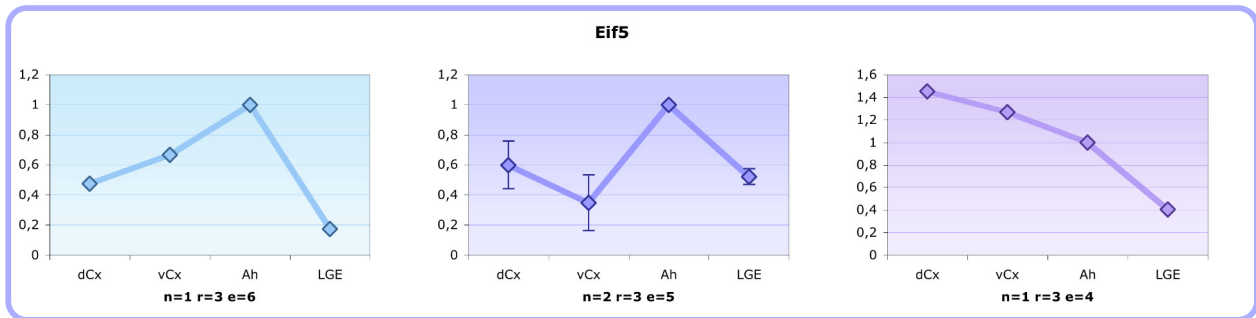
- **Fig. 2** Microdissected tissue RT-PCR profiling for Ah-specific expression candidates. Expression values are normalized against Gapdh expression and are shown in relative units to Ah expression. Replicate experiments are superimposed to show the observed variability and intra-experiment standard deviation is adopted. n, number of experiments; r, number of sample replicates per experiment; e, number of dissected embryos per sample.

Temporal kinetics

In order to obtain insight on the relationship among the spatial expression profiles described above and the formation of the corticostriatal boundary, we studied temporal progression of these profiles around E12.5. To this aim, samples were collected by manual microdissection on embryos at both E11.5 and E13.5, and subsequently profiled by RT-PCR. Sample dissection was performed in the same manner employed at E12.5, so that lateral ganglionic eminence (LGE), corticostriatal boundary (Ah), ventral cortex (vCx) and dorsal cortex (dCx) were collected separately. It should be noted that, due to tissue dynamics and the difference in dissection quality (due to different embryo size and shape), it is not possible to presume perfect population identity among analogous tissue samples collected at the different time points, given that the only guidelines available in dissection are morphological.

E11.5**E12.5****E13.5**

- **Fig. 3** Time course of microdissected tissue RT-PCR profiling for Ah-specific expression candidates. Expression values are normalized against Gapdh expression and are shown in relative units to Ah expression. Averages of replicate experiments and inter-experiment standard deviation are shown, when applicable. n, number of experiments; r, number of sample replicates per experiment; e, number of dissected embryos per sample.

E11.5**E12.5****E13.5**

From the comparison of E11.5, E12.5 and E13.5 profiles, it is apparent that most expression profiles are probably already established by E11.5, but they are no longer apparent by E13.5: the expression peak previously located in the Ah sample is smoothed or located more dorsally (as it is the case for *Anapc5*, *Atp5b*, *Ddah1*, *Eif5*, *Rpl35*, *Ldhb*, *Psb7*). In other words, boundary-associated molecular diversification begun by

E11.5 is mainly confined to the Ah region at E12.5 but subsequently diffuses to further districts. This might reflect a wave of gene regulation propagating over a static population, or it might be an epiphenomenon of the expansion-migration of a specific subpopulation originally centered around the Ah. This subpopulation might include the interneuronal cohorts, which - initially confined to the ventral forebrain - reach the corticostriatal boundary at E12.5 and enter the pallial field by E13.5.

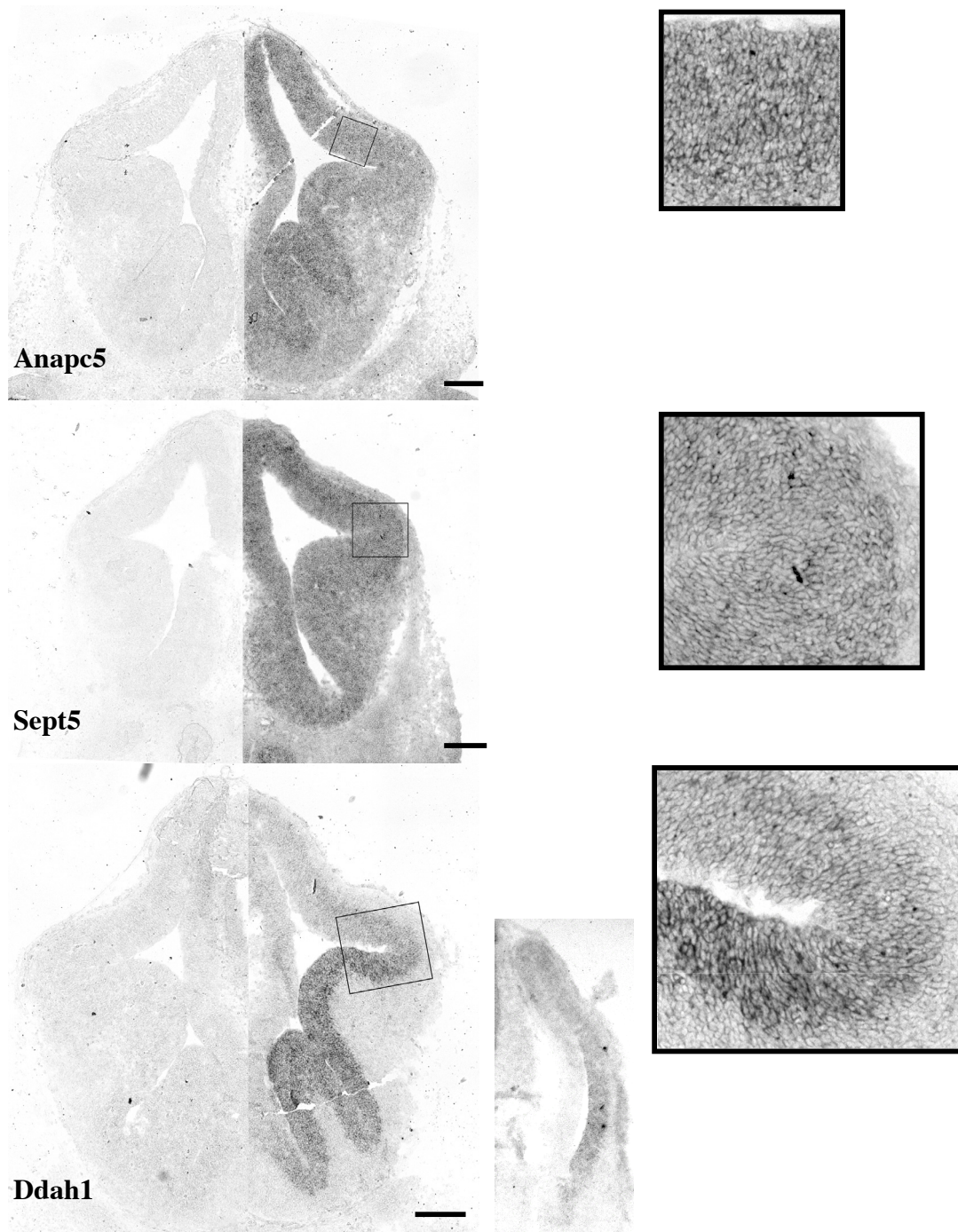
Comparison between repeated experiments shows additionally that, at a given stage, transcription profiles of different litters presumed synchronous often display conspicuous variability. Given the dynamism of the process under analysis, these inconsistencies might be due to even subtle heterochronies among litters (thus indicating that between E12.5 and E13.5 an important transition takes place in this area), and might be exacerbated by small differences in the microdissection procedure, leading to more dorsally- or ventrally-biased Ah samples (thus underlining the tight succession of fields with different molecular identity located along the corticostriatal boundary).

It must be noted that RT-PCR, while very efficient in detecting gene expression in a quantitative manner and on a large number of samples (thus allowing the accurate scrutiny of a defined time window in replicate analyses), it is constrained in its spatial sensitivity by the sensitivity of the sample microdissection procedure. In particular, molecular events restricted to very small areas, being diluted in the surrounding tissue, may fall below statistical significance; also, sharp discontinuities in expression patterns cannot be appreciated. To circumvent these limitations, an entirely different technique, not based on microdissection, needs be used; we have therefore decided to perform *in situ* hybridizations of some of the selected targets.

In situ hybridization

We have decided to test the spatial distribution of some of our target mRNAs on E12.5 mouse frontal sections, which are most informative in regards to the corticostriatal corner. We have selected as candidates the two transcripts whose spatial pattern appeared somewhat in disaccord with RT-PCR results, *Sept5* and *Ddah1*, in order to verify if dissection variability might have affected the retrieval of the gene expressing region. A gene for which patterned expression appeared well established, *Anapc5*, was also chosen. Hybridization results, referring to rostral sections where the corticostriatal

sulcus is clearly visible, are shown and compared with negative control results on an analogous section.



- **Fig. 4** Gene expression localization for *Anapc5*, *Sept5* and *Ddah1* as revealed through in situ hybridization. E12.5 coronal sections were used; control (sense) probes on the left, hybridizing (antisense) probes on the right. Magnifications shown in boxes. A caudal section is additionally shown for *Ddah1*. Bar, 100 μ m.

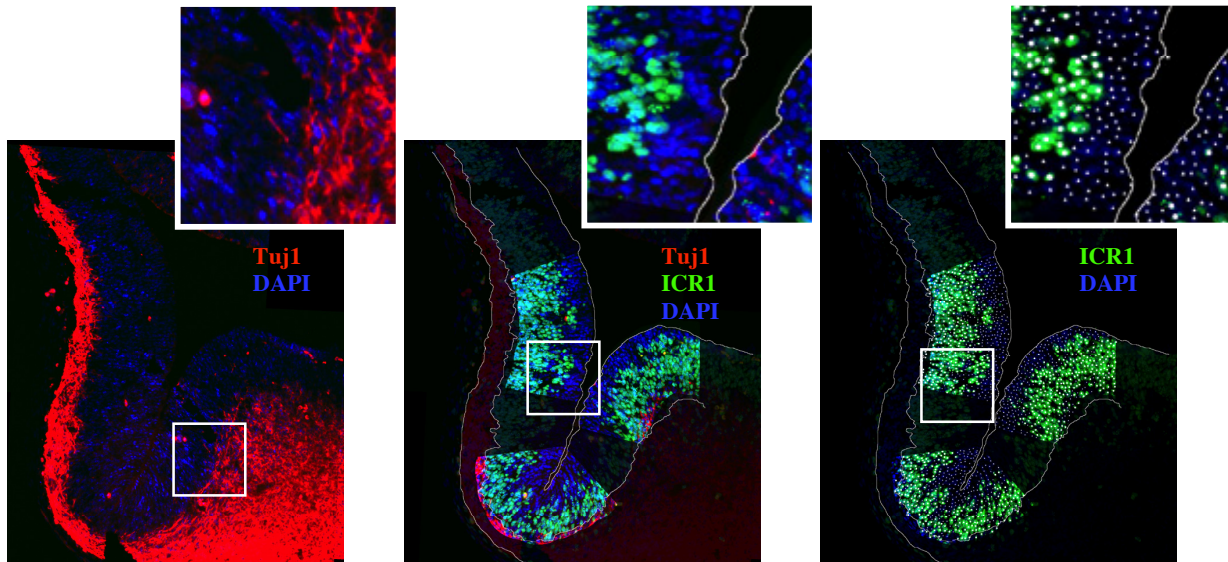
From these preliminary data, it appears that none of the tested candidates shows a clear upregulation in the area of interest; the patterns of expression observed in both the microarray hybridization experiment and the RT-PCR confirmation may be an artifact of the dissection technique. This appears to be the case for *Ddah1*, in which three elements combined to give rise to an apparent expression peak at the corticostriatal margin: the gene is expressed exclusively in the periventricular proliferative layer; this expression is furthermore not homogeneous throughout the telencephalon, but is higher in the basal ganglia and much lower in the cortex, with a higher-ventral to almost null-dorsal gradient, which is preserved rostrocaudally; finally, at this stage the postmitotic population of basal ganglia is much more abundant than in the cortex, which has determined such a dilution of the signal in the LGE sample that the expression appeared to peak at the Ah sample. We were aware that the microdissection technique would be subject to this kind of errors, but although this gene's expression may not be significant in the study of boundary events, it is nevertheless interesting due to its known function as a regulator of nitric oxide (NO) signaling. NO has been found to participate in regulating the switch from proliferation to neurogenesis (Moreno-Lopez et al., 2004) and its peculiar distribution, strictly limited to the proliferative layers, may be related to this function.

Although not in line with what we expected, the results are therefore not devoid of information: in the case of *Sept5* and *Anapc5*, we can observe that, although the expression is widespread as expected for genes that are part of common cell cycle mechanisms, there is a preference for neural tissue and, as expected, in particular its primary, i.e. ventricular, proliferative compartments (this can be appreciated mostly in the subpallium, where there is at this stage a large post-proliferative population).

Functional assays

A further step in our analysis calls for an extension of the observed tissue characteristics from simple gene expression data to functional information, to verify if the molecular signatures of cellular processes that were observed in the microarray hybridization experiments are in fact associated with discernible coherent behaviors in the area of our interest.

Microarray data shows a group of cell cycle regulators among the genes that appeared to be selectively upregulated in the Ah sample as compared to the Cx and LGE samples, namely, Septin5, Anaphase promoting complex subunit 5 and a transcribed locus similar to human protooncogene PIM1. In particular, all of these genes seem to act as positive regulators of cell cycle progression, and should therefore promote proliferation. We sought therefore to verify if there appeared to be an acceleration of cell cycle in this area, and to this end we have employed the cumulative S-phase labeling method described by Takahashi et al., 1993 with the features previously referenced.



- **Fig. 5** Sequential steps of image processing in cell cycle length calculations following the cumulative S phase labeling system. Sections are stained for a post-mitotic marker (Tuj1, red) used to outline the proliferative region. Regions of roughly equal area corresponding to cortex, corticostriatal corner and lateral ganglionic eminence are also outlined and total (DAPI staining, blue) and halogen-labeled cells (B44 or ICR1, green) are separately counted (white dots).

Cell cycle analysis

These analyses were performed on pairs of sections from two embryos and are thus to be considered strictly preliminary; the current results are shown in the table below.

$$\text{fraction labelled} = \frac{T_s + \text{labelling time}}{T_c}$$

Cx		Ah		LGE	
labeling time (h)	fraction labeled	labeling time (h)	fraction labeled	labeling time (h)	fraction labeled
1	0,52040816	1	0,53812636	1	0,54803493
1	0,55607477	1	0,48076923	1	0,49295775
2,5	0,63937622	2,5	0,68253968	2,5	0,63157895
2,5	0,67573696	2,5	0,65367965	2,5	0,61507128

y=a+bx		y=a+bx		y=a+bx	
a	0,45869805	a	0,40367321	a	0,45194382
b	0,07954342	b	0,10577458	b	0,06855252

Tc (=1/b)	12,5717506	Tc (=1/b)	9,45406721	Tc (=1/b)	14,5873565
Ts (=a/b)	5,76663748	Ts (=a/b)	3,8163537	Ts (=a/b)	6,5926657
Tc-Ts	6,80511316	Tc-Ts	5,6377135	Tc-Ts	7,99469084

- Table 2

From these preliminary data, a strong cell cycle acceleration seems to characterize the corticostriatal corner. These results, if confirmed by larger datasets, might help understanding how the small ventricular layer surrounding the Ah could generate, in a relatively short time, the disproportionately large structure of the paleocortex which is classically considered to arise from it (Fernandez et al., 1998).

Cocultures

To complement the microdissection/microarray and RT-PCR gene expression technique with a gene expression explorative tool that focuses more specifically on boundary events, we have chosen to massively recreate such boundary events *in vitro* by mixing and culturing together cells dissected from different telencephalic regions. Due to neuroblasts' tendency to aggregate in culture, each cell is then surrounded by a number of other cells, made up of a variable fraction of each population. We have decided to mix the two cell populations with a 1:1 ratio, as this should give rise to the highest number of heterotypic contact events. Transcriptional programs induced by the contact events can then be identified by comparing the cocultured samples with unmixed cultures of either dissected area via array hybridization and verified via quantitative RT-PCR.

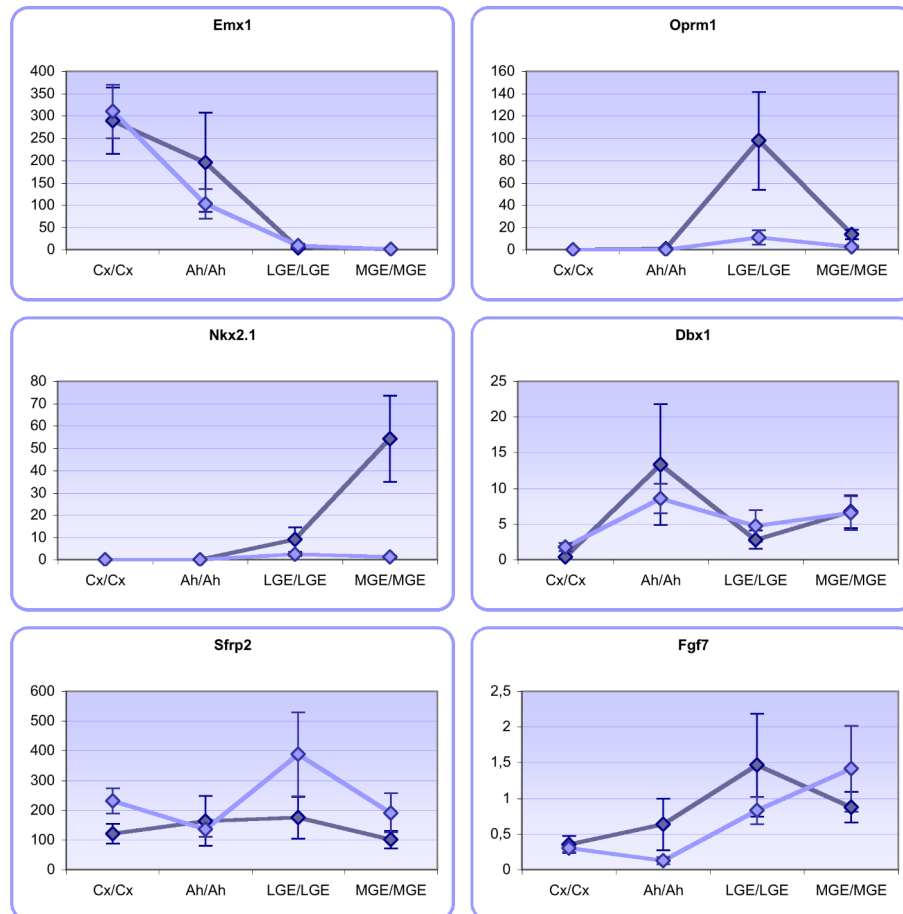
Dissection quality and biological identity in culture

Several preliminary tests were used to verify the correctness and biological plausibility of our technique. In order to establish the correctness of the microdissection procedure, acutely dissected material from E11.5 cortices, corticostriatal boundaries, lateral ganglionic eminences and medial ganglionic eminences was tested for the presence and relative abundance of transcripts with known localized gene expression through RT-PCR. The same was done after 24 hours in culture, to verify if distinctive regional identities were preserved. Finally, samples were also tested for regional markers paying special attention to antihem-specific markers, to discern if boundary-related patterns were activated by the contact among cells from these adjacent areas.

RT-PCR on acutely dissected and cultured material

As shown in Fig. 6, all genes show a correct profile both in the acute and cultured samples; some differences in relative expression between the acute and cultured sample may relate to the progression of regional diversification programs during culturing time (see for example *Nkx2.1*, whose cultured profile resembles more closely the one shown by acute E12.5 material as shown in Fig. 1). Thus, the E11.5 dissected material represents correctly the desired regions as outlined by their gene expression pattern, and such specific expression is not lost over 24 hours of culturing, but appears instead to progress

toward a state resembling the physiological E12.5. These are necessary validations to ensure that contact events that may take place in cocultures happen indeed between cells retaining their regional identity.

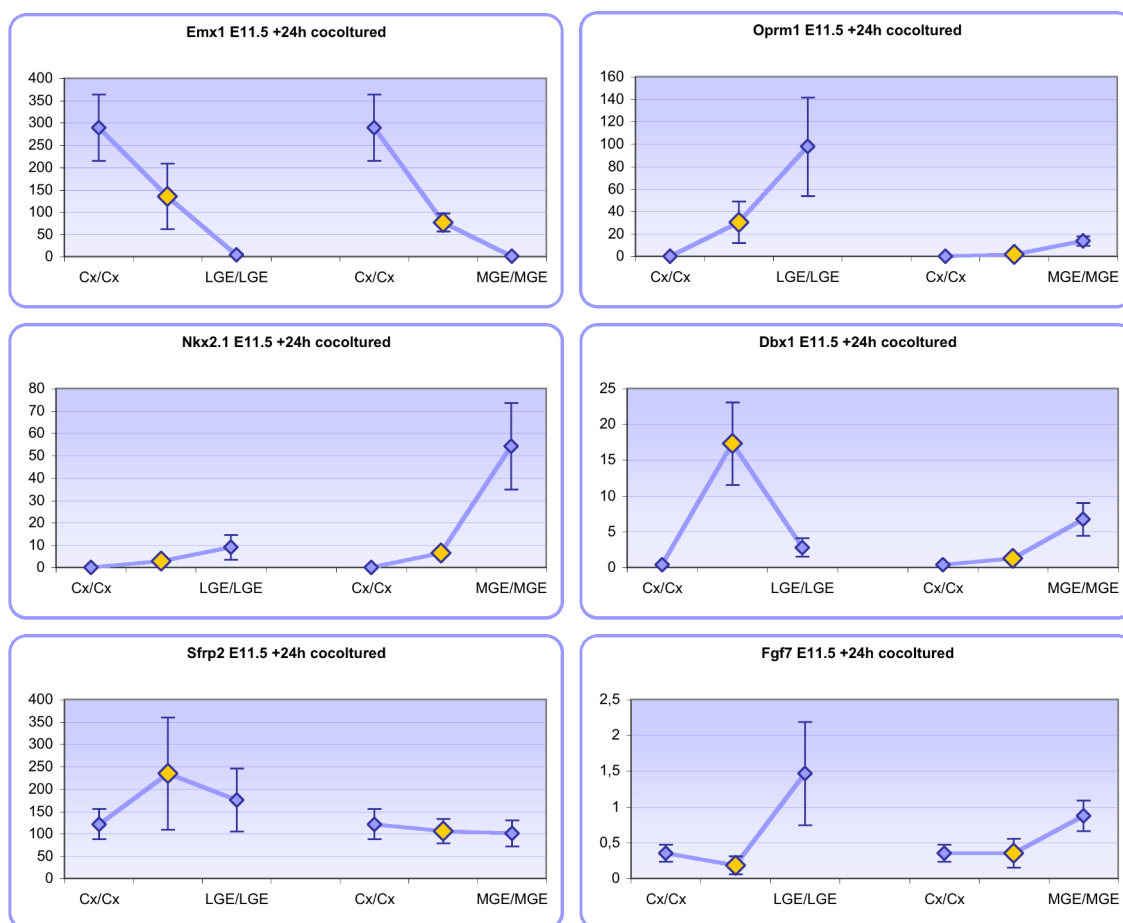


- **Fig. 6** Microdissected and cultured material RT-PCR profiling for area markers. E11.5 microdissected material (light blue) and the same material after 24h in culture (purple) were compared to verify the correctness of the microdissection procedure and the maintenance of area identity after culturing. Expression values are normalized against Gapdh expression and are shown in arbitrary units. Refer to Fig. 1 for markers' known localization.

RT-PCR on cocultured material

Comparison of heterotypic cocultures with homotypic cultures (Fig. 7) shows that areal markers of cortex (Emx1), striatum (Oprm1) and pallidus (Nkx2.1) are not

affected by coculturing: they show an expression that is roughly the average of the two contributing fields. However, Cx/LGE cocultures show an interesting pattern in regards to antihem-specific genes: Dbx1 is sharply upregulated, while Sfrp2 may be slightly upregulated as well and Fgf7 downregulated, although statistical significance of these latter two results is not high enough to draw irrefutable conclusions. It is important to observe that none of these effects are found in the Cx/MGE cocultures, thus reinforcing the idea that these events are indeed the specific in vitro recapitulation of the events triggered in vivo at the corticostriatal boundary by the juxtaposition of cortical and striatal tissue.



- **Fig. 7** Cocultured material RT-PCR profiling for area markers. Each heterotypic coculture (Cx/LGE and Cx/MGE, shown in yellow) is compared with the relevant homotypic cultures. Expression values are normalized against Gapdh expression and are shown in arbitrary units. Refer to Fig. 1 for markers' known localization.

Microarray hybridization

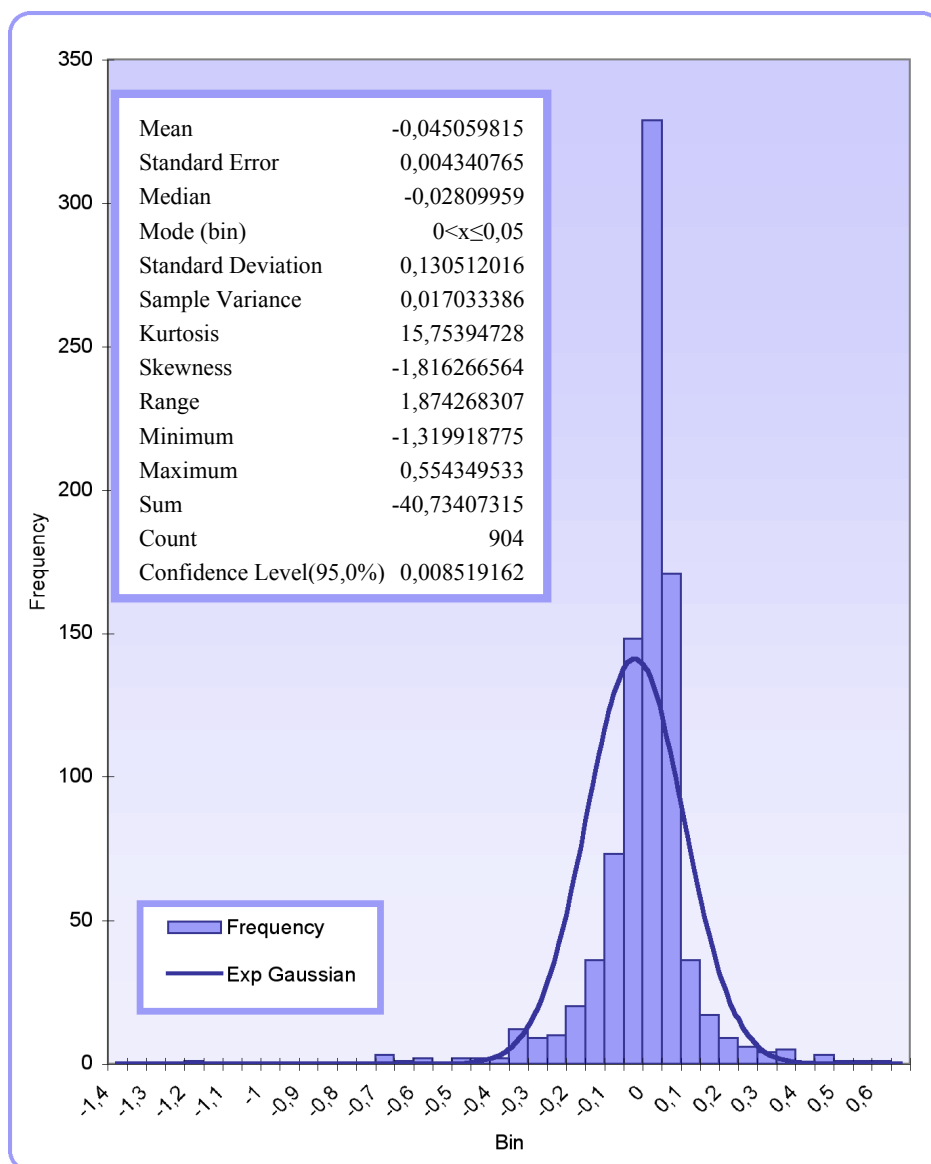
After the validation experiments and the indication that the Cx/LGE coculture technique can induce boundary-specific events, we have used these cocultures as well as their respective homotypical cultures to hybridize Affymetrix Mouse Genome chips. Two classes of events can be expected: coculture-specific up- or downregulations, as suggested by the RT-PCR results, which represent boundary-specific events; and regional identity shifts, if one of the populations' identities spreads to the entire cell population. The latter may happen through a selection mechanism (differential proliferation and/or apoptosis rates), which is supposed to shift the entire molecular signature of the selected population closer to that of one of the contributing fields; it should also be noted, however, that slight differences in plating densities due to cell count variability could have similar results. A different mechanism involves instruction, the induction of a set of genes related to a particular regional fate by a field into another. These mechanisms are involved in boundary positioning, maintenance and refinement and can shed light on molecular events in the region of our interest.

Whole-transcriptome dynamics

As an initial step of validation, we wished to compare the cocultured sample to the two homogeneous cultures in order to verify how the transcriptomes as wholes relate to each other. We expect the cocultured sample to be equidistant from the two contributing samples, that is, showing for the major fraction of genes an expression that is intermediate between the cortex and LGE samples' expressions. A net shift, that is, a cocultured sample's general expression profile that resembles more closely one of the two homogeneous samples, would be observed if the two populations were numerically unbalanced, either for an incorrect cell quantitation before plating, or for differential kinetic properties (in terms of proliferation and/or apoptosis rates), either pre-existent or triggered by the coculture. We were particularly concerned with proliferation rates, as it is known that at this stage, the lateral ganglionic eminence has a large post-proliferative population while the cortex is almost entirely proliferating.

We have therefore selected a list of genes with significant variance between the three samples by means of an ANOVA test (Zar, 1999) with $p \leq 0,01$; then, for each gene of the list, we have compared the relative distance between the cocultured samples and

each homotypical culture and plotted the results in the histogram shown below, where negative values represent genes for which the cocultured sample's expression was closer to that of the cortical sample, positive values for genes closer to LGE's expression, and 0 for equally-distanced genes.



- **Fig. 8** Distribution of cocultured (CL) expression values relative to cortical (CC, negative) and striatal (LL, positive) values. The histogram was built dispensing the 904 values filtered by ANOVA with $p \leq 0,01$ in 0,05 sized bins. The expected Gaussian distribution, bearing the same mean and standard deviation as the sample distribution, is superimposed onto the histogram.

Several interesting notes can be made about our data. First of all, values group tightly around the null value, as the $0 < x < 0,05$ bin is the most represented (36%) and as a whole, the $-0,05 < x < 0,1$ interval contains 72% of the genes. This addresses our question regarding whole-genome dynamics confirming that, in most cases, the cocultured samples was equally distant from the two homotypic cultures, and therefore neither gross cell plating mistakes nor differential kinetics took place.

However, if compared to the null hypothesis (a standard deviation curve with the same mean and standard deviation as our distribution, superimposed in the graph), it is clear that there is a higher incidence of extreme deviations (as shown by the very high kurtosis) and a certain asymmetry (note also the negative skewness) as more genes seem to resemble a cortical pattern than a striatal one. This suggests that non-casual events are taking place in which the expression pattern of certain genes acquires the characteristics of one of the contributing fields and that, in particular, these events seem to happen mostly in a cortex-bound fashion.

Local boundary patterning events

We are interested in genes whose expression is sensitive to coculturing; the first behavior we have investigated is boundary-specific gene activation or repression, represented by patterns in which the cocultured sample shows a divergent expression value from both homotypical cultures. To filter such patterns, ANOVA test (Zar, 1999) with $p\text{-value} \leq 0,01$ was used to select genes displaying significant differences between samples,; then, a 000111000 or 111000111 Pavlidis Template Matching (Pavlidis and Noble, 2001) filter with $p\text{-value} \leq 0,05$ was applied to identify the subset of genes that were selectively upregulated in the cocultured sample, as shown in Table 3.

	CC	CL	LL	Filter	Number of filtered genes
Upregulated in boundary				ANOVA 000111000	6 genes
Downregulated in boundary				ANOVA 111000111	30 genes

- Table 3

The following genes were selected by our filter (\log_2 expression levels are reported):

gene name	p-value	CC	σ_{CC}	CL	σ_{CL}	LL	σ_{LL}
upregulated							
ubiquitin-conjugating enzyme E2I	0,02932	8,7098	0,0476	8,8565	0,0175	8,8022	0,0223
splicing factor 1	0,00164	10,894	0,1075	11,141	0,0478	10,799	0,0632
heterogeneous nuclear ribonucleoprotein L-like	0,0412	11,944	0,0549	12,021	0,0653	11,779	0,0302
PHD finger protein 2	0,01517	9,9212	0,0327	10,114	0,0732	9,702	0,1423
phosphofructokinase, liver, B-type	0,03181	9,7789	0,0802	10,012	0,0534	9,411	0,243
transforming growth factor beta regulated gene 4	0,01501	8,4361	0,0276	8,7095	0,0706	8,5862	0,0648
downregulated							
chaperonin subunit 4 (delta)	0,00901	6,5559	0,0131	6,2814	0,1095	6,823	0,1593
plasminogen	0,00139	4,4278	0,0896	4,1993	0,0427	4,4339	0,0673
coiled-coil domain containing 71	0,00173	9,1867	0,0146	9,0072	0,0908	9,2268	0,0436
DNA segment, Chr 11, Wayne State University 99, expressed	0,01577	10,766	0,056	10,625	0,0977	10,907	0,0587
RB1-inducible coiled-coil 1	6,20E-04	9,961	0,0328	9,7504	0,079	10,037	0,0299
parotid secretory protein	0,00324	3,5066	0	3,3938	0,0333	3,5915	0,0479
NA	0,03256	3,849	0,0281	3,7349	0,0363	3,7767	0
NA	0,00309	6,744	0,1476	6,2344	0,087	6,5886	0,1395
VATPase, H ⁺ transporting, lysosomal V1 subunit E1	0,00218	7,9441	0,0767	7,4444	0,2032	8,0635	0,2022
plakophilin 2	0,01979	4,3525	0,0424	4,1812	0,1177	4,5624	0,1021
open reading frame 28	0,02085	7,3318	0,1192	6,8747	0,0522	7,0562	0,0842
dynein, axonemal, heavy chain 11	9,19E-04	7,0997	0,1728	6,6251	0,1232	7,05	0,0118
mitogen activated protein kinase kinase kinase 2	6,93E-04	3,4842	0,01	3,3154	0,0706	3,4704	0,0175
nucleolar protein 12	0,04683	10,872	0,072	10,734	0,0887	11,188	0,1354
RIKEN cDNA 2310076L09 gene	0,00128	4,7379	0,0567	4,5465	0,0182	4,7189	0,0693
ornithine transcarbamylase	0,04996	2,865	0,0706	2,805	0,0351	3,0004	0,0207
triadin	0,03756	3,802	0,0926	3,5281	0,0515	3,6249	0,044
oogenesisin 1	0,00684	3,0583	0,0876	2,8083	0,0276	2,9482	0,0321
sulfide quinone reductase-like (yeast)	3,83E-05	4,4702	0,024	4,2841	0,0393	4,4479	0,0079
protein phosphatase 1, regulatory (inhibitor) subunit 12C	0,01627	6,6354	0,0691	6,3448	0,0529	6,4784	0,0759
F11 receptor	0,00297	5,7944	0,0316	5,6678	0,0253	5,7537	0,0333
HLA-B-associated transcript 1A	9,51E-04	6,3665	0,0741	6,1024	0,0673	6,3631	0,0786
DEAD (Asp-Glu-Ala-Asp) box polypeptide 39	0,00474	4,131	0,0406	4,0221	0,0467	4,1854	0,0421
immunoglobulin heavy chain 6 (heavy chain of IgM)	0,00769	4,9391	0,0301	4,7777	0,0179	4,8707	0,0596
superoxide dismutase 2, mitochondrial	0,00156	11,449	0,03	11,267	0,0681	11,405	0,0157
TAF13 RNA polymerase II, TATA box binding protein (TBP)-associated factor	0,00166	11,215	0,0529	11,097	0,0327	11,251	0,0217
TBC1 domain family, member 14	6,23E-04	6,4636	0,134	5,9502	0,0947	6,5134	0,1739
caspase 3	0,03569	11,452	0,0226	11,396	0,0607	11,546	0,0156
EPS8-like 1	0,02832	4,1215	0,1352	3,9414	0,0687	4,3827	0,122
ADP-ribosylarginine hydrolase	0,04235	6,0861	0,0693	5,9093	0,017	5,9685	0,0205

- Table 4

Homotypical expression shift

Identity shift induction events were selected with SAM filtering (Tusher et al., 2001) (Chu et al., 2002), grouping the CL samples alternatively with the CC samples or the LL samples and selecting genes whose expression deviated significantly between the two groups, according to the possible dynamic patterns shown in Table 5.

		CC	CL	LL	Filter	Number of filtered genes
Striatal-like expression	High in LGE and Ah, low in Cx				SAM CCvsCL&LL	23 genes (25 probes)
	Low in LGE and Ah, high in Cx				SAM CCvsCL&LL	0 genes
Cortical-like expression	High in Cx and Ah, low in LGE				SAM CC&CLvsLL	105 genes (131 probes)
	Low in Cx and AH, high in LGE				SAM CC&CLvsLL	4 genes (4 probes)

- Table 5

What is apparent from these results is that field contact is able to give rise to both striatal-like and cortical-like patterns, and that the latter are prominent. This is in accord with the distance distribution calculated above, that shows a significant number of outliers in both directions, but more markedly so in cortical direction. In fact, the list of genes obtained through SAM filtering is largely superimposable with the list of distribution outliers, as shown by the following table, in which we have listed the most up- and downregulated genes in each category identified by SAM filtering and added the direction and amount of shift from 0 (equal distance). For clarity purposes, we have only included those genes whose distribution is at least 2 standard deviations from the mean. False discovery rate was set to 0, except in bracketed genes, where it is 0,1.

Gene name	CC	σ_{CC}	CL	σ_{CL}	LL	σ_{LL}	direction	shift
neurogenic differentiation 6	9,914884	0,49	9,441976	0,45	3,9879684	0,86	C	-1,3199188
early B-cell factor 2	8,140759	0,52	7,5332465	0,4	4,1720815	0,42	C	-0,7310066
[Wnt inhibitory factor 1]	5,2550235	0,74	5,182246	0,52	2,994645	0,24	C	-0,7166552
bone morphogenetic protein 7	7,761494	0,83	7,4424644	0,6	4,244198	0,2	C	-0,7124579
solute carrier family 14 (urea transporter), member 1	7,2294846	0,67	7,2506423	0,76	4,280848	0,63	C	-0,6908131
aldolase 3, C isoform	12,908837	0,23	12,559987	0,33	7,5644383	0,56	C	-0,633375
nescient helix loop helix 1	8,601616	0,53	8,3219185	0,15	5,048435	0,2	C	-0,6158986
neurogenin 2	10,268504	0,66	9,20869	0,41	5,5779643	0,76	C	-0,547695

basic helix-loop-helix domain containing, class B5	11,8995440,3	11,459279	0,27	7,2409425	0,65	C	-0,5455688	
early B-cell factor 2	10,2774840,57	9,552289	0,8	6,1518197	0,72	C	-0,4821968	
dopachrome tautomerase	9,053779	0,74	7,9908996	0,57	5,080642	0,32	C	-0,4554167
neurogenic differentiation 1	10,7908170,22	10,1253195	0,19	6,7120724	1,14	C	-0,446851	
[serine (or cysteine) peptidase inhibitor, clade B, member 2]	7,2011495	0,67	6,943245	0,35	4,6990848	0,82	C	-0,4417595
Fez family zinc finger 2	11,07244	0,21	10,459607	0,16	7,0379243	0,24	C	-0,4308302
T-box brain gene 1	10,1341060,12	10,004529	0,47	6,9761276	1,03	C	-0,421323	
RWD domain containing 3	8,344067	0,15	7,987129	0,42	5,4746184	0,29	C	-0,4161606
glypican 3	9,589362	0,7	9,326318	0,46	6,5031466	0,49	C	-0,4066931
early B-cell factor 2	7,031938	0,4	6,6401772	0,24	4,5457015	0,56	C	-0,405048
neurogenic differentiation 1	11,3632580,1	10,717735	0,17	7,388035	0,95	C	-0,3938803	
[citrate lyase beta like]	7,13959	0,84	7,1277237	0,4	5,1874146	0,32	C	-0,3723796
calcium binding protein 1	5,81991770,19	5,69293	0,27	4,0844483	0,27	C	-0,3719869	
frizzled homolog 9 (Drosophila)	9,399796	0,23	8,9126	0,26	6,27574	0,07	C	-0,3683367
tumor necrosis factor receptor superfamily, member 19	10,3850490,37	10,021209	0,16	7,145294	0,14	C	-0,3674558	
transcription factor AP-2, gamma	9,75702	0,14	9,152671	0,18	6,433706	1,04	C	-0,3606726
[pleiomorphic adenoma gene-like 1]	7,947834	0,3	7,8575416	0,91	5,748087	0,27	C	-0,3556231
protein phosphatase 1, regulatory (inhibitor) subunit 14A	8,107574	0,02	7,2248216	0,2	4,947605	0,78	C	-0,3513865
LIM and cysteine-rich domains 1	8,697996	0,48	8,4155655	0,19	6,0901394	0,27	C	-0,3493639
nuclear factor I/X	8,872458	0,12	8,496061	0,46	6,1214557	0,49	C	-0,3454921
tumor necrosis factor receptor superfamily, member 19	7,20149	0,37	6,5397534	0,08	4,585218	0,29	C	-0,33438
RWD domain containing 3	8,025755	0,12	7,6381745	0,48	5,525392	0,07	C	-0,3340849
[fibroblast growth factor 17]	4,431453	0,55	4,3723044	0,1	3,2507992	0,13	C	-0,3316462
transcription factor AP-2, gamma	8,434414	0,26	7,646519	0,07	5,3747106	0,61	C	-0,3292705
retinoic acid induced 2	7,240731	0,34	7,094967	0,4	5,3013697	0,25	C	-0,318196
sine oculis-related homeobox 3 homolog (Drosophila)	7,843733	0,39	10,349914	0,37	11,461871	0,19	L	0,22250024
prepronociceptin	6,254251	0,19	8,351048	0,09	9,34194	0,5	L	0,2291903
zinc finger homeobox 3	6,3649063	0,13	8,508597	0,66	9,457087	0,22	L	0,23650437
tachykinin 1	7,1640472	0,51	9,466107	0,43	10,222903	0,37	L	0,24730564
GS homeobox 2	5,9242744	0,5	8,0073395	0,12	8,705182	0,24	L	0,2714512
distal-less homeobox 2	7,7982774	0,64	10,432032	0,43	11,122001	0,28	L	0,27569902
[glutamic acid decarboxylase 2]	4,598132	0,17	6,7094646	0,67	8,00111	0,42	L	0,29773854
distal-less homeobox 1	7,31093170,76	10,313058	0,09	11,373093	0,1	L	0,31742974	
distal-less homeobox 5	7,004831	0,29	9,797115	0,29	10,584743	0,36	L	0,32421093
netrin 1	7,258967	0,36	10,331119	0,2	11,280725	0,33	L	0,33904213
distal-less homeobox 1, antisense	5,9659085	0,7	8,7646	0,19	9,873254	0,17	L	0,35682544
LIM homeobox protein 8	4,96920870,35	7,6735873	0,4	8,738091	0,61	L	0,42240384	
distal-less homeobox 6	4,6579385	0,65	7,309273	0,44	8,432686	0,51	L	0,43598645
ISL1 transcription factor, LIM/homeodomain	7,4664483	0,64	11,331433	0,34	12,332085	0,24	L	0,43650486
ISL1 transcription factor, LIM/homeodomain	6,4190555	0,26	9,980371	0,34	10,994064	0,35	L	0,4626
glutamic acid decarboxylase 1	6,1128693	0,17	9,858364	0,12	10,876286	0,33	L	0,51913189
solute carrier family 32 (GABA vesicular transporter), member 1	5,28185840,41	8,831852	0,81	10,010727	0,73	L	0,55434953	

- Table 6

Striatal-like features of the cocultures

An analysis of the resulting genes is intriguing in its implications. The set of genes regulated in a striatal-like manner is small, however they are all very tightly interconnected in function and identity.

An emerging GABA-ergic signature

We can see, among the most upregulated genes, several members of the Dlx family of homeobox genes as well as Islet1 and Gsh2, all known to be involved in the patterning of ventral forebrain cells; enzymes involved in GABA production, such as Gad1 (also known as Gad67) and Gad2 (also known as Gad65), and transportation, such as Slc6a1 and Slc32a1, are upregulated in a striatal-like manner. All these are fundamental components of the molecular signature of GABA-ergic interneuron population (Kaufman et al., 1991) which around E12,5 start leaving their original basal birthplace and migrating toward the cortex.

Cortical-like features of the coculture

The situation is more complex in regards to the cortical-like patterns acquired by the cocultured sample. The number and significance of the genes in this set is much higher, and as expected the variety of functions and molecular pathways is greater, maybe representing more than one process or molecular signature that is activated by cell contact. Also, in this case we find both upregulated and downregulated genes, further suggesting that a more complex network of events is taking place.

Involvement of retinoic acid signaling

One subset of functionally-related genes is involved in retinoic acid (RA) signaling, which has been implicated in neurogenesis and neuronal differentiation (Guan et al., 2001). Expression of the retinoic acid receptor beta (Rarb), low in the cortex and high in the striatum, strongly decreases - in a cortical-like manner - in cocultured samples; conversely, the retinaldehyde binding protein 1 (Rlbp1), a transporter involved in RA synthesis, and retinoic acid induced 2 (Rai2), both higher in the cortex than in the striatum, acquire upon coculturing a high, cortical-like expression. It appears, therefore, that cocultured cells become equipped to respond to RA signaling in a cortical manner, both in

terms of up- and downregulated elements.

A master gene for transcription factor regulation

An even more striking set is represented by proneural transcription factors, such as neurogenic differentiation 1, 2 and 6 (NeuroD1, NeuroD2 and NeuroD6), neurogenin1 and 2 (Ngn1 and Ngn2), other basic helix-loop-helix factors such as transcription factor 4 (Tcf4), transcription factor AP-2 gamma (Tcfap2c) and nescient helix loop helix 1 (Nhlh1). Many of these factors are expressed in the proliferative layers, but are markers of ongoing differentiation or intermediate progenitor stages, rather than staminal state; t-box brain gene 2/eomesodermin homolog (xenopus laevis) (Eomes/Tbr2) and t-box brain gene 1 (Tbr1), which are also increased to cortical-like amounts in cocultured samples, are another example of transcription factors involved in a progressive differentiation process. In fact, it appears that the sequential expression of Paired box gene 6 (Pax6), Tbr2 and Tbr1 is associated with a proliferative state transition from radial glia to intermediate precursors and finally postmitotic neurons (Englund et al., 2005).



Several hints from our gene list, such as the Tbr transition we just mentioned, suggested a possible involvement of the cortical neuronogenesis master gene Pax6 in a coordinated gene expression profile switch. As probes for the Pax6 transcript itself are not present on our chip, we have chosen to use a transcriptional signature comparison to verify if a Pax6-induced transcription pattern can be applied to our results. We have employed the list of genes published by Magdalena Götz's lab (Holm et al., 2006) from the microarray profiling on Affymetrix chips of Pax6-deficient cortices and basal ganglia at E12 and E15. We have focused on E12 data and compared the Pax6-dependent gene set with our filtered coculture-stimulated genes, in both cortical and striatal direction; the results are listed below.

	Gene name	Mean	Distribution
E12 Cortex			
Transcription factors and DNA binding proteins	neurogenic differentiation 6	-4,18	-1,3199188
	transcription factor AP-2, gamma	-3,14	-0,3606726
	T-box brain gene 2	-2,75	-0,2770417
	sine oculis-related homeobox 3 homolog (Drosophila)	-2,34	[-0,1419211]
	neurogenin 1	-2,2	[-0,2410611]
	nuclear factor I/a	-2,15	[-0,13349797]



	neurogenin 2	-2,11	-0,547695
	nuclear factor I/X	-2,08	-0,3454921
	neurogenic differentiation 2	-2	-0,1588943
	nuclear factor I/b	-1,92	-0,1424492
	T-box brain gene 1	-1,61	-0,421323
	distal-less homeobox 1	2,01	0,35682544
	zinc finger homeodomain 4	2,23 [0,08133659]	
	distal-less homeobox 2	2,77	0,27569902
	orthodenticle homolog 2 (Drosophila)	3,24	0,18875593
	ankyrin repeat and SOCS box-containing protein 4	5,91 [0,12612088]	
Signal transduction	glypican 3	2,41	-0,4066931
	Wnt inhibitory factor 1	2,7 [-0,7166552]	
Calcium ion binding	annexin A5	1,59	
Transporters	retinaldehyde binding protein 1	-3,55 [-0,2687342]	
	solute carrier family 15 (H ⁺ /peptide transporter), member 2	-2,62	-0,2992616
Growth factors	transforming growth factor, beta 2	-2,05	-0,2510943
	inhibin beta-B	-1,86	
	fibroblast growth factor 17	2,33 [-0,3316462]	
Cytoskeleton	N-myc downstream regulated gene 2	-2,04 [-0,11690142]	
	calponin 2	1,7 [0,03374680]	
Metabolism	aldolase 3, C isoform	-5,52	-0,633375
Neurotransmitter metabolism	netrin 1	2,08	0,33904213
Chemokine	chemokine (C-X-C motif) ligand 14	1,86 [-0,0162281]	
RIKEN/Est	proline rich 15	-4,38 [-0,00669499]	
	RIKEN cDNA 2010011I20 gene	-1,86 [-0,0309867]	
	protein phosphatase 2 (formerly 2A), regulatory subunit B (PR 52), beta isoform	-1,71	-0,2358557
E12 GE			
Transcription factors and DNA binding proteins	neurogenin 2	-8,75	-0,547695
	neurogenic differentiation 6	-4,11	-1,3199188
	neurogenic differentiation 1	-3,85	-0,446851
	T-box brain gene 2	-3,33	-0,2770417
	neurogenin 1	-2,23 [-0,2410611]	
	transcription factor AP-2, gamma	-2	-0,3606726
	basic helix-loop-helix domain containing, class B5	-1,95	-0,5455688
	T-box brain gene 1	-1,91	-0,421323
Transporters	retinaldehyde binding protein 1	-1,61 [-0,2687342]	
Metabolism	retinaldehyde binding protein 1-like 1	-1,89 [-0,0590323]	

Legend:

Pax6 ^{-/-} expression patterns (Holm et al 2006)

	Pax6-dependent
	Pax6-repressed

Coculture expression patterns (our results)

	Cortical-like upregulation
	Striatal-like upregulation

Genes in brackets were filtered with FDR=0,1; otherwise, FDR=0

- Table 7

It should be noted that, out of the 226 genes representing the Pax6-dependent signature, only 80 identical probes were available on our chips; this number is further reduced when we limit our analysis to E12. However, even with small numbers, results are striking:

- 10/13 (76,9%) of transcription factors and 14/24 (58,3%) of genes overall that appeared downregulated in the absence of Pax6 in the E12 cortex and GE are also significantly upregulated, cortex-like, in cocultured samples; these values increase to 13/13 (100%) of transcription factors and 23/24 (95,8%) overall if maximum false discovery rate is set at 0,1;
- only 1 highly significant gene behaves in disaccord with this pattern (glypican 3) and three lower significance ones (Wnt inhibitory factor 1, fibroblast growth factor 17, and chemokine (C-X-C motif) ligand 14) as they are upregulated in both the cocultures and the Pax^{-/-} cortex;
- no significant downregulation of Pax6-repressed genes (whose expression was higher in Pax6 deficient samples) can be observed in our cocultured sample; it should be noted, however, that only 3 genes showed significant downregulation in our coculture;
- conversely, 4/12 (33,3%), or 7/12 (58,3%) with a FDR \leq 0,1, of apparently Pax-repressed genes appeared upregulated, in a striatal-like direction, in our cocultured sample.

These results support the idea that a Pax6-mediated effect is responsible for the main molecular signature we observed in coculture experiments, especially in regards to transcription factors. However, it has to be emphasized that a Pax6-opposing signature, typical of subpallial interneurons, was also evident. Given that Pax6 is a fundamental player in pallial-subpallial identity distinction (Stoykova et al., 1996) and particularly in limiting GABA-ergic patterns to the subpallium (Kroll and O'Leary, 2005), as well as being essential for the formation of corticostriatal boundary structure (Stoykova et al., 1997), what we have reproduced might very well represent an element of the molecular tug-of-war that positions and defines the pallial-subpallial boundary.

Discussion

Acute preparations

Features of the isolated population

Concerning our results with acute preparations, microarray data shows that we have isolated a highly plastic and metabolically active population, undergoing rapid protein turnover, increased energy production and consumption and cytoskeletal rearrangement; the cell cycle progression also appears to be accelerated, as shown by S-phase labeling. This is not in accord with the typical features of boundary tissue, which is generally characterized by a lowered proliferation and metabolism (Bally-Cuif and Hammerschmidt, 2003), nor does it seem appropriate for a local, self-renewing staminal behavior; instead, it appears the signature of a dynamic, expanding and perhaps migrating group of cells. In situ hybridization experiments, although still underway, seem to support the idea that these characteristics are indeed not a feature of the boundary structure, although the identity of the population we are observing is yet to be determined.

Putative identity of the population

A possibility is that the increased metabolism, migration and proliferation are a feature of the early ventrolateral pallial neuroepithelium. The enhanced activity may reflect the necessity of a large expansion together with a substantial spatial relocation, which can take the form of either radial or tangential migration, as is the case for lateral cortical stream cells, which are involved in amygdala and pyriform cortex formation (Carney et al., 2006). An expansion of the ventralmost cortex would explain why RT-PCR experiments performed at E13.5 show in many cases an increase of signal in the vCx sample, sometimes reaching higher levels than in the Ah: the very narrow region, which is dissected as part of the Ah sample at E12.5, is widened by later stages and thus makes up a large part of the vCx sample by E13.5. In the light of the fast pace of this process, the high variability seen in replicates can therefore be caused by even slight embryonic stage and dissection differences among experimental sessions, as morphological indications available to discern the position of this region are very poor. The verification of

these hypotheses requires therefore a different tool, as for example the in situ hybridization technique we have begun to use.

Tissue distribution patterns of analyzed genes

In situ hybridizations failed to reveal boundary- or ventral pallium-specific gene expression domains; however, a few interesting observations can be done on our preliminary data.

Anaphase promoting complex, subunit 5 (Anapc5) seems to be located preferentially at the external margin of the proliferative layers: this is in accord with the mechanism of interkinetic nuclear migration (Messier, 1978), which postulates that the proliferation of cortical neurons is associated with a radial migration along radial glia fibers that brings the neuroblasts' soma in contact with the ventricular surface at the time of mitosis, while the S phase of the cell cycle occur closest to the pial surface (Takahashi et al., 1992). Thus, an outward location as the one observed can be associated to a late-S/G2 phase peak of expression, necessary to pave the way to the timely subsequent occurrence of anaphase.

While both Anapc5 and Sept5, being both involved in common cell cycle mechanisms, show a widespread distribution, a very clear regional confinement is observed for Ddah1, whose expression is exclusively found in neural proliferative layers and more markedly so in the ganglionic eminences, while the cortex shows a much lower expression with a negative ventral-to-dorsal gradient. In evaluating the implications of this peculiar distribution, it is important to consider the gene's role in neurogenesis homeostasis.

Ddah1 and NO signaling

Ddah1 gene appears to regulate positively the production of nitric oxide by depleting arginine derivatives such as N(omega)-methyl-L-arginine and N(omega)-N(omega)-dimethyl-L-arginine which compete for nitric oxide synthase (NOS) activity, thus removing a self-inhibitory loop and enhancing as a result nitric oxide production (Frey et al., 2006). As nitric oxide signaling normally seems to promote the conversion of neural stem cells into more advanced neural precursors and neurons (Cheng et al., 2003), it is interesting to observe that this gene is expressed by cellular layers where proliferation is

still ongoing. The higher expression in the basal ganglia may be explained by the much more pronounced and precocious formation of a post-proliferative compartment in the LGE than in the cortex. The same applies to the higher Ddah1 expression in the ventral-lateral pallium as compared to the dorsal-medial pallium, possibly reflecting the orientation of the main cortical neuronogenetic gradient.

Cocultures

As the acute results, although interesting, do not seem to rely information about the pallial-subpallial boundary and the patterning events taking place at the margin between different fields, we have chosen the artificial in vitro recreation of contact events as a tool for addressing these aspects.

Recreation of contact events

In order to understand what processes can be identified through the use of this technique, it is necessary to understand in what cases cells with a certain molecular identity come into contact with cells with a different identity and what is the physiological outcome of this contact event. In early patterning, cells that are initially homogeneous in expression patterns acquire molecular differences in response to external stimuli: contact is necessary for refinement and progression of these differences. Then, as a difference is established, a boundary can form at the interface between these regions. Positioning of this boundary results from the equilibration of contrasting influences within and between cells located around the interface and, in turn, the boundary region can acquire local molecular features which are not found in the original populations. Finally, as the boundary is established, the smoothing of the interface between the two adjacent fields may require that cells or groups of cells that have ended up surrounded by different tissue be “reprogrammed” to fit correctly with their position. In regards to the classes of genes that are predominantly involved in this processes, we expect to find genes involved in signaling and signal transduction, such as soluble factors, receptors or transcription factors.

Molecular counterparts of contact events

Therefore, two major classes of events can be expected when cells from different fields come into contact artificially: contact-specific events, representing emerging events of boundary establishment and local pattern formation, not found in either of the contributing populations; or identity shift events, in which the coculture acquires features typical of one of the contributing populations but not the other. We have employed different statistical techniques to identify candidates for these two classes and found a

small number of candidates for the first group, displaying a very low fold change if compared to the average of the contributing fields, while for the second class of events, a larger set of candidates appeared, from which it appeared that cortical features have a stronger tendency to be found in cocultured cells than striatal.

Contact-specific events

Regarding the relatively weak results in boundary-specific gene expression, this could be due to different factors. Even if there are contact-induced events, the culture time may be too short to give rise to significant gene expression changes (cells for these experiments were cultured for 24 hours, although it is possible that a shorter time was available for cell-to-cell contact as dissociated cells require some time to aggregate). Also, the culturing conditions may induce correct contact-type events only in a fraction of cells, thus diluting the gene expression variations. Not all cells in culture are part of an aggregate; even among those that are, there may be differences between cells located on the surface of an aggregate, in contact with the medium, and cells entirely surrounded by other cells. Even for a cell entirely embedded in the aggregate, it is a matter of chance whether the cells it comes in contact with are of the same tissutal identity, of the opposite identity or a combination, in different proportions, of both. As it is not known what proportions of heterotypical contact are able to induce a certain change, different programs could be induced by different proportions: for example, a cell entirely surrounded by a different tissue might be reprogrammed rather than acquire a boundary behavior. All these components could mask a real effect, as any gene expression variation in a subpopulation would be diluted with the rest of the cells and thus bring expression changes very close to experimental noise, thus making it harder to verify these data even by other techniques such as RT-PCR, as they would suffer from the same problems.

Identity shift events

Regarding the second class of events, in which a tissue's features are later found in the entire population, we can postulate two possible mechanisms to account for this effect: population kinetics asymmetries and instructive regulation.

Kinetic regulation

Cell contact may have a stimulating effect on the proliferation kinetics of a small subpopulation expressing high levels of a certain molecular signature, which expands clonally and thus justifies the higher abundance of that profile in the average of the entire sample. In this view, individual cells do not change their transcriptional profile, but the population as a whole does, as its components reach a different numerical balance. This mechanism is found in developmental processes, as for example in regulation through Wnt of cell cycle progression (Panhuysen et al., 2004) and is necessary to modulate relative abundances of local subpopulations. In our results, this model could be applied to explain the set of genes that acquire striatal behavior (see table 6 in Results): as they all point to a basal, GABA-ergic identity, they may represent an interneuronal precursor pool whose proliferation is enhanced by contact with cortical cells, perhaps representing a migration-triggered intermediate progenitor step in the production of this type of cells. The fact that all genes acquiring striatal characteristics do so by expression increase supports the idea that even a small population, if overexpressing those markers to a sufficient extent, could account for our observed results.

Instructive regulation

A radically different mechanism can also take place, in which cell-to-cell contact has an instructive effect, so that one or both cells change their expression profile as a result; such changes can be both an increase or decrease of gene expression. This may represent either a contact-dependent boundary refinement process, in which misplaced cells are “absorbed”, molecular identity-wise, into the surrounding tissue, or also a dynamic equilibrium between adjacent populations which is maintained *in vivo* by the interplay of long range acting opposing factors and is disrupted as the tissue is disaggregated while in culture. In that case, certain regional-specific molecular features that are generally kept in check by an opposing signal, as for example a morphogen gradient, could be induced through contact in neighboring cells. The fact that cortical features seem to spread on striatum-originated cells suggests that the counteracting mechanism that is required to maintain striatal identity has been disrupted or lost.

RA signaling

An interesting candidate in this case could be retinoic acid (RA) signaling, which is known to have a role in defining molecular identity of neurons born in the striatum (Wang and Liu, 2005) and, interacting with BMP signaling, may have a role in relaying positional information along the dorsoventral axis. In particular, while RA appears to enhance or sustain BMP signaling (Li et al., 2001) (Helfring et al., 2000), BMP attenuates the RA pathway by reducing the synthesis (Hoffman et al., 2006) of RA and the transduction of its signal (Means and Gudas, 1996). This interaction has a positional function in the patterning of the forelimb (Mic and Duester, 2003) and facial structures (Lee et al., 2001) and it is reasonable to foresee the possibility of a similar role in the telencephalon.

It is therefore interesting to note that three genes involved in RA processing and signaling, the retinoic acid receptor (RAR) beta (Rarb), retinaldehyde binding protein 1 (Rlbp1) and retinoic acid induced 2 (Rai2) are among the genes whose expression in cocultured material acquires cortex-like expression. It is important to note that the gene expression change is positive in two cases (Rlbp1 and Rai2) but negative in the case of Rarb, which suggests an instructive rather than kinetic mechanism: a downregulation effect taking place in a limited subpopulation would be likely diluted in the general signal.

The loss of Rarb in the cocultured sample should not be viewed as a complete loss of RA signaling responsiveness, although it is known that Rarb upregulation is instrumental in the striatum's higher competence to RA signals (Liao et al., 2005); instead, it might represent shifting of the cocultured striatal tissue to a cortical-like RA responsiveness profile. It should be noted that the striatum itself is a major source of RA, which is in turn an important regulator of identity and differentiation of local neurons (Toresson et al., 1999); therefore, the morphogen's dilution in the culture medium may account for the expression pattern shift. However, LGE samples cultured in the same condition do not show a reduction in this gene's levels; therefore, unless a very tight dose-dependent threshold is involved, the contact with cortical cells appears to be instrumental in this gene's decrease in expression. This could be mediated by secretion of BMP ligands by cortical cells (Furuta et al., 1997) or the reduction of a paracrine or adhesion-mediated reciprocal sustenance loop by striatal cells.

An interesting note is that, although RA signaling is Gsh2-dependent and Pax6 is known to antagonize Gsh2, the RA pathway/gene group is not directly connected to its Pax6 counterpart, as Pax6 removal does not rescue RA defects (i.e. Raldh3 loss) from Gsh2 $-/-$ mutants, although a large subsets of defects is indeed rescued (Waclaw et al., 2004).

Pax6 signature upregulation

The coordinated expression of Pax6-dependent genes that we have observed in the cocultured sample may be of extreme interest in our search for boundary events, as Pax6 seems to cover a high-level role in regulating several aspects of cortical patterning; most interesting in our case is its role in contrasting expression of basal genes in the ventral cortex (Stoykova et al., 1996) by repressing both striatal fates (Kroll and O’Leary, 2005) and interneuron migration into the cortex (Götz et al., 1998) (Chapouton et al., 1999). Pax6 is able to act upon cell surface characteristics, and therefore adhesion, migration and cell sorting (Talamillo et al., 2003) as well as being required for the development of pallial-subpallial boundary structural features (Stoykova et al., 1997). There are indications, from work in chimaeras, that such effects are cell-autonomous (Quinn et al., 2007), but in other cases, a non-cell-autonomous mechanism driven by Pax6 was also observed in reelin regulation (Stoykova et al., 2003) and this sort of inductive mechanism could be taking place in our case in response to a contact with a striatal population.

It is important to note that a striatal signature, represented by GABA metabolism genes and subpallial transcription factors, is not only present but upregulated, in opposition with typical Pax6 effect. This suggests that we are looking at two separate populations, one of which is overexpressing Pax6 and the subsequent (ventral) cortical identity, and one showing, in opposition, upregulation of striatal markers. This comes to no surprise, as cortical and striatal populations were mixed in our cocultured samples; it is however extremely interesting that they reacted to coculturing by overexpressing certain typical identity signatures whose expression domains are very tightly separated in vivo along the pallial-subpallial boundary, as if they “reacted” to the intermingling of cellular identities by reinforcing (and perhaps extending through instructive mechanisms) their own, as would happen during boundary establishment in vivo.

Conclusions

In the search for boundary events, our experiments have opened several fascinating lines of research that can be pursued in several ways.

We have identified a group of genes and processes upregulated in the area surrounding the corticostriatal boundary; we suspect the tissue expressing these genes may be involved in a burst of proliferation and migration, possibly in the perspective of expanding to give rise to parts of the paleocortex. In this regards, it will be necessary to verify the tissue distribution of these transcripts with better accuracy and over a larger period of time.

A small set of genes was also characterized by its peculiar expression found only when cells from different fields are cultured together. As these may represent boundary establishment and secondary patterning events, we wish to select and confirm candidates and try to characterize further their localization both in wild type and boundary-impaired mice such as Pax6 null mutants. Among transcriptional programs reactive to heterotypic contact in culture, some seem to represent the striatal and ventral cortical responses to reciprocal contact, strengthening identity features and regulating responsiveness to signaling molecules. The next information we wish to obtain is to assess whether such gene expression patterns are limited by the tissue of origin (i.e., cortical-like gene expression is only found, albeit upregulated, in cells originated from cortical dissected material) or if instructive events also take place. As antibodies are available for many of the identified genes, we plan to analyze their pattern of expression in individual cells, whose origin can be tracked through the use of wild type and constitutively fluorescent embryos for the preparation of heterotypic cocultures.

As a final note, our experiments provide hints on events related to different levels and steps of boundary positioning, establishment, patterning and function. Many features are still to be studied, as this particular boundary region is not yet well characterized, and our current results may be a starting point to shed light on this yet enigmatic structure.

List of abbreviations

Genes

Actb	actin, beta, cytoplasmic
Anapc5	anaphase-promoting complex subunit 5
Atp5b	ATP synthase, H ⁺ transporting mitochondrial F1 complex, beta subunit
COUP-TFI	chicken ovalbumin upstream promoter transcription factor 1, also known as nuclear receptor subfamily 2, group F, member 1 (Nr2f1)
Dbx1	developing brain homeobox 1
Ddah1	dimethylarginine dimethylaminohydrolase 1
Dlx2	distal-less homeobox 2
Eif5	eukaryotic translation initiation factor 5
ems	empty spiracles
Emx1	empty spiracles homolog 1 (Drosophila)
Emx2	empty spiracles homolog 2 (Drosophila)
En2	Egrailed 2
Eomes	eomesodermin homolog (xenopus laevis), also known as t-box brain gene 2 (Tbr2)
Fgf7	fibroblast growth factor 7
Fgf8	fibroblast growth factor 8
Fgf15	fibroblast growth factor 15
Fgf17	fibroblast growth factor 17
Fgf18	fibroblast growth factor 18
Fgfr1	fibroblast growth factor receptor 1
Fgfr2	fibroblast growth factor receptor 2
Fgfr3	fibroblast growth factor receptor 3
Foxg1	Forkhead box gene 1
Gad1	glutamic acid decarboxylase 1, also known as Gad67
Gad2	glutamic acid decarboxylase 2, also known as Gad65
Gapdh	glyceraldehyde-3-phosphate dehydrogenase
Gbx2	gastrulation brain homeobox 2
Isl1	ISL1 transcription factor, LIM/homeodomain
Ldhb	lactate dehydrogenase B
Lhx2	LIM homeobox protein 2
Lhx5	LIM homeobox protein 5
Mash1	mammalian achaete scute homolog 1, also known as achaete-scute complex homolog 1 (Drosophila) (Ascl1)
NeuroD1	neurogenic differentiation 1
NeuroD2	neurogenic differentiation 2
NeuroD6	neurogenic differentiation 6
Ngn1	neurogenin 1
Ngn2	neurogenin 2
Nhlh1	nescient helix loop helix 1
Nkx2.1	NK2 homeobox 1
Oprm1	opioid receptor, mu 1

otd	orthodenticle
Otx2	orthodenticle homologue 2
Pax6	paired box gene 6
Psmb7	proteasome (prosome, macropain) subunit, beta type
Rai2	retinoic acid induced 2
Rarb	retinoic acid receptor beta,
Rlbp1	retinaldehyde binding protein 1
Rpl35	ribosomal protein L35
Sept5	septin 5
Sfrp2	secreted frizzled-related protein 2
Shh	Sonic Hedgehog
Slc32a1	solute carrier family 32 (GABA vesicular transporter), member 1
Slc6a1	solute carrier family 6 (neurotransmitter transporter, GABA), member 1
Sp8	trans-acting transcription factor 8
Tbp	TATA box binding protein
Tbr1	t-box brain gene 1
Tbr2	t-box brain gene 2, also known as eomesodermin homolog (xenopus laevis) (Eomes)
Tcf4	transcription factor 4
Tcfap2c	transcription factor AP-2 gamma
Tgfa	transforming growth factor alpha
Wnt1	wingless-related MMTV integration site 1
Wnt2b	wingless-related MMTV integration site 2b
Wnt3a	wingless-related MMTV integration site 3a
Wnt5a	wingless-related MMTV integration site 5a
Wnt8	wingless-related MMTV integration site 8

Molecules

GABA	γ -aminobutyric acid
BMP	bone morphogenetic protein
Fgf	fibroblast growth factor
Wnt	Wingless analogue
Shh	sonic hedgehog
EGF	epidermal growth factor
NO	nitric oxide
RA	retinoic acid

Gene families

bHLH	basic helix-loop-helix factor
Emx	empty spiracle homeobox
Dlx	distal-less homeobox
Lhx	LIM homeobox
Gsh	GS homeobox
Hes	hairy and enhancer of split
Id	inhibitor of DNA binding

Reagents and techniques

BCIP	5-bromo-4-chloro-3-indolyl phosphate, toluidine salt
BFGF	basic fibroblast growth factor
BrdU	bromodeoxyuridine
BSA	bovine serum albumin
DAPI	4,6diamidino2phenylindole, dihydrochloride
DMEM-F12	Dulbecco's Modified Eagle's Medium : Ham's Nutrient Mixture F-12
DTT	dithiothreitol
EDTA	tetra(acetoxymethyl ester)
EGF	epidermal growth factor
FBS	fetal bovine serum
IdU	iododeoxyuridine
NBT	nitro blue tetrazolium chloride
NTE	NaCl Tris EDTA buffer
NTP	nucleoside 5'-triphosphates
PCR	polymerase chain reaction
PBS	phosphate buffered saline
RT-PCR	real time polymerase chain reaction
SSC	sodium chloride/sodium citrate buffer
UTP	uridine 5'-triphosphates

Embryonic structures and terms

Ah	antihem
ANR	anterior neural ridge
AP	anteroposterior
CNS	central nervous system
dCx	dorsal cortex
E	embryonic day
LGE	lateral ganglionic eminence
MGE	medial ganglionic eminence
MHB	midbrain-hindbrain boundary
VCx	ventral cortex
ZLI	zona limitans intrathalamica

Appendices

Appendix A

RT-PCR results for areal markers in acutely dissected E11.5 samples, acutely dissected E12.5 samples and E11.5 samples cultured for 24 hours. SD, standard deviation; fg, femtograms.

Emx1

Well / Set	Avg C(t)	C(t) SD	Avg fg	fg SD
Ah E11	22,85	0,27	0,6178	0,1451
Ah E12	21,53	1,03	2,376	1,616
Ah/Ah	23,79	0,42	0,2981	0,0885
Cx E11	20,67	0,21	3,529	0,5736
Cx/Cx	21,73	0,22	1,511	0,277
Cx/LGE	27,28	0,34	0,01751	0,005132
Cx/MGE	28	0,21	0,009578	0,001556
LGE E11	23,67	0,39	0,3257	0,1086
LGE E12	25,43	0,28	0,07689	0,01697
LGE/LGE	28,05	0,2	0,009214	0,001414
MGE E11	27,04	0,51	0,02215	0,007732
MGE E12	27,41	0,63	0,01723	0,008066
MGE/MGE	29,6	0,32	0,002685	0,000725
dCx E12	22,62	1,01	0,9798	0,66
vCx E12	21,16	0,11	2,369	0,209

Nkx2.1

Well / Set	Avg C(t)	C(t) SD	Avg fg	fg SD
Ah E11	36,42	0,96	0,00006475	0,00004269
Ah E12	33,21	0	0,0005614	0
Ah/Ah	35,73	1,34	0,0001241	0,00007964
Cx E11	35,63	0,58	0,0001006	0,00004435
Cx/Cx	N/A	N/A		
Cx/LGE	33,76	0,14	0,0003746	0,00003897
Cx/MGE	32,74	0,04	0,0007987	0,00002314
LGE E11	26,53	0,32	0,08679	0,02167
LGE E12	30,61	0,17	0,003978	0,0005078
LGE/LGE	28,42	0,63	0,02246	0,008549
MGE E11	27,47	0,47	0,0446	0,01703
MGE E12	24,35	0,3	0,4434	0,09953
MGE/MGE	25,71	0,23	0,1586	0,02851
dCx E12	35,71	0	0,00008642	0
vCx E12	30,74	0,14	0,003621	0,0003857

Oprm1

Well / Set	Avg C(t)	C(t) SD	Avg fg	fg SD
Ah E11	33,62	0	0,000309	0
Ah E12	30,62	0,51	0,003346	0,001238
Ah/Ah	32,26	0,48	0,0009333	0,0002913
Cx E11	38,27	0	0,000008711	0
Cx/Cx	34,94	0	0,000112	0
Cx/LGE	30,42	0,57	0,003929	0,001415
Cx/MGE	34,26	0,43	0,0002007	0,00007042
LGE E11	24,5	0,6	0,3834	0,1925
LGE E12	26,81	0,02	0,05794	0,0009188
LGE/LGE	24,97	0,26	0,2425	0,0513
MGE E11	26,38	0,56	0,08849	0,03843
MGE E12	27,22	0,27	0,04315	0,008714
MGE/MGE	27,31	0,19	0,03969	0,005589
dCx E12	34,61	0,14	0,0001455	0,00001573
vCx E12	35,38	0	0,00008023	0

Dbx1

Well / Set	Avg C(t)	C(t) SD	Avg fg	fg SD
Ah E11	27,74	0,23	0,05139	0,007936
Ah E12	26,61	0,12	0,1135	0,009307
Ah/Ah	29,13	0,57	0,02034	0,007371
Cx E11	29,09	0,39	0,02021	0,005916
Cx/Cx	32,3	0,28	0,002029	0,0004047
Cx/LGE	32,14	0,11	0,002237	0,0001776
Cx/MGE	35,89	0,4	0,0001616	0,00004121
LGE E11	26,14	0,47	0,1675	0,05993
LGE E12	31,94	0,31	0,002637	0,0005757
LGE/LGE	30,58	0,34	0,006925	0,001539
MGE E11	25,63	0,35	0,2335	0,0608
MGE E12	27,35	0,23	0,06765	0,01117
MGE/MGE	29,09	0,25	0,01971	0,003248
dCx E12	31,06	0,14	0,004823	0,0004757
vCx E12	28,31	0,53	0,03627	0,01299

Sfrp2

Well / Set	Avg C(t)	C(t) SD	Avg fg	fg SD
Ah E11	24,32	0,16	0,8199	0,08817
Ah E12	20,81	0,05	8,923	0,2985
Ah/Ah	26,1	0,4	0,2502	0,06098
Cx E11	22,61	0,21	2,645	0,4008
Cx/Cx	24,72	0,32	0,6352	0,1285
Cx/LGE	29,21	0,46	0,03031	0,008596
Cx/MGE	30,37	0,23	0,0133	0,002001
LGE E11	20,23	0,37	13,66	3,517
LGE E12	22,83	0,11	2,263	0,1639
LGE/LGE	25,26	0,26	0,4352	0,07111
MGE E11	21,24	0,34	6,829	1,649
MGE E12	22,06	0,19	3,825	0,4986
MGE/MGE	25,82	0,17	0,2948	0,03448
dCx E12	21,82	0,27	4,555	0,8161
vCx E12	23,11	0,03	1,86	0,04135

Gapdh

Well / Set	Avg C(t)	C(t) SD	Avg fg	fg SD
Ah E11	14,9	0,13	598	53,46
Ah E12	12,83	0,07	2469	111,1
Ah/Ah	16,95	0,41	152,4	41,4
Cx E11	13,96	0,05	1139	36,59
Cx/Cx	15,1	0,11	523,1	40,01
Cx/LGE	20,55	0,39	12,93	3,248
Cx/MGE	20,55	0,15	12,53	1,295
LGE E11	12,31	0,16	3526	372,2
LGE E12	11,92	0,06	4599	196,2
LGE/LGE	16,22	0,35	248,2	59,03
MGE E11	12,3	0,15	3564	366,8
MGE E12	11,73	0,08	5219	287,9
MGE/MGE	15,96	0,25	292,5	51,34
dCx E12	12,85	0,04	2432	58,32
vCx E12	12,39	0,02	3336	48,03

Fgf7

Well / Set	Avg C(t)	C(t) SD	Avg fg	fg SD
Ah E11	31,01	0,36	0,0007547	0,0002168
Ah E12	25,82	0,14	0,03531	0,003619
Ah/Ah	30,69	0,42	0,0009708	0,0002893
Cx E11	28,95	0,21	0,00342	0,0005308
Cx/Cx	29,81	0,34	0,001844	0,0004897
Cx/LGE	35,8	0,8	0,00002355	0,00001058
Cx/MGE	34,9	0,6	0,00004413	0,00002066
LGE E11	26,07	0,17	0,0293	0,003671
LGE E12	26,02	0,76	0,03525	0,01813
LGE/LGE	28,9	0,34	0,00363	0,0009222
MGE E11	25,4	0,4	0,05038	0,01628
MGE E12	24,84	1,07	0,0978	0,06488
MGE/MGE	29,33	0,09	0,002562	0,0001766
dCx E12	27,78	0,33	0,008392	0,002032
vCx E12	28,6	0,11	0,00442	0,0003521

Tbp

Well / Set	Avg C(t)	C(t) SD	Avg fg	fg SD
Ah E11	22,8	0,36	2,101	0,5898
Ah E12	19,41	0,22	23,78	3,813
Ah/Ah	23,46	0,34	1,295	0,3044
Cx E11	21,06	0,22	7,189	1,142
Cx/Cx	22,2	0,49	3,299	1,006
Cx/LGE	26,99	0,45	0,103	0,02918
Cx/MGE	27,5	0,07	0,0678	0,00342
LGE E11	19,11	0,2	29,5	4,402
LGE E12	19,07	0,69	33,86	15,57
LGE/LGE	22,39	0,39	2,823	0,7889
MGE E11	19,66	0,24	19,87	3,241
MGE E12	18,76	0,2	37,96	5,34
MGE/MGE	22,44	0,2	2,651	0,4
dCx E12	19,67	0,23	19,77	3,189
vCx E12	20,04	0,69	16,77	7,75

Actb

Well / Set	Avg C(t)	C(t) SD	Avg fg	fg SD
Ah E11	18,4	0,22	21,71	3,884
Ah E12	17,03	0,47	68,05	24,34
Ah/Ah	18,25	0,44	25,46	8,941
Cx E11	16,53	0,2	95,33	13,96
Cx/Cx	17,19	0,18	56,34	8,203
Cx/LGE	21	0,29	2,765	0,5835
Cx/MGE	23,96	0,18	0,2574	0,03823
LGE E11	14,05	0,33	708,2	195,7
LGE E12	17,72	0,26	37,47	7,788
LGE/LGE	16,65	0,2	86,65	12,99
MGE E11	16,34	0,42	116,9	41,25
MGE E12	16,55	0,04	93,44	3,234
MGE/MGE	17,81	0,27	35,05	7,744
dCx E12	18,05	0,76	33,51	18,15
vCx E12	17,97	0,13	30,22	3,135

Appendix B

Results of Affymetrix hybridization of acutely dissected E12.5 embryonal regions (Ah, Cx and LGE), filtered for a positive ≥ 3 fold change between Cx and Ah and LGE and Ah.

Probe id	Gene name	Ah	Cx	LGE
1415690_at	mitochondrial ribosomal protein L27	273,39	80,11	25,56
1415864_at	2,3-bisphosphoglycerate mutase	131	37,54	3,91
1415895_at	small nuclear ribonucleoprotein N	1677,91	453,61	656,47
1415896_x_at	small nuclear ribonucleoprotein N	1474,53	374,66	571,79
1416088_a_at	ribosomal protein S15	4705,46	1376,34	1067,28
1416183_a_at	lactate dehydrogenase B	2000,18	593,65	390,7
1416240_at	proteasome (prosome, macropain) subunit, beta type 7	2288,84	498,62	101,85
1416243_a_at	ribosomal protein L35	4963,78	1206,03	603,25
1416269_at	ATP synthase, H ⁺ transporting, mitochondrial F0 complex, subunit f, isoform 2	1871,27	356,12	323,03
1416313_at	myeloid/lymphoid or mixed-lineage leukemia (trithorax homolog, Drosophila); translocated to, 11	3717,95	966,58	989,05
1416365_at	heat shock protein 90kDa alpha (cytosolic), class B member 1	786,62	218,9	73,63
1416483_at	tetratricopeptide repeat domain 3	2544,98	607,27	320,49
1416494_at	NADH dehydrogenase (ubiquinone) Fe-S protein 5	454,49	121,16	106,41
1416495_s_at	NADH dehydrogenase (ubiquinone) Fe-S protein 5	883,83	269,93	74,02
1416829_at	ATP synthase, H ⁺ transporting mitochondrial F1 complex, beta subunit	3587,54	761,67	540,61
1416902_a_at	cytochrome c oxidase, subunit Vb	2356,28	638,42	333,48
1416906_at	anaphase-promoting complex subunit 5	1824,25	379,14	38,73
1416979_at	proteasome maturation protein	1334,38	303,44	194,3
1417005_at	kinesin 2	2606,68	798,01	538,82
1417028_a_at	tripartite motif protein 2	1112,44	249,15	67,11
1417176_at	casein kinase 1, epsilon	1269,77	323,74	333,94
1417219_s_at	thymosin, beta 10	4578,32	1166,43	1544,51
1417258_at	chaperonin subunit 5 (epsilon)	2260,91	649,69	753,47
1417428_at	guanine nucleotide binding protein (G protein), gamma 3 subunit	2168,18	588,2	1284
1418139_at	doublecortin	2586,1	680,86	533,9
1418178_at	internexin neuronal intermediate filament protein, alpha	1792,27	345,74	935,44
1418562_at	splicing factor 3b, subunit 1	1349,01	334,08	233,66
1418717_at	mitochondrial ribosomal protein S25	260,06	30,06	83,56
1419038_a_at	casein kinase 2, alpha 1 polypeptide	2862,77	524,48	133,94
1419584_at	tetratricopeptide repeat domain 28	2669,9	688,08	357,26
1419845_at	distal-less homeobox 1, antisense	307,66	56,16	144,87
1420622_a_at	heat shock protein 8 /// similar to heat shock protein 8 /// heat shock protein 8 pseudogene /// similar to heat shock protein 8	3705,73	987,98	1127,53
1420874_at	twinfilin, actin-binding protein, homolog 1 (Drosophila)	191,82	56,65	35,1
1421027_a_at	myocyte enhancer factor 2C	467,6	72,78	41,36

1421144_at	retinitis pigmentosa GTPase regulator interacting protein 1	2861,02	411,88	383,55
1421193_a_at	pre B-cell leukemia transcription factor 3	464,29	98,55	291,55
1421323_a_at	GTPase activating protein (SH3 domain) binding protein 2	3009,43	923	336,62
1421534_at	deafness, autosomal dominant 5 homolog (human)	1615,48	171,5	40,18
1421754_at	cDNA sequence AY036118	1407,55	249,46	479,24
1421955_a_at	Nedd4 (ubiquitin-like)	991,37	234,78	125,79
1421986_at	eukaryotic translation initiation factor 4E member 2	59,44	7,37	92,12
1422146_at	sema domain, seven thrombospondin repeats (type 1 and type 1-like), transmembrane domain (TM) and short cytoplasmic domain, (semaphorin) 5B	1104,15	97,5	281,28
1422432_at	diazepam binding inhibitor	1642,28	345,82	385,1
1422564_at	actin-like 6B	640,92	143,92	93,34
1422589_at	RAB3A, member RAS oncogene family	686,14	193,75	456,38
1422751_at	transducin-like enhancer of split 1, homolog of Drosophila E(spl)	1804,53	411,51	332,49
1422943_a_at	heat shock protein 1	297,79	71,74	179,15
1423030_at	valosin containing protein /// similar to Transitional endoplasmic reticulum ATPase (TER ATPase) (15S Mg(2+)-ATPase p97 subunit) (Valosin-containing protein) (VCP)	1045,93	255,16	87,54
1423111_at	ATP synthase, H ⁺ transporting, mitochondrial F1 complex, alpha subunit, isoform 1	2313,54	450,62	335,06
1423280_at	stathmin-like 2	2097,55	389,86	462,05
1423281_at	stathmin-like 2	2056,33	323,75	400,27
1423537_at	growth associated protein 43	1021,4	188,73	184
1423568_at	proteasome (prosome, macropain) subunit, alpha type 7	743,05	208,87	27,25
1423715_a_at	Nedd8 (ubiquitin-like)	2500,27	643,59	342,42
1423813_at	kinesin family member 22	157,03	45,44	45,98
1424269_a_at	myosin, light polypeptide 6, alkali, smooth muscle and non-muscle /// predicted gene, EG433297 /// predicted gene, EG667952 /// similar to Myosin light polypeptide 6 (Myosin light chain alkali 3) (Myosin light chain 3) (MLC-3) (LC17)	1285,11	354,46	280,19
1424398_at	DEAH (Asp-Glu-Ala-His) box polypeptide 36	1049,79	278,53	238,28
1424403_a_at	RUN and FYVE domain containing 3	268,72	70,89	99,25
1425784_a_at	olfactomedin 1	1194,58	292,98	63,79
1425966_x_at	ubiquitin C	2212,54	649,38	1288,75
1426060_at	Cul4, cullin ubiquitin-ligase gene family, promoter of tumor progression	330,04	63,62	73,74
1426061_x_at	Cul4, cullin ubiquitin-ligase gene family, promoter of tumor progression	518,99	70,49	172,55
1426504_a_at	ring finger protein 121	275,79	42,31	94,44
1426514_at	RIKEN cDNA 4631426J05 gene	157,12	13,07	46,4
1426578_s_at	SNAP-associated protein, secretion & endocytosis	1038,42	257,41	359,29
1426645_at	heat shock protein 90kDa alpha (cytosolic), class A member 1	1254,84	364,27	142,09
1426793_a_at	ribosomal protein L14	888,99	189,53	44,49
1426804_at	SWI/SNF related, matrix associated, actin dependent regulator of chromatin, subfamily a, member 4	1962	501,73	367,45
1426865_a_at	neural cell adhesion molecule 1	1807,47	280,17	371,68
1426930_at	bruno-like 4, RNA binding protein (Drosophila)	1457,28	329,52	425,34
1427019_at	protein tyrosine phosphatase, receptor type Z, polypeptide 1	1517,54	421,24	601,12
1427256_at	chondroitin sulfate proteoglycan 2 (NG-2 or versican)	1597,05	459,94	711,24
1427260_a_at	tropomyosin 3, gamma	3118,05	873,9	442,02
1427266_at	polybromo 1	802,47	222,72	357,29

1427347_s_at	tubulin, beta 2a /// tubulin, beta 2b /// similar to tubulin, beta 3 /// similar to tubulin, beta 3	2306,6	485,83	620,61
1427640_a_at	runt-related transcription factor 1; translocated to, 1 (cyclin D-related)	234,85	47,48	132,79
1427863_at	histone cluster 1, H3d	953,42	89,67	237,93
1429298_at	dimethylarginine dimethylaminohydrolase 1	1608,21	425,24	442,47
1429761_at	reticulon 1	2896,65	647,42	505,21
1429772_at	plexin A2	1296,63	349,58	135,94
1430791_at	RIKEN cDNA 6330415B21 gene	621,15	167,7	121,23
1431225_at	SRY-box containing gene 11	6801,8	959	2585,71
1431326_a_at	tropomodulin 2	249,56	64,48	53,47
1431328_at	protein phosphatase 1, catalytic subunit, beta isoform	2233,87	368,73	868,64
1432158_a_at	trafficking protein particle complex 2	1223,79	250,57	335,32
1433689_s_at	ribosomal protein S9	2098,6	624,8	81,22
1434375_at	RIKEN cDNA B930006L02 gene	1763,2	463,28	212,42
1434499_a_at	lactate dehydrogenase B	3511,64	1010,77	1163,78
1434853_x_at	makorin, ring finger protein, 1	1856,44	459,41	206,46
1435113_x_at	stathmin-like 3	4730,56	1194,65	1064,15
1435129_at	Protein tyrosine phosphatase 4a2	5471,35	429,98	1264,43
1435137_s_at	RIKEN cDNA 1200015M12 gene /// RIKEN cDNA 1200016E24 gene /// RIKEN cDNA A130040M12 gene /// RIKEN cDNA E430024C06 gene	292,92	53,97	66,42
1435178_x_at	anaphase-promoting complex subunit 5	3322,2	985,48	735,95
1435395_s_at	ATP synthase, H ⁺ transporting, mitochondrial F0 complex, subunit f, isoform 2	3688,38	891,7	734,36
1435767_at	sodium channel, voltage-gated, type III, beta	727,88	185,04	205,19
1435872_at	similar to human protooncogene PIM1, encoding a protein kinase	1231,08	188,41	222,36
1436760_a_at	ribosomal protein S8	3839,86	899,11	665
1436985_at	zinc finger protein 644	490,06	132,29	236,41
1437148_at	actin related protein 2/3 complex, subunit 2	2925,97	880,92	1132,79
1437195_x_at	mitogen activated protein kinase 10	594,53	144,18	246,09
1437224_at	reticulon 4	908,53	176,91	170,89
1437234_x_at	protein arginine N-methyltransferase 2	2053,66	499,53	304,04
1437246_x_at	ribosomal protein S6 /// predicted	2715,86	757,76	576,47
1437281_x_at	XPA binding protein 2	1104,62	302,66	528,96
1437784_at	runt-related transcription factor 1; translocated to, 1 (cyclin D-related)	459,4	116,44	181,86
1437841_x_at	cold shock domain containing C2, RNA binding (pippin)	1604,67	289,59	1244,08
1438194_at	RIKEN cDNA 2900019G14 gene	458,09	100,6	49,97
1438403_s_at	gb:BF537798 /DB_XREF=gi:11625166 /DB_XREF=602053404F1 /CLONE=IMAGE:4192561 /FEA=EST /CNT=31 /TID=Mm.218611.2 /TIER=Stack /STK=10 /UG=Mm.218611 /LL=54409 /UG_GENE=Ramp2 /UG_TITLE=receptor (calcitonin) activity modifying protein 2	523,78	153,2	139
1438714_at	zinc finger protein 207	1428,92	100,73	311,21
1439634_at	RIKEN cDNA 4930505D03 gene	56,74	15,41	5,33
1440154_at	Pre B-cell leukemia transcription factor 3	53,52	12,2	35,06
1440346_at	Jumonji domain containing 3, PKC target	670,41	152,02	102,13
1440862_at	Transcribed locus	380,71	16,56	108,84
1441656_at	RIKEN cDNA B930068K11 gene	367,81	83,13	254,47
1442408_at	sulfatase 2	206,15	40	59,94

1442786_s_at	RUN and FYVE domain containing 3	1601,13	391,94	126,71
1444001_at	Spermatid perinuclear RNA binding protein	162,57	6,41	9,99
1444020_at	chondroitin sulfate proteoglycan 3 (neurocan)	2236,36	79,94	488,86
1445727_at	ubiquitin protein ligase E3A	28,41	3,91	6,39
1446682_at	Transcribed locus	431,13	22,72	88,99
1447298_at	RIKEN cDNA C130071C03 gene	320,3	23,38	37,71
1447483_s_at	RIKEN cDNA 2610002F03 gene	3,91	17,6	27,8
1448113_at	stathmin 1 /// similar to Stathmin (Phosphoprotein p19) (pp19) (Oncoprotein 18) (Op18) (Leukemia-associated phosphoprotein p18) (pp17) (Prosolin) (Metablastin) (Pr22 protein) (Leukemia-associated gene protein)	545,97	127,42	162,22
1448145_at	WW domain containing E3 ubiquitin protein ligase 2	253,27	28,98	63,57
1448166_a_at	proteasome (prosome, macropain) subunit, beta type 1	2042,75	548,22	445,13
1448172_at	malate dehydrogenase 1, NAD (soluble)	1992,37	537,38	430,12
1448251_at	RIKEN cDNA 9030425E11 gene	199,09	54,53	62,12
1448361_at	tetratricopeptide repeat domain 3	4287,59	1090,29	958,11
1448405_a_at	EP300 interacting inhibitor of differentiation 1	4753,13	1294,98	1585,35
1448406_at	EP300 interacting inhibitor of differentiation 1	2561,67	693,51	162,6
1448430_a_at	nascent polypeptide-associated complex alpha polypeptide /// predicted gene, EG628277 /// similar to nascent polypeptide-associated complex alpha polypeptide /// similar to nascent polypeptide-associated complex alpha polypeptide	3732,69	925,51	711,04
1448533_at	tubulin folding cofactor B	1584,08	402,33	156,71
1448628_at	secretogranin III	633,65	184,96	165,42
1448754_at	retinol binding protein 1, cellular	721,74	72,49	268,54
1448770_a_at	ATPase inhibitory factor 1	3628,61	1103,08	1055,39
1448895_a_at	catenin (cadherin associated protein), alpha 2	671,3	169,08	72,74
1449069_at	zinc finger protein 148, induces mouse ES cells expansion	1150,02	261,04	320,34
1450008_a_at	catenin (cadherin associated protein), beta 1	1077,11	204,91	19,04
1450720_at	acid phosphatase 1, soluble	1075,04	290,08	238,83
1450815_s_at	coiled-coil-helix-coiled-coil-helix domain containing 2 /// RIKEN cDNA 2410018M08 gene	3176,29	950,84	592,09
1450849_at	heterogeneous nuclear ribonucleoprotein U	687,48	130,38	265,51
1451020_at	glycogen synthase kinase 3 beta	907,21	189,38	267,35
1451070_at	guanosine diphosphate (GDP) dissociation inhibitor 1	2585,24	726,42	1122,93
1452240_at	bruno-like 4, RNA binding protein (Drosophila)	2055,25	513,61	794,39
1452357_at	glycoprotein Ib, beta polypeptide /// septin 5	1716,49	407,61	541,61
1452433_at	gb:BB662083 /DB_XREF=gi:16495838 /DB_XREF=BB662083 /CLONE=D830021I19 /FEA=mRNA /CNT=22 /TID=Mm.218310.1 /TIER=ConsEnd /STK=0 /UG=Mm.218310 /UG_TITLE=Murine (DBA2) mRNA fragment for gag related peptide	177,72	33,84	56,98
1452844_at	POU domain, class 6, transcription factor 1	457,86	132,56	184,68
1453015_at	RIKEN cDNA 5830471E12 gene	2350,34	628,13	532,99
1453729_a_at	ribosomal protein L37	4555,61	1218,54	969,97
1453818_a_at	RIKEN cDNA 9030025P20 gene	144,91	26,81	33,04
1454373_x_at	ubiquitin C	322,93	59,53	104,41
1454454_at	Elav2 - HuR	984,84	149,61	67,24
1454664_a_at	eukaryotic translation initiation factor 5	2760,43	794,65	308,04
1454674_at	fasciculation and elongation protein zeta 1 (zygin I)	3656,81	932,28	843,99

1454758_a_at	TSC22 domain family, member 1	3491,34	902,24	359,56
1455867_at	SRY-box containing gene 4	225,29	55,25	117,22
1455976_x_at	diazepam binding inhibitor	4163,59	1177,99	475,2
1456054_a_at	pumilio 1 (Drosophila)	2812,82	693,13	749,74
1456393_at	RIKEN cDNA 2310002J21 gene	3304,66	592,32	490,98
1456565_s_at	mitogen activated protein kinase kinase kinase 12	107,15	27,04	13,42
1457047_at	Transcribed locus	173,84	18,64	43,69
1458439_a_at	RIKEN cDNA 2310047C04 gene	583,78	170,85	87,35
1459672_at	Topoisomerase (DNA) I	127,28	12,26	60,37
1459801_at	UDP-Gal:betaGlcNAc beta 1,3-galactosyltransferase, polypeptide 5	346,23	37,58	49,08
1459860_x_at	tripartite motif protein 2	3773,1	673,46	469,92
	gb:BB473929 /DB_XREF=gi:16439785 /DB_XREF=BB473929 /CLONE=D330003M06 /FEA=EST /CNT=5 /TID=Mm.214471.1			
1460084_at	/TIER=ConsEnd /STK=3 /UG=Mm.214471 /UG_TITLE=ESTs, Weakly similar to ENV1_HUMAN RETROVIRUS-RELATED ENV POLYPROTEIN (H.sapiens)	135,03	31,76	11,95
1460187_at	secreted frizzled-related sequence protein 1	65,81	264,59	12,1
1460432_a_at	eukaryotic translation initiation factor 3, subunit 6	2380,3	670,67	521,65

Appendix C

RT-PCR results for selected makers on acutely dissected E12.5 samples. SD, standard deviation; fg, femtograms.

Replicate experiment 1

Dbx1

	C(t)	C(t) SD	fg	fg SD
Ah E11.5	26,08	0,09	0,189	0,01176
Ah E12.5	25,38	0,06	0,3133	0,01417
Ah E13.5	27,97	0,15	0,04828	0,005369
LGE E11.5	37,52	0	4,96E-05	0
LGE E12.5	34,5	0,4	0,0004365	0,0001363
LGE E13.5		0		0
dCx E11.5	27,83	0,15	0,05369	0,005458
dCx E12.5	31,4	0,58	0,004102	0,00163
dCx E13.5	26,96	0,27	0,1002	0,02002
vCx E11.5	28,22	0,15	0,04055	0,004264
vCx E12.5	30,75	0,19	0,006534	0,0009625
vCx E13.5	27,03	0,24	0,09504	0,01695

Ddah1

	C(t)	C(t) SD	fg	fg SD
Ah E11.5	20,86	0,2	2,64	0,3989
Ah E12.5	17,72	0,17	28,12	3,613
Ah E13.5	16,98	0,15	49,08	5,247
LGE E11.5	25,28	0,07	0,09243	0,005133
LGE E12.5	18,5	0,19	15,66	2,211
LGE E13.5	18,05	0,17	2,19E+01	2,801
dCx E11.5	19,81	0,13	5,79	0,5796
dCx E12.5	18,93	0,22	11,36	1,925
dCx E13.5	16,6	0,22	65,29	10,35
vCx E11.5	21,98	0,12	1,126	0,1013
vCx E12.5	20,18	0,24	4,42E+00	0,8612
vCx E13.5	16,16	0,23	91,89	15,35

Anapc5

	C(t)	C(t) SD	fg	fg SD
Ah E11.5	20,35	0,1	3,687	0,308
Ah E12.5	18,31	0,11	20,71	1,923
Ah E13.5	18,92	0,32	12,81	3,174
LGE E11.5	25,04	0,45	0,07474	0,02996
LGE E12.5	21,01	0,99	2,857	1,907
LGE E13.5	23,55	0,12	2,47E-01	0,02474
dCx E11.5	17,45	0,16	43,35	5,575
dCx E12.5	18,91	0,29	12,85	2,94
dCx E13.5	15,01	0,65	396,3	232,8
vCx E11.5	20,52	0,16	3,21E+00	0,4374
vCx E12.5	21,39	0,29	1,58E+00	0,4058
vCx E13.5	15,83	0,51	186,1	86,28

Sept5

	C(t)	C(t) SD	fg	fg SD
Ah E11.5	24,13	0,12	0,09023	0,008465
Ah E12.5	21,73	0,1	0,644	0,05205
Ah E13.5	26,43	0,08	0,01369	0,0009592
LGE E11.5	29,84	0,37	0,0008692	0,000236
LGE E12.5	24,16	0,18	0,08813	0,01311
LGE E13.5	30,27	0,43	6,27E-04	0,0002357
dCx E11.5	22,9	0,15	0,247	0,03115
dCx E12.5	25,26	0,6	0,03979	0,01724
dCx E13.5	20,8	0,49	1,484	0,507
vCx E11.5	25,64	0,28	0,02664	0,005682
vCx E12.5	26,94	0,23	9,14E-03	0,001728
vCx E13.5	20,57	0,29	1,693	0,3694

Atp5b

	C(t)	C(t) SD	fg	fg SD
Ah E11.5	17,79	0,05	14,9	0,6614
Ah E12.5	15,1	0,33	179,5	52,41
Ah E13.5	12,59	0,47	1824	718,3
LGE E11.5	21,81	1,16	0,6913	0,7104
LGE E12.5	16,29	0,1	58,47	5,5
LGE E13.5	14,28	0,15	3,65E+02	47,77
dCx E11.5	14,81	0,1	223,8	20,78
dCx E12.5	14,97	0,22	197,2	40,36
dCx E13.5	10,51	0,67	1,35E+04	8663
vCx E11.5	17,81	0,36	1,56E+01	5,448
vCx E12.5	16,02	0,10	7,45E+01	6,605
vCx E13.5	13,26	0,15	918,6	117,1

Eif5

	C(t)	C(t) SD	fg	fg SD
Ah E11.5	18,57	0,32	13,66	3,277
Ah E12.5	16,71	0,28	52,22	10,18
Ah E13.5	15,69	0,32	110,1	23,99
LGE E11.5	23,72	0,53	0,3387	0,1268
LGE E12.5	17,82	0,26	23,32	4,556
LGE E13.5	18,06	0,15	1,93E+01	2,128
dCx E11.5	15,9	0,2	93,65	14,37
dCx E12.5	16,47	0,15	61,51	6,779
dCx E13.5	14,1	0,42	359,7	113,2
vCx E11.5	18,84	0,42	11,42	3,638
vCx E12.5	17,92	0,07	2,14E+01	1,105
vCx E13.5	15,22	0,08	151	8,701

Rpl35

	C(t)	C(t) SD	fg	fg SD
Ah E11.5	16,3	0,22	18,6	3,017
Ah E12.5	14,43	0,29	68,26	14,73
Ah E13.5	11,67	0,25	456,3	81,56
LGE E11.5	23,26	4,33	0,9325	0,8749
LGE E12.5	15,34	0,33	36,52	7,71
LGE E13.5	14,15	0,22	8,23E+01	13,32
dCx E11.5	13,3	0,13	146,5	13,1
dCx E12.5	13,68	0,22	113,4	18,25
dCx E13.5	10,07	0,49	1432	4,78E+02
vCx E11.5	16,96	0,48	12,23	3,532
vCx E12.5	14,63	0,13	5,83E+01	5,008
vCx E13.5	12,06	0,46	358,5	98,72

Psmb7

	C(t)	C(t) SD	fg	fg SD
Ah E11.5	19,42	0,59	3,452	1,564
Ah E12.5	17,38	0,1	13,26	0,9099
Ah E13.5	15,15	0,1	64,49	4,773
LGE E11.5	25,03	0,35	0,06136	0,01475
LGE E12.5	20,25	0,2	1,763	0,2418
LGE E13.5	18,6	0,52	5,982	2,196
dCx E11.5	16,49	0,22	25,24	3,85
dCx E12.5	19,7	0,18	2,603	0,312
dCx E13.5	13,84	0,39	168	48,57
vCx E11.5	19,64	0,4	2,793	0,7556
vCx E12.5	20,6	0,27	1,363	0,2587
vCx E13.5	15,43	0,45	55,09	15,51

Ldhh

	C(t)	C(t) SD	fg	fg SD
Ah E11.5	23,07	0,19	0,1183	0,01497
Ah E12.5	21,05	0,08	0,4978	0,02785
Ah E13.5	19,59	0,18	1,43	0,1732
LGE E11.5	30,33	0,33	0,0006656	0,0001637
LGE E12.5	24,54	0,38	0,04237	0,01226
LGE E13.5	25,54	0,21	2,03E-02	0,003198
dCx E11.5	20,36	0,92	1,02	0,6959
dCx E12.5	24,45	0,06	0,04358	0,001946
dCx E13.5	18,27	0,11	3,66E+00	0,2849
vCx E11.5	23,8	0,19	7,00E-02	0,009178
vCx E12.5	25,45	0,11	2,14E-02	0,001645
vCx E13.5	18,9	0,24	2,35	0,3818

Gapdh

	C(t)	C(t) SD	fg	fg SD
Ah E11.5	16,12	0,2	161,9	19,13
Ah E12.5	13,08	0,35	1034	203,6
Ah E13.5	11,09	0,25	3415	540,8
LGE E11.5	19,84	1,3	23,04	18,16
LGE E12.5	13,19	0,22	955,5	132
LGE E13.5	12,47	0,21	1,48E+03	184,7
dCx E11.5	11,83	0,64	2339	967,7
dCx E12.5	11,62	0,3	2500	459,7
dCx E13.5	9,74	0,14	7699	635,8
vCx E11.5	15,74	0,09	202,7	11,34
vCx E12.5	12,03	0,30	1,95E+03	366,7
vCx E13.5	10,95	0,17	3695	385,9

Replicate experiment 2**Dbx1**

	C(t)	C(t) SD	fg	fg SD
Ah E11.5	28,16	0,21	0,009188	0,001426
Ah E12.5	30,44	0,19	0,001646	0,0002455
Ah E13.5	34,42	0,7	9,39E-05	5,03E-05
LGE E11.5	31,72	0,53	0,0006693	0,000254
LGE E12.5	33,57	0,01	0,000155	1,26E-06
LGE E13.5	N/A	N/A		
dCx E11.5	33,20	0,35	0,0002108	5,89E-05
dCx E12.5	33,59	0,94	0,0001986	0,0001486
dCx E13.5	33,92	0,26	0,0001214	2,39E-05
vCx E11.5	32,07	0,6	0,0005294	0,0002346
vCx E12.5	30,86	0,45	0,001261	0,0004541
vCx E13.5	34,57	0,68	8,18E-05	3,57E-05

Anapc5

	C(t)	C(t) SD	fg	fg SD
Ah E11.5	20,33	0,36	1,212	0,3304
Ah E12.5	23,12	0,41	0,1268	0,04398
Ah E13.5	23,15	0,32	1,21E-01	2,85E-02
LGE E11.5	20,79	0,24	0,8137	0,1485
LGE E12.5	22,76	0,44	0,1715	5,62E-02
LGE E13.5	24,64	0,49	0,03799	0,01666
dCx E11.5	24,90	0,34	0,02933	8,62E-03
dCx E12.5	21,76	0,56	0,3977	0,1473
dCx E13.5	23,60	0,05	0,08124	3,34E-03
vCx E11.5	20,14	0,69	1,58	0,8065
vCx E12.5	21,88	0,22	0,3356	0,05911
vCx E13.5	26,85	0,22	5,85E-03	1,00E-03

Ddah1

	C(t)	C(t) SD	fg	fg SD
Ah E11.5	19,31	0,11	3,244	0,2269
Ah E12.5	22,21	0,56	0,491	0,1766
Ah E13.5	21,77	0,73	6,83E-01	2,66E-01
LGE E11.5	19,08	0,36	3,909	0,9409
LGE E12.5	20,72	0,31	1,276	2,59E-01
LGE E13.5	24,33	0,15	0,1103	0,01108
dCx E11.5	22,97	1,29	0,4133	3,74E-01
dCx E12.5	20,18	2,96	7,387	9,012
dCx E13.5	21,72	0,47	0,6701	1,86E-01
vCx E11.5	20,15	0,32	1,886	0,37
vCx E12.5	19,46	0,42	3,047	0,833
vCx E13.5	25,72	0,43	4,49E-02	1,25E-02

Gapdh

	C(t)	C(t) SD	fg	fg SD
Ah E11.5	17,93	0,33	9,572	2,395
Ah E12.5	21,34	0,07	0,821	0,04308
Ah E13.5	20,93	0,43	1,152	0,3707
LGE E11.5	18,45	0,27	6,555	1,259
LGE E12.5	20,52	0,12	1,48	0,1311
LGE E13.5	22,18	0,15	0,4545	0,04882
dCx E11.5	21,39	0,33	0,8158	0,2021
dCx E12.5	19,22	0,63	4,105	1,711
dCx E13.5	19,21	0,45	3,955	1,236
vCx E11.5	16,36	0,07	28,54	1,479
vCx E12.5	19,03	0,28	4,355	0,9021
vCx E13.5	24,07	0,64	0,1306	0,06213

Sept5

	C(t)	C(t) SD	fg	fg SD
Ah E11.5	25,25	0,26	0,03704	0,006295
Ah E12.5	27,51	0,18	0,007538	0,000926
Ah E13.5	26,30	1,06	0,02317	0,01711
LGE E11.5	24,91	0,52	0,04966	0,01946
LGE E12.5	25,26	0,74	0,04177	0,02293
LGE E13.5	29,06	0,34	0,002605	0,0006585
dCx E11.5	29,53	0,38	0,001879	0,0004503
dCx E12.5	28,14	0,96	0,006159	0,004465
dCx E13.5	28,59	0,31	0,003613	0,0007749
vCx E11.5	28,17	0,26	0,004808	0,0009167
vCx E12.5	26,62	0,72	0,01596	0,00864
vCx E13.5	30,63	0,35	0,000867	0,0001898

Replicate experiment 3**Anapc5**

	C(t)	C(t) SD	fg	fg SD
Ah E12.5	17,33	0,13	153,3	16,38
LGE E12.5	16,92	0,33	220,3	54,39
dCx E12.5	17,44	0,34	144,5	40,44
vCx E12.5	17,19	0,22	173,5	31,19

Sept5

	C(t)	C(t) SD	fg	fg SD
Ah E12.5	23,03	0,27	1,43	0,2189
LGE E12.5	21,48	1,37	4,671	3,507
dCx E12.5	24,17	0,16	0,7365	0,06661
vCx E12.5	22,48	0,18	1,954	0,2063

Atp5b

	C(t)	C(t) SD	fg	fg SD
Ah E12.5	12,81	0,27	1010	177,8
LGE E12.5	12,9	0,38	963,6	266,5
dCx E12.5	12,26	0,1	1473	105,4
vCx E12.5	13,61	0,21	564,3	85,77

Eif5

	C(t)	C(t) SD	fg	fg SD
Ah E12.5	16,66	0,53	179,5	51,19
LGE E12.5	16,27	0,24	221,4	33,29
dCx E12.5	15,78	0,31	304,3	61,84
vCx E12.5	16,79	0,53	166,2	48,29

Ddah1

	C(t)	C(t) SD	fg	fg SD
Ah E12.5	18,23	0,51	47,87	20,99
LGE E12.5	17,09	0,48	118,1	44,82
dCx E12.5	19,32	0,14	18,32	2,011
vCx E12.5	19,32	1,34	28,95	22,46

Rpl35

	C(t)	C(t) SD	fg	fg SD
Ah E12.5	13,12	0,16	370,6	40,7
LGE E12.5	13,39	0,12	307,5	25,22
dCx E12.5	12,2	0,2	695	92,69
vCx E12.5	13,34	0,33	324,9	67,42

Ldhb

	C(t)	C(t) SD	fg	fg SD
Ah E12.5	20,02	0,18	2,701	0,3376
LGE E12.5	20,67	0,45	1,789	0,4935
dCx E12.5	21,1	0,93	1,519	0,7844
vCx E12.5	21,17	0,23	1,222	0,2009

Gapdh

	C(t)	C(t) SD	fg	fg SD
Ah E12.5	14,34	0,36	750,6	175,1
LGE E12.5	13	0,15	1661	149
DCx E12.5	13,12	0,96	1788	893,1
VCx E12.5	13,3	0,58	1455	441,6

Psmb7

	C(t)	C(t) SD	fg	fg SD
Ah E12.5	15,2	0,27	55,06	10,01
LGE E12.5	15,15	0,1	56,47	4,076
dCx E12.5	14,5	0,31	90,23	20,8
vCx E12.5	15,25	0,81	61,69	36,3

Appendix D

Results of Affymetrix hybridization of cultured E11.5 embryonal regions (Cx/Cx, Cx/LGE and LGE/LGE), filtered through SAM with false discovery rate = 0, applied to either CC and CL together against LL or CC against CL and LL.

probe_id	gene_name	CC mean	σ_{CC}	CL mean	σ_{CL}	LL mean	σ_{LL}
1415917_at	methylenetetrahydrofolate dehydrogenase (NADP+ dependent), methenyltetrahydrofolate cyclohydrolase, formyltetrahydrofolate synthase	10,44724	0,045	10,437473	0,085	10,045541	0,02
1416304_at	LPS-induced TN factor	9,478869	0,161	9,4448395	0,3478	3,342935	0,239
1416340_a_at	mannosidase 2, alpha B1	9,823885	0,129	9,718333	0,075	9,286214	0,058
1416368_at	glutathione S-transferase, alpha 4	11,888051	0,307	11,606816	0,2	10,467362	0,049
1416474_at	neighbor of Punc E11	8,328998	0,161	8,142169	0,291	7,026404	0,196
1416561_at	glutamic acid decarboxylase 1	6,1128693	0,167	9,858364	0,124	10,876286	0,329
1416658_at	frizzled-related protein	7,2781644	0,55	6,988922	0,154	5,226461	0,217
1416673_at	beta-site APP-cleaving enzyme 2	6,855944	0,423	6,598952	0,166	5,469441	0,082
1416711_at	T-box brain gene 1	10,134106	0,124	10,004529	0,471	6,9761276	1,035
1416723_at	transcription factor 4	12,346923	0,081	11,941522	0,026	10,717525	0,287
1416724_x_at	transcription factor 4	11,497753	0,033	11,157033	0,099	9,820203	0,019
1416783_at	tachykinin 1	7,1640472	0,51	9,466107	0,428	10,222903	0,373
1416855_at	growth arrest specific 1	12,70865	0,306	12,126607	0,275	10,546509	0,352
1417143_at	endothelial differentiation, lysophosphatidic acid G-protein-coupled receptor, 2	8,708894	0,391	8,199013	0,25	6,761419	0,299
1417293_at	heparan sulfate 6-O-sulfotransferase 1	8,561794	0,044	8,9312525	0,026	8,900971	0,106
1417323_at	proline/serine-rich coiled-coil 1	11,314902	0,06	11,17452	0,067	10,591048	0,08
1417437_at	X-ray repair complementing defective repair in Chinese hamster cells 6	9,351628	0,027	9,252312	0,048	8,919318	0,096
1417600_at	solute carrier family 15 (H+/peptide transporter), member 2	9,478207	0,318	8,736657	0,279	6,3424053	0,587
1417612_at	immediate early response 5	11,021865	0,065	10,802028	0,1	9,959128	0,093
1418028_at	dopachrome tautomerase	9,053779	0,739	7,9908996	0,574	5,080642	0,321
1418047_at	neurogenic differentiation 6	9,914884	0,487	9,441976	0,452	3,9879684	0,864
1418086_at	protein phosphatase 1, regulatory (inhibitor) subunit 14A	8,107574	0,023	7,2248216	0,202	4,947605	0,776
1418147_at	transcription factor AP-2, gamma	8,985564	0,138	8,24817	0,096	6,5452037	0,388
1418260_at	hormonally upregulated Neu-associated kinase	10,314447	0,197	10,171566	0,11	9,521491	0,039
1418271_at	basic helix-loop-helix domain containing, class B5	11,899544	0,302	11,459279	0,272	7,2409425	0,651
1418281_at	RAD51 homolog (S, cerevisiae)	10,63473	0,025	10,539166	0,018	10,038674	0,011
1418286_a_at	ephrin B1	11,234788	0,05	11,051559	0,123	10,349761	0,099
1418317_at	LIM homeobox protein 2	12,163724	0,109	12,169095	0,166	10,4028425	0,195
1418382_at	adenomatous polyposis coli down-regulated 1	8,00689	0,469	7,7354393	0,073	6,333463	0,194
1418494_at	early B-cell factor 2	10,277484	0,575	9,552289	0,798	6,1518197	0,717
1418540_a_at	protein tyrosine phosphatase, receptor type, E	6,9289474	0,233	6,757301	0,048	5,782133	0,239
1418599_at	procollagen, type XI, alpha 1	9,272325	0,258	8,995202	0,329	7,6305695	0,276
1418790_at	Fez family zinc finger 2	11,07244	0,209	10,459607	0,16	7,0379243	0,24
1418879_at	RIKEN cDNA 9030611O19 gene	6,162554	0,111	6,492327	0,111	7,8231874	0,156
1418890_a_at	RAB3D, member RAS oncogene family	6,9859433	0,115	6,8077273	0,088	6,0421715	0,117
1418910_at	bone morphogenetic protein 7	7,761494	0,835	7,4424644	0,601	4,244198	0,201

1418925_at	cadherin EGF LAG seven-pass G-type receptor 1	8,127513	0,16	7,682944	0,1146,309543	0,301	
1418995_at	neurogenic differentiation 2	9,797711	0,305	9,444602	0,34	7,9038677	0,122
1419533_at	nescient helix loop helix 1	8,601616	0,526	8,3219185	0,153	5,048435	0,203
1419589_at	CD93 antigen	4,9591427	0,4	6,0453744	0,308	9,07846	0,149
1419845_at	distal-less homeobox 1, antisense	5,9659085	0,703	8,7646	0,193	9,873254	0,17
1420028_s_at	minichromosome maintenance deficient 3 (S, cerevisiae)	11,428409	0,157	11,347716	0,111	10,707954	0,154
1420150_at	splA/ryanodine receptor domain and SOCS box containing 1	8,408797	0,308	8,278838	0,193	6,5557117	0,058
1420649_at	zinc finger homeobox 3	8,565907	0,111	10,241558	0,144	10,991191	0,163
1420650_at	zinc finger homeobox 3	6,3649063	0,132	8,508597	0,661	9,457087	0,223
1420695_at	dachshund 1 (Drosophila)	7,55838	0,083	7,2633147	0,297	6,2255387	0,077
1420824_at	sema domain, immunoglobulin domain (Ig), transmembrane domain (TM) and short cytoplasmic domain, (semaphorin) 4D	8,700654	0,073	8,520827	0,064	7,9291606	0,088
1420905_at	interleukin 17 receptor A	8,115547	0,107	7,862347	0,094	6,8716016	0,128
1421074_at	cytochrome P450, family 7, subfamily b, polypeptide 1	7,8185983	0,172	7,389767	0,19	5,9722753	0,355
1421255_a_at	calcium binding protein 1	5,8199177	0,192	5,69293	0,269	4,0844483	0,265
1421601_at	GS homeobox 2	5,9242744	0,504	8,0073395	0,12	8,705182	0,243
1421841_at	fibroblast growth factor receptor 3	10,781316	0,219	10,29938	0,169	9,096661	0,18
1422272_at	per-hexamer repeat gene 4	8,793976	0,316	8,354191	0,061	7,161568	0,227
1422561_at	a disintegrin-like and metallopeptidase (reprolysin type) with thrombospondin type 1 motif, 5 (aggrecanase-2)	7,5249524	0,421	7,2304626	0,283	5,6805496	0,107
1422649_at	contactin 6	9,775765	0,237	9,395932	0,095	7,437444	0,359
1422670_at	Rho family GTPase 2	11,257258	0,36	11,0372505	0,269	9,452605	0,384
1422694_at	tweety homolog 1 (Drosophila)	9,188865	0,287	8,844415	0,522	7,275889	0,202
1422720_at	ISL1 transcription factor, LIM/homeodomain	6,4190555	0,259	9,980371	0,343	10,994064	0,349
1422756_at	solute carrier family 32 (GABA vesicular transporter), member 1	5,2818584	0,415	8,831852	0,813	10,1010727	0,725
1422811_at	solute carrier family 27 (fatty acid transporter), member 1	8,922513	0,016	8,8055725	0,385	7,8077626	0,07
1422818_at	neural precursor cell expressed, developmentally down-regulated gene 9	9,661597	0,18	9,595841	0,215	8,670299	0,094
1422839_at	neurogenin 2	10,268504	0,664	9,20869	0,412	5,5779643	0,758
1423428_at	receptor tyrosine kinase-like orphan receptor 2	7,541229	0,199	6,6626487	0,096	4,965325	0,299
1423493_a_at	nuclear factor I/X	8,872458	0,122	8,496061	0,465	6,1214557	0,487
1424010_at	microfibrillar-associated protein 4	8,196796	0,125	7,6482944	0,072	5,664003	0,263
1424089_a_at	transcription factor 4	10,416396	0,165	10,217413	0,096	8,622951	0,045
1424113_at	laminin B1 subunit 1	8,224769	0,256	7,897671	0,19	6,1909547	0,632
1424138_at	rhomboid family 1 (Drosophila)	10,319368	0,131	10,153058	0,14	9,332883	0,258
1424351_at	WAP four-disulfide core domain 2	9,209998	0,12	8,670787	0,014	7,192842	0,312
1424534_at	monocyte to macrophage differentiation-associated 2	10,068578	0,165	9,221771	0,082	7,069256	0,166
1424596_s_at	LIM and cysteine-rich domains 1	8,697996	0,475	8,4155655	0,194	6,0901394	0,267
1424680_at	expressed sequence BB146404	4,471388	0,056	4,8311534	0,153	6,299235	0,168
1424767_at	cadherin 22	7,2909837	0,278	8,710846	0,223	9,304454	0,176
1424816_at	cat eye syndrome chromosome region, candidate 5 homolog (human)	7,724806	0,078	7,63318	0,05	7,1865406	0,091
1425212_a_at	tumor necrosis factor receptor superfamily, member 19	8,649161	0,352	7,9311867	0,227	6,3772483	0,106
1425650_at	transducin-like enhancer of split 4, homolog of Drosophila E(spl)	6,130712	0,2	7,0228143	0,223	6,974701	0,174
1425788_a_at	enoyl Coenzyme A hydratase domain containing 2	7,494697	0,023	7,144094	0,147	6,4304504	0,122
1425892_a_at	prepronociceptin	6,254251	0,189	8,351048	0,085	9,34194	0,503

1425926_a_at	orthodenticle homolog 2 (Drosophila)	7,89009860,7299,918029	0,11810,644703	0,118
1425985_s_at	mannan-binding lectin serine peptidase 1	9,209004	0,0518,524899	0,2166,7453384
1426001_at	omesodermin homolog (Xenopus laevis)	9,303855	0,4848,678428	0,2376,8564873
1426208_x_at	pleiomorphic adenoma gene-like 1	13,2694470,09913,121266	0,13311,760026	0,15
1426288_at	low density lipoprotein receptor-related protein 4	10,1759060,3229,618566	0,2267,836907	0,581
1426342_at	STT3, subunit of the oligosaccharyltransferase complex, homolog B (S, cerevisiae)	12,8541140,10412,726284	0,07612,310227	0,067
1426412_at	neurogenic differentiation 1	10,7908170,21710,12531950,1916,7120724	1,141	
1426413_at	neurogenic differentiation 1	11,3632580,10210,717735	0,17	7,388035
1426621_a_at	protein phosphatase 2 (formerly 2A), regulatory subunit B (PR 52), beta isoform	9,672828	0,4579,308	0,5677,3085747
1426642_at	fibronectin 1	10,6609390,11810,451466	0,2089,591816	0,216
1426652_at	minichromosome maintenance deficient 3 (S, cerevisiae)	10,3029450,09910,148589	0,0599,528046	0,05
1427138_at	coiled-coil domain containing 88C	9,93904	0,0229,699353	0,16
1427139_at	a disintegrin-like and metallopeptidase (reprolysin type) with thrombospondin type 1 motif, 10	8,448825	0,0948,371662	0,0867,8507934
1427300_at	LIM homeobox protein 8	4,96920870,3527,6735873	0,4048,738091	0,609
1427465_at	ATPase, Na ⁺ /K ⁺ transporting, alpha 2 polypeptide	8,187486	0,3827,7194886	0,3465,865763
1427523_at	sine oculis-related homeobox 3 homolog (Drosophila)	7,843733	0,38910,349914	0,37111,461871
1427529_at	frizzled homolog 9 (Drosophila)	9,399796	0,2288,9126	0,2616,27574
1427600_at	tumor necrosis factor receptor superfamily, member 19	7,20149	0,3736,5397534	0,0774,585218
1427680_a_at	nuclear factor I/B	11,7897450,10411,612149	0,25210,031983	0,26
1427894_at	vasorin	7,667627	0,1887,5062394	0,1086,785528
1427981_a_at	cysteine sulfinic acid decarboxylase	8,766112	0,1178,634196	0,0997,9093494
1428114_at	solute carrier family 14 (urea transporter), member 1	7,22948460,6657,2506423	0,7614,280848	0,628
1428452_at	RIKEN cDNA 2810025M15 gene	12,5784	0,01812,268501	0,07211,550868
1428662_a_at	homeobox only domain	13,0133250,13512,73452	0,08910,42246	0,426
1430167_a_at	RWD domain containing 3	8,025755	0,1157,6381745	0,48
1431704_a_at	Ral GEF with PH domain and SH3 binding motif 2	7,249044	0,1247,007605	0,0486,296446
1431946_a_at	amyloid beta (A4) precursor protein-binding, family A, member 2 binding protein	6,882405	0,2346,680448	0,0955,327638
1434148_at	transcription factor 4	11,8950570,1911,68316650,09210,515801	0,054	
1434149_at	transcription factor 4	10,6315370,19310,210971	0,3358,747504	0,15
1434557_at	huntingtin interacting protein 1	10,24735	0,01610,243963	0,03
1434599_a_at	tight junction protein 2	8,901383	0,1488,876641	0,0867,922382
1434755_at	coronin, actin binding protein, 2B	10,3450250,31210,488576	0,1039,33209	0,23
1435026_at	sparc/osteonectin, cwcv and kazal-like domains proteoglycan 2	9,759515	0,21610,050795	0,2458,144885
1435172_at	omesodermin homolog (Xenopus laevis)	9,955776	0,3169,22441	0,2316,8303504
1435732_x_at	ATPase, H ⁺ transporting, lysosomal V0 subunit C	12,4565430,05912,691461	0,03312,690131	0,017
1436030_at	cache domain containing 1	11,91319	0,17	11,59739
1436031_at	cache domain containing 1	8,613742	0,1578,429844	0,2187,210354
1436363_a_at	nuclear factor I/X	10,8615570,20910,242074	0,2357,9987826	0,569
1436364_x_at	nuclear factor I/X	10,4984430,0929,98863	0,0747,759274	0,573
1436392_s_at	transcription factor AP-2, gamma	9,75702	0,14	9,152671
1438245_at	nuclear factor I/B	10,4668610,22	9,991178	0,0758,628647
1438602_s_at	mannan-binding lectin serine peptidase 1	9,542633	0,3198,848826	0,3447,1208415
1438654_x_at	monocyte to macrophage differentiation-associated 2	10,53835	0,1619,56033	0,0816,8682733
1448026_at	NA	10,7144470,06310,3828	0,0359,717156	0,13

1448147_at	tumor necrosis factor receptor superfamily, member 19	10,3850490,365	10,021209	0,163	7,145294	0,14
1448162_at	vascular cell adhesion molecule 1	7,302859	0,413	8,421432	0,088	8,797626 0,124
1448288_at	nuclear factor I/B	12,4824170,121	11,940526	0,1	10,662869	0,266
1448395_at	secreted frizzled-related protein 1	11,1702040,353	10,875619	0,224	9,503719	0,035
1448494_at	growth arrest specific 1	10,88844	0,239	10,222196	0,394	8,209825 0,35
1448877_at	distal-less homeobox 2	7,79827740,637	10,432032	0,428	11,122001	0,283
1448977_at	transcription factor AP-2, gamma	8,434414	0,255	7,646519	0,071	5,3747106 0,613
1449070_x_at	adenomatosis polyposis coli down-regulated 1	9,305401	0,271	9,048274	0,113	7,5342097 0,432
1449101_at	early B-cell factor 2	7,031938	0,401	6,6401772	0,238	4,5457015 0,564
1449102_at	early B-cell factor 2	8,140759	0,516	7,5332465	0,396	4,1720815 0,421
1449277_at	chemokine (C-C motif) ligand 19	7,78715370,076	8,193654	0,032	8,280808	0,029
1449470_at	distal-less homeobox 1	7,31093170,764	10,313058	0,089	11,373093	0,101
1449531_at	leprecan-like 2	7,31357960,132	7,1269126	0,143	6,4874167	0,133
1449581_at	EMI domain containing 1	9,134604	0,107	8,610936	0,026	6,8189826 0,075
1449848_at	guanine nucleotide binding protein, alpha 14	9,586734	0,219	9,147803	0,176	7,4204926 0,597
1449863_a_at	distal-less homeobox 5	7,004831	0,295	9,797115	0,287	10,5847435 0,361
1450567_a_at	procollagen, type II, alpha 1	8,647019	0,175	8,25681	0,158	6,9901004 0,117
1450723_at	ISL1 transcription factor, LIM/homeodomain	7,46644830,642	11,331433	0,335	12,332085	0,244
1450922_a_at	transforming growth factor, beta 2	8,582274	0,145	8,102532	0,606	6,199367 0,451
1450923_at	transforming growth factor, beta 2	9,041976	0,197	8,449615	0,002	6,646176 0,652
1450990_at	glypican 3	9,589362	0,704	9,326318	0,46	6,5031466 0,491
1451119_a_at	fibulin 1	9,951879	0,132	9,7221365	0,169	8,75926 0,205
1451461_a_at	aldolase 3, C isoform	12,9088370,234	12,559987	0,329	7,5644383	0,564
1451520_at	spastic paraplegia 20, spartin (Troyer syndrome) homolog (human)	8,827738	0,082	8,715211	0,105	8,302268 0,039
1451776_s_at	homeobox only domain	11,77583	0,36	11,4987955	0,032	9,076661 0,504
1451809_s_at	RWD domain containing 3	8,344067	0,148	7,987129	0,415	5,4746184 0,293
1451935_a_at	serine protease inhibitor, Kunitz type 2	9,81409	0,142	9,593839	0,102	8,505717 0,355
1452142_at	solute carrier family 6 (neurotransmitter transporter, GABA), member 1	7,24768450,56	9,457203	0,371	10,385129	0,206
1452227_at	RIKEN cDNA 2310045A20 gene	10,6716640,171	10,518197	0,212	9,729485	0,138
1452358_at	retinoic acid induced 2	7,240731	0,343	7,094967	0,402	5,3013697 0,249
1452507_at	distal-less homeobox 6	4,65793850,654	7,309273	0,435	8,432686	0,509
1452830_s_at	carbamoyl-phosphate synthetase 2, aspartate transcarbamylase, and dihydroorotase	9,909005	0,034	9,840629	0,113	9,322101 0,169
1454906_at	retinoic acid receptor, beta	4,97592350,254	5,0223536	0,164	7,278211	0,056
1454974_at	netrin 1	7,258967	0,363	10,331119	0,199	11,280725 0,332
1455343_at	pleckstrin homology domain containing, family A member 7	6,192496	0,071	6,097252	0,039	5,3127475 0,088
1455892_x_at	predicted gene, EG622147	9,432467	0,152	9,284042	0,313	8,418137 0,054
1456140_at	similar to OPR	9,277352	0,314	8,783128	0,348	6,7904954 0,521
1460716_a_at	core binding factor beta	12,7380440,043	12,44471	0,05	11,849785	0,133

Bibliography

- Aboitiz, F. 1999. Evolution of isocortical organization. A tentative scenario including roles of reelin, p35/cdk5 and the subplate zone. *Cereb Cortex*. 9:655-61.
- Armentano, M., S.J. Chou, G.S. Tomassy, A. Leingartner, D.D. O'Leary, and M. Studer. 2007. COUP-TFI regulates the balance of cortical patterning between frontal/motor and sensory areas. *Nat Neurosci*. 10:1277-86.
- Assimacopoulos, S., E.A. Grove, and C.W. Ragsdale. 2003. Identification of a Pax6-dependent epidermal growth factor family signaling source at the lateral edge of the embryonic cerebral cortex. *J Neurosci*. 23:6399-403.
- Aubert, J., H. Dunstan, I. Chambers, and A. Smith. 2002. Functional gene screening in embryonic stem cells implicates Wnt antagonism in neural differentiation. *Nat Biotechnol*. 20:1240-5.
- Baehrecke, E.H. 2002. How death shapes life during development. *Nat Rev Mol Cell Biol*. 3:779-87.
- Bally-Cuif, L., and M. Hammerschmidt. 2003. Induction and patterning of neuronal development, and its connection to cell cycle control. *Curr Opin Neurobiol*. 13:16-25.
- Bertrand, N., D.S. Castro, and F. Guillemot. 2002. Proneural genes and the specification of neural cell types. *Nat Rev Neurosci*. 3:517-30.
- Bielle, F., A. Griveau, N. Narboux-Neme, S. Vigneau, M. Sigrist, S. Arber, M. Wassef, and A. Pierani. 2005. Multiple origins of Cajal-Retzius cells at the borders of the developing pallium. *Nat Neurosci*. 8:1002-12.
- Bishop, K.M., G. Goudreau, and D.D. O'Leary. 2000. Regulation of area identity in the mammalian neocortex by Emx2 and Pax6. *Science*. 288:344-9.
- Bovolenta, P. 2005. Morphogen signaling at the vertebrate growth cone: a few cases or a general strategy? *J Neurobiol*. 64:405-16.
- Broccoli, V., E. Boncinelli, and W. Wurst. 1999. The caudal limit of Otx2 expression positions the isthmic organizer. *Nature*. 401:164-8.
- Carney, R.S., T.B. Alfonso, D. Cohen, H. Dai, S. Nery, B. Stoica, J. Slotkin, B.S. Bregman, G. Fishell, and J.G. Corbin. 2006. Cell migration along the lateral cortical stream to the developing basal telencephalic limbic system. *J Neurosci*. 26:11562-74.
- Caubit, X., M.C. Tiveron, H. Cremer, and L. Fasano. 2005. Expression patterns of the three Teashirt-related genes define specific boundaries in the developing and

- postnatal mouse forebrain. *J Comp Neurol.* 486:76-88.
- Caviness, V.S., Jr., T. Goto, T. Tarui, T. Takahashi, P.G. Bhide, and R.S. Nowakowski. 2003. Cell output, cell cycle duration and neuronal specification: a model of integrated mechanisms of the neocortical proliferative process. *Cereb Cortex.* 13:592-8.
- Cayuso, J., and E. Marti. 2005. Morphogens in motion: growth control of the neural tube. *J Neurobiol.* 64:376-87.
- Chapouton, P., A. Gartner, and M. Gotz. 1999. The role of Pax6 in restricting cell migration between developing cortex and basal ganglia. *Development.* 126:5569-79.
- Charron, F., and M. Tessier-Lavigne. 2005. Novel brain wiring functions for classical morphogens: a role as graded positional cues in axon guidance. *Development.* 132:2251-62.
- Cheng, A., S. Wang, J. Cai, M.S. Rao, and M.P. Mattson. 2003. Nitric oxide acts in a positive feedback loop with BDNF to regulate neural progenitor cell proliferation and differentiation in the mammalian brain. *Dev Biol.* 258:319-33.
- Chu, G., B. Narasimhan, R. Tibshirani, and V. Tusher. 2002. SAM "Significance Analysis of Microarrays" Users Guide and Technical Document.
- Ciani, L., and P.C. Salinas. 2005. WNTs in the vertebrate nervous system: from patterning to neuronal connectivity. *Nat Rev Neurosci.* 6:351-62.
- Creuzet, S.E., S. Martinez, and N.M. Le Douarin. 2006. The cephalic neural crest exerts a critical effect on forebrain and midbrain development. *Proc Natl Acad Sci U S A.* 103:14033-8.
- de Carlos, J.A., L. Lopez-Mascaraque, and F. Valverde. 1996. Dynamics of cell migration from the lateral ganglionic eminence in the rat. *J Neurosci.* 16:6146-56.
- Dehay, C., and H. Kennedy. 2007. Cell-cycle control and cortical development. *Nat Rev Neurosci.* 8:438-50.
- Dupin, E., G. Calloni, C. Real, A. Goncalves-Trentin, and N.M. Le Douarin. 2007. Neural crest progenitors and stem cells. *C R Biol.* 330:521-9.
- Ellis, R.E., and H.R. Horvitz. 1991. Two *C. elegans* genes control the programmed deaths of specific cells in the pharynx. *Development.* 112:591-603.
- Englund, C., A. Fink, C. Lau, D. Pham, R.A. Daza, A. Bulfone, T. Kowalczyk, and R.F. Hevner. 2005. Pax6, Tbr2, and Tbr1 are expressed sequentially by radial glia, intermediate progenitor cells, and postmitotic neurons in developing neocortex. *J Neurosci.* 25:247-51.
- Fernandez, A.S., C. Pieau, J. Reperant, E. Boncinelli, and M. Wassef. 1998. Expression

of the *Emx-1* and *Dlx-1* homeobox genes define three molecularly distinct domains in the telencephalon of mouse, chick, turtle and frog embryos: implications for the evolution of telencephalic subdivisions in amniotes. *Development*. 125:2099-111.

- Finkelstein, R., and E. Boncinelli. 1994. From fly head to mammalian forebrain: the story of *otd* and *Otx*. *Trends Genet*. 10:310-5.
- Forster, E., Y. Jossin, S. Zhao, X. Chai, M. Frotscher, and A.M. Goffinet. 2006. Recent progress in understanding the role of Reelin in radial neuronal migration, with specific emphasis on the dentate gyrus. *Eur J Neurosci*. 23:901-9.
- Frey, D., O. Braun, C. Briand, M. Vasak, and M.G. Grutter. 2006. Structure of the mammalian NOS regulator dimethylarginine dimethylaminohydrolase: A basis for the design of specific inhibitors. *Structure*. 14:901-11.
- Fuccillo, M., A.L. Joyner, and G. Fishell. 2006. Morphogen to mitogen: the multiple roles of hedgehog signaling in vertebrate neural development. *Nat Rev Neurosci*. 7:772-83.
- Fujimori, T., S. Miyatani, and M. Takeichi. 1990. Ectopic expression of N-cadherin perturbs histogenesis in *Xenopus* embryos. *Development*. 110:97-104.
- Furuta, Y., D.W. Piston, and B.L. Hogan. 1997. Bone morphogenetic proteins (BMPs) as regulators of dorsal forebrain development. *Development*. 124:2203-12.
- Gamse, J., and H. Sive. 2000. Vertebrate anteroposterior patterning: the *Xenopus* neurectoderm as a paradigm. *Bioessays*. 22:976-86.
- Garcia-Lopez, R., C. Vieira, D. Echevarria, and S. Martinez. 2004. Fate map of the di-encephalon and the zona limitans at the 10-somites stage in chick embryos. *Dev Biol*. 268:514-30.
- Gilbert, S.F. 2003. *Developmental Biology*. Sinauer Associates, Inc., Sunderland, MA.
- Gleeson, J.G., and C.A. Walsh. 2000. Neuronal migration disorders: from genetic diseases to developmental mechanisms. *Trends Neurosci*. 23:352-9.
- Gotz, M., A. Wizenmann, S. Reinhardt, A. Lumsden, and J. Price. 1996. Selective adhesion of cells from different telencephalic regions. *Neuron*. 16:551-64.
- Griesel, G., D. Treichel, P. Collombat, J. Krull, A. Zembrzycki, W.M. van den Akker, P. Gruss, A. Simeone, and A. Mansouri. 2006. *Sp8* controls the anteroposterior patterning at the midbrain-hindbrain border. *Development*. 133:1779-87.
- Grove, E.A., and T. Fukuchi-Shimogori. 2003. Generating the cerebral cortical area map. *Annu Rev Neurosci*. 26:355-80.
- Grove, E.A., S. Tole, J. Limon, L. Yip, and C.W. Ragsdale. 1998. The hem of the embryonic cerebral cortex is defined by the expression of multiple Wnt genes and

- is compromised in Gli3-deficient mice. *Development*. 125:2315-25.
- Guan, K., H. Chang, A. Rolletschek, and A.M. Wobus. 2001. Embryonic stem cell-derived neurogenesis. Retinoic acid induction and lineage selection of neuronal cells. *Cell Tissue Res*. 305:171-6.
- Guillemot, F., Z. Molnar, V. Tarabykin, and A. Stoykova. 2006. Molecular mechanisms of cortical differentiation. *Eur J Neurosci*. 23:857-68.
- Helvering, L.M., R.L. Sharp, X. Ou, and A.G. Geiser. 2000. Regulation of the promoters for the human bone morphogenetic protein 2 and 4 genes. *Gene*. 256:123-38.
- Hippenmeyer, S., I. Kramer, and S. Arber. 2004. Control of neuronal phenotype: what targets tell the cell bodies. *Trends Neurosci*. 27:482-8.
- Hoffman, L.M., K. Garcha, K. Karamboulas, M.F. Cowan, L.M. Drysdale, W.A. Horton, and T.M. Underhill. 2006. BMP action in skeletogenesis involves attenuation of retinoid signaling. *J Cell Biol*. 174:101-13.
- Holm, P.C., M.T. Mader, N. Haubst, A. Wizenmann, M. Sigvardsson, and M. Gotz. 2007. Loss- and gain-of-function analyses reveal targets of Pax6 in the developing mouse telencephalon. *Mol Cell Neurosci*. 34:99-119.
- Inoue, T., T. Tanaka, M. Takeichi, O. Chisaka, S. Nakamura, and N. Osumi. 2001. Role of cadherins in maintaining the compartment boundary between the cortex and striatum during development. *Development*. 128:561-9.
- Irving, C., A. Malhas, S. Guthrie, and I. Mason. 2002. Establishing the trochlear motor axon trajectory: role of the isthmus organizer and Fgf8. *Development*. 129:5389-98.
- Jarov, A., K.P. Williams, L.E. Ling, V.E. Koteliansky, J.L. Duband, and C. Fournier-Thibault. 2003. A dual role for Sonic hedgehog in regulating adhesion and differentiation of neuroepithelial cells. *Dev Biol*. 261:520-36.
- Jones, L., G. Lopez-Bendito, P. Gruss, A. Stoykova, and Z. Molnar. 2002. Pax6 is required for the normal development of the forebrain axonal connections. *Development*. 129:5041-52.
- Kaufman, D.L., C.R. Houser, and A.J. Tobin. 1991. Two forms of the gamma-aminobutyric acid synthetic enzyme glutamate decarboxylase have distinct intraneuronal distributions and cofactor interactions. *J Neurochem*. 56:720-3.
- Kent, W.J., C.W. Sugnet, T.S. Furey, K.M. Roskin, T.H. Pringle, A.M. Zahler, and D. Haussler. 2002. The human genome browser at UCSC. *Genome Res*. 12:996-1006.
- Kiecker, C., and A. Lumsden. 2005. Compartments and their boundaries in vertebrate brain development. *Nat Rev Neurosci*. 6:553-64.

- Kim, A.S., S.A. Anderson, J.L. Rubenstein, D.H. Lowenstein, and S.J. Pleasure. 2001. Pax-6 regulates expression of SFRP-2 and Wnt-7b in the developing CNS. *J Neurosci.* 21:RC132.
- Kitajima, K., U. Koshimizu, and T. Nakamura. 1999. Expression of a novel type of classic cadherin, PB-cadherin in developing brain and limb buds. *Dev Dyn.* 215:206-14.
- Kriegstein, A., S. Noctor, and V. Martinez-Cerdeno. 2006. Patterns of neural stem and progenitor cell division may underlie evolutionary cortical expansion. *Nat Rev Neurosci.* 7:883-90.
- Kroll, T.T., and D.D. O'Leary. 2005. Ventralized dorsal telencephalic progenitors in Pax6 mutant mice generate GABA interneurons of a lateral ganglionic eminence fate. *Proc Natl Acad Sci U S A.* 102:7374-9.
- Kuida, K., T.F. Haydar, C.Y. Kuan, Y. Gu, C. Taya, H. Karasuyama, M.S. Su, P. Rakic, and R.A. Flavell. 1998. Reduced apoptosis and cytochrome c-mediated caspase activation in mice lacking caspase 9. *Cell.* 94:325-37.
- Lee, S.H., K.K. Fu, J.N. Hui, and J.M. Richman. 2001. Noggin and retinoic acid transform the identity of avian facial prominences. *Nature.* 414:909-12.
- Lee, S.M., P.S. Danielian, B. Fritsch, and A.P. McMahon. 1997. Evidence that FGF8 signaling from the midbrain-hindbrain junction regulates growth and polarity in the developing midbrain. *Development.* 124:959-69.
- Li, J.Y., and A.L. Joyner. 2001. Otx2 and Gbx2 are required for refinement and not induction of mid-hindbrain gene expression. *Development.* 128:4979-91.
- Li, X., E.M. Schwarz, M.J. Zuscik, R.N. Rosier, A.M. Ionescu, J.E. Puzas, H. Drissi, T.J. Sheu, and R.J. O'Keefe. 2003. Retinoic acid stimulates chondrocyte differentiation and enhances bone morphogenetic protein effects through induction of Smad1 and Smad5. *Endocrinology.* 144:2514-23.
- Liao, W.L., H.F. Wang, H.C. Tsai, P. Chambon, M. Wagner, A. Kakizuka, and F.C. Liu. 2005. Retinoid signaling competence and RARbeta-mediated gene regulation in the developing mammalian telencephalon. *Dev Dyn.* 232:887-900.
- Liem, K.F., Jr., T.M. Jessell, and J. Briscoe. 2000. Regulation of the neural patterning activity of sonic hedgehog by secreted BMP inhibitors expressed by notochord and somites. *Development.* 127:4855-66.
- Lim, Y., and J.A. Golden. 2007. Patterning the developing diencephalon. *Brain Res Rev.* 53:17-26.
- Liu, A., and L.A. Niswander. 2005. Bone morphogenetic protein signaling and vertebrate nervous system development. *Nat Rev Neurosci.* 6:945-54.
- Lupo, G., W.A. Harris, and K.E. Lewis. 2006. Mechanisms of ventral patterning in the

- vertebrate nervous system. *Nat Rev Neurosci.* 7:103-14.
- Lyuksyutova, A.I., C.C. Lu, N. Milanese, L.A. King, N. Guo, Y. Wang, J. Nathans, M. Tessier-Lavigne, and Y. Zou. 2003. Anterior-posterior guidance of commissural axons by Wnt-frizzled signaling. *Science.* 302:1984-8.
- Mallamaci, A., L. Muzio, C.H. Chan, J. Parnavelas, and E. Boncinelli. 2000. Area identity shifts in the early cerebral cortex of *Emx2*^{-/-} mutant mice. *Nat Neurosci.* 3:679-86.
- Mallamaci, A., and A. Stoykova. 2006. Gene networks controlling early cerebral cortex arealization. *Eur J Neurosci.* 23:847-56.
- Marin, O., and J.L. Rubenstein. 2001. A long, remarkable journey: tangential migration in the telencephalon. *Nat Rev Neurosci.* 2:780-90.
- Martinez-Barbera, J.P., M. Signore, P.P. Boyl, E. Puelles, D. Acampora, R. Gogoi, F. Schubert, A. Lumsden, and A. Simeone. 2001. Regionalisation of anterior neuroectoderm and its competence in responding to forebrain and midbrain inducing activities depend on mutual antagonism between OTX2 and GBX2. *Development.* 128:4789-800.
- Mason, I. 2007. Initiation to end point: the multiple roles of fibroblast growth factors in neural development. *Nat Rev Neurosci.* 8:583-96.
- Means, A.L., and L.J. Gudas. 1996. FGF-2, BMP-2, and BMP-4 regulate retinoid binding proteins and receptors in 3T3 cells. *Cell Growth Differ.* 7:989-96.
- Meier, P., A. Finch, and G. Evan. 2000. Apoptosis in development. *Nature.* 407:796-801.
- Messier, P.E. 1978. Microtubules, interkinetic nuclear migration and neurulation. *Experientia.* 34:289-96.
- Metin, C., J.P. Baudoin, S. Rakic, and J.G. Parnavelas. 2006. Cell and molecular mechanisms involved in the migration of cortical interneurons. *Eur J Neurosci.* 23:894-900.
- Mic, F.A., and G. Duester. 2003. Patterning of forelimb bud myogenic precursor cells requires retinoic acid signaling initiated by *Raldh2*. *Dev Biol.* 264:191-201.
- Minowada, G., L.A. Jarvis, C.L. Chi, A. Neubuser, X. Sun, N. Hacohen, M.A. Krasnow, and G.R. Martin. 1999. Vertebrate *Sprouty* genes are induced by FGF signaling and can cause chondrodysplasia when overexpressed. *Development.* 126:4465-75.
- Molnar, Z., C. Metin, A. Stoykova, V. Tarabykin, D.J. Price, F. Francis, G. Meyer, C. Dehay, and H. Kennedy. 2006. Comparative aspects of cerebral cortical development. *Eur J Neurosci.* 23:921-34.

- Molyneaux, B.J., P. Arlotta, J.R. Menezes, and J.D. Macklis. 2007. Neuronal subtype specification in the cerebral cortex. *Nat Rev Neurosci.* 8:427-37.
- Monuki, E.S., F.D. Porter, and C.A. Walsh. 2001. Patterning of the dorsal telencephalon and cerebral cortex by a roof plate-Lhx2 pathway. *Neuron.* 32:591-604.
- Moreno-Lopez, B., C. Romero-Grimaldi, J.A. Noval, M. Murillo-Carretero, E.R. Matarredona, and C. Estrada. 2004. Nitric oxide is a physiological inhibitor of neurogenesis in the adult mouse subventricular zone and olfactory bulb. *J Neurosci.* 24:85-95.
- Muzio, L., B. DiBenedetto, A. Stoykova, E. Boncinelli, P. Gruss, and A. Mallamaci. 2002. Emx2 and Pax6 control regionalization of the pre-neuronogenic cortical primordium. *Cereb Cortex.* 12:129-39.
- Nadarajah, B., and J.G. Parnavelas. 2002. Modes of neuronal migration in the developing cerebral cortex. *Nat Rev Neurosci.* 3:423-32.
- Nery, S., H. Wichterle, and G. Fishell. 2001. Sonic hedgehog contributes to oligodendrocyte specification in the mammalian forebrain. *Development.* 128:527-40.
- O'Leary, D.D. 1989. Do cortical areas emerge from a protocortex? *Trends Neurosci.* 12:400-6.
- O'Leary, D.D., S.J. Chou, and S. Sahara. 2007. Area patterning of the mammalian cortex. *Neuron.* 56:252-69.
- Ohkubo, Y., C. Chiang, and J.L. Rubenstein. 2002. Coordinate regulation and synergistic actions of BMP4, SHH and FGF8 in the rostral prosencephalon regulate morphogenesis of the telencephalic and optic vesicles. *Neuroscience.* 111:1-17.
- Osterfield, M., M.W. Kirschner, and J.G. Flanagan. 2003. Graded positional information: interpretation for both fate and guidance. *Cell.* 113:425-8.
- Panhuysen, M., D.M. Vogt Weisenhorn, V. Blanquet, C. Brodski, U. Heinzmann, W. Beisker, and W. Wurst. 2004. Effects of Wnt1 signaling on proliferation in the developing mid-/hindbrain region. *Mol Cell Neurosci.* 26:101-11.
- Patten, I., and M. Placzek. 2002. Opponent activities of Shh and BMP signaling during floor plate induction in vivo. *Curr Biol.* 12:47-52.
- Pavlidis, P., and W.S. Noble. 2001. Analysis of strain and regional variation in gene expression in mouse brain. *Genome Biol.* 2:RESEARCH0042.
- Quinn, J.C., M. Molinek, B.S. Martynoga, P.A. Zaki, A. Faedo, A. Bulfone, R.F. Hevner, J.D. West, and D.J. Price. 2007. Pax6 controls cerebral cortical cell number by regulating exit from the cell cycle and specifies cortical cell identity by a cell autonomous mechanism. *Dev Biol.* 302:50-65.
- Raff, M.C., B.A. Barres, J.F. Burne, H.S. Coles, Y. Ishizaki, and M.D. Jacobson. 1993.

- Programmed cell death and the control of cell survival: lessons from the nervous system. *Science*. 262:695-700.
- Ragsdale, C.W., and E.A. Grove. 2001. Patterning the mammalian cerebral cortex. *Curr Opin Neurobiol*. 11:50-8.
- Raible, F., and M. Brand. 2004. Divide et Impera--the midbrain-hindbrain boundary and its organizer. *Trends Neurosci*. 27:727-34.
- Rash, B.G., and E.A. Grove. 2006. Area and layer patterning in the developing cerebral cortex. *Curr Opin Neurobiol*. 16:25-34.
- Rhinn, M., K. Lun, M. Luz, M. Werner, and M. Brand. 2005. Positioning of the mid-brain-hindbrain boundary organizer through global posteriorization of the neuroectoderm mediated by Wnt8 signaling. *Development*. 132:1261-72.
- Rhinn, M., A. Picker, and M. Brand. 2006. Global and local mechanisms of forebrain and midbrain patterning. *Curr Opin Neurobiol*. 16:5-12.
- Ross, S.E., M.E. Greenberg, and C.D. Stiles. 2003. Basic helix-loop-helix factors in cortical development. *Neuron*. 39:13-25.
- Saarimäki-Vire, J., P. Peltopuro, L. Lahti, T. Naserke, A.A. Blak, D.M. Vogt Weisenhorn, K. Yu, D.M. Ornitz, W. Wurst, and J. Partanen. 2007. Fibroblast growth factor receptors cooperate to regulate neural progenitor properties in the developing midbrain and hindbrain. *J Neurosci*. 27:8581-92.
- Saeed, A.I., V. Sharov, J. White, J. Li, W. Liang, N. Bhagabati, J. Braisted, M. Klapa, T. Currier, M. Thiagarajan, A. Sturn, M. Snuffin, A. Rezantsev, D. Popov, A. Ryltsov, E. Kostukovich, I. Borisovsky, Z. Liu, A. Vinsavich, V. Trush, and J. Quackenbush. 2003. TM4: a free, open-source system for microarray data management and analysis. *Biotechniques*. 34:374-8.
- Sahara, S., Y. Kawakami, J.C. Izpisua Belmonte, and D. O'Leary D. 2007. Sp8 exhibits reciprocal induction with Fgf8 but has an opposing effect on anterior-posterior cortical area patterning. *Neural Develop*. 2:10.
- Salie, R., V. Niederkofler, and S. Arber. 2005. Patterning molecules; multitasking in the nervous system. *Neuron*. 45:189-92.
- Sambrook, J., E. F. Fritsch, and T. Maniatis. 1989. Molecular cloning. 2nd ed. New York: Cold Spring Harbor Laboratory Press.
- Sanchez-Camacho, C., J. Rodriguez, J.M. Ruiz, F. Trousse, and P. Bovolenta. 2005. Morphogens as growth cone signaling molecules. *Brain Res Brain Res Rev*. 49:242-52.
- Scholpp, S., I. Foucher, N. Staudt, D. Peukert, A. Lumsden, and C. Houart. 2007. Otx11, Otx2 and Irx1b establish and position the ZLI in the diencephalon. *Development*. 134:3167-76.

- Schuermans, C., and F. Guillemot. 2002. Molecular mechanisms underlying cell fate specification in the developing telencephalon. *Curr Opin Neurobiol.* 12:26-34.
- Shimamura, K., S. Hirano, A.P. McMahon, and M. Takeichi. 1994. Wnt-1-dependent regulation of local E-cadherin and alpha N-catenin expression in the embryonic mouse brain. *Development.* 120:2225-34.
- Shimogori, H., T. Takemoto, T. Mikuriya, and H. Yamashita. 2007. Edaravone protects the vestibular periphery from free radical-induced toxicity in response to perilymphatic application of (+/-)-alpha-amino-3-hydroxy-5-methyl-isoxazole-4-propionic acid. *Eur J Pharmacol.* 554:223-8.
- Shimogori, T., V. Banuchi, H.Y. Ng, J.B. Strauss, and E.A. Grove. 2004. Embryonic signaling centers expressing BMP, WNT and FGF proteins interact to pattern the cerebral cortex. *Development.* 131:5639-47.
- Stoykova, A., R. Fritsch, C. Walther, and P. Gruss. 1996. Forebrain patterning defects in Small eye mutant mice. *Development.* 122:3453-65.
- Stoykova, A., M. Gotz, P. Gruss, and J. Price. 1997. Pax6-dependent regulation of adhesive patterning, R-cadherin expression and boundary formation in developing forebrain. *Development.* 124:3765-77.
- Stoykova, A., O. Hatano, P. Gruss, and M. Gotz. 2003. Increase in reelin-positive cells in the marginal zone of Pax6 mutant mouse cortex. *Cereb Cortex.* 13:560-71.
- Takahashi, T., R.S. Nowakowski, and V.S. Caviness, Jr. 1992. BUdR as an S-phase marker for quantitative studies of cytokinetic behaviour in the murine cerebral ventricular zone. *J Neurocytol.* 21:185-97.
- Takahashi, T., R.S. Nowakowski, and V.S. Caviness, Jr. 1993. Cell cycle parameters and patterns of nuclear movement in the neocortical proliferative zone of the fetal mouse. *J Neurosci.* 13:820-33.
- Talamillo, A., J.C. Quinn, J.M. Collinson, D. Caric, D.J. Price, J.D. West, and R.E. Hill. 2003. Pax6 regulates regional development and neuronal migration in the cerebral cortex. *Dev Biol.* 255:151-63.
- Testaz, S., A. Jarov, K.P. Williams, L.E. Ling, V.E. Koteliansky, C. Fournier-Thibault, and J.L. Duband. 2001. Sonic hedgehog restricts adhesion and migration of neural crest cells independently of the Patched- Smoothed-Gli signaling pathway. *Proc Natl Acad Sci U S A.* 98:12521-6.
- Toresson, H., A. Mata de Urquiza, C. Fagerstrom, T. Perlmann, and K. Campbell. 1999. Retinoids are produced by glia in the lateral ganglionic eminence and regulate striatal neuron differentiation. *Development.* 126:1317-26.
- Toresson, H., S.S. Potter, and K. Campbell. 2000. Genetic control of dorsal-ventral identity in the telencephalon: opposing roles for Pax6 and Gsh2. *Development.* 127:4361-71.

- Tusher, V.G., R. Tibshirani, and G. Chu. 2001. Significance analysis of microarrays applied to the ionizing radiation response. *Proc Natl Acad Sci U S A*. 98:5116-21.
- Vandesompele, J., K. De Preter, F. Pattyn, B. Poppe, N. Van Roy, A. De Paepe, and F. Speleman. 2002. Accurate normalization of real-time quantitative RT-PCR data by geometric averaging of multiple internal control genes. *Genome Biol*. 3:RESEARCH0034.
- Waclaw, R.R., B. Wang, and K. Campbell. 2004. The homeobox gene *Gsh2* is required for retinoid production in the embryonic mouse telencephalon. *Development*. 131:4013-20.
- Wang, H.F., and F.C. Liu. 2005. Regulation of multiple dopamine signal transduction molecules by retinoids in the developing striatum. *Neuroscience*. 134:97-105.
- Watanabe, Y., R. Toyoda, and H. Nakamura. 2004. Navigation of trochlear motor axons along the midbrain-hindbrain boundary by neuropilin 2. *Development*. 131:681-92.
- Wurst, W., and L. Bally-Cuif. 2001. Neural plate patterning: upstream and downstream of the isthmic organizer. *Nat Rev Neurosci*. 2:99-108.
- Ye, W., K. Shimamura, J.L. Rubenstein, M.A. Hynes, and A. Rosenthal. 1998. FGF and Shh signals control dopaminergic and serotonergic cell fate in the anterior neural plate. *Cell*. 93:755-66.
- Yun, K., A. Mantani, S. Garel, J. Rubenstein, and M.A. Israel. 2004. *Id4* regulates neural progenitor proliferation and differentiation in vivo. *Development*. 131:5441-8.
- Yun, K., S. Potter, and J.L. Rubenstein. 2001. *Gsh2* and *Pax6* play complementary roles in dorsoventral patterning of the mammalian telencephalon. *Development*. 128:193-205.
- Zar, J.H. 1999. *Biostatistical Analysis*. Prentice Hall, NJ.
- Zhao, Y., H.Z. Sheng, R. Amini, A. Grinberg, E. Lee, S. Huang, M. Taira, and H. Westphal. 1999. Control of hippocampal morphogenesis and neuronal differentiation by the LIM homeobox gene *Lhx5*. *Science*. 284:1155-8.
- Zhu, Y., M.S. Hsu, and J.E. Pintar. 1998. Developmental expression of the mu, kappa, and delta opioid receptor mRNAs in mouse. *J Neurosci*. 18:2538-49.

Acknowledgements

The following people were essential in the production of this work, providing valuable guidance, help and support.

Prof. Giorgio Casari

Prof. Antonello Mallamaci

The members of the Cerebral Cortex Development lab:

Marco Brancaccio

Assunta Diodato

Nicola Antonio Maiorano

Chiara Pivetta

Elisa Puzzolo

Giulia Spigoni

Helena Krnac for Affymetrix chip technical support

Paola Roncaglia for statistical analysis

Prof. Stefano Gustincich

Prof. John Nicholls

Tullio Bigiarini for technical support of all kinds

My family, friends and all students and staff at SISSA.

- a S. e al futuro.